

# **Review of Aeronautical Fatigue and Structural Integrity Work in Canada (2017 - 2019)**

**Authors:** Min Liao

**Report No.:** LTR-SMM-2019-0063

**RDIMS No.:** N/A

**Date:** April 2019



NATIONAL RESEARCH COUNCIL CANADA (NRC)

AEROSPACE

# **Review of Aeronautical Fatigue and Structural Integrity Work in Canada (2017 - 2019)**

Volume 1 of 1

Report No.: LTR-SMM-2019-0063

RDIMS No.: N/A

Date: April 2019

Authors: Min Liao

Classification:	Unclassified	Distribution:	Unlimited
For:	International Committee on Aeronautical Fatigue and Structural Integrity (ICAF)		
Reference:	-		
Submitted by:	R. Kearsey, Director/A, Structures and Materials Performance Laboratory		
Approved by:	I. Yimer, Director in General, Aerospace Research Center		

Pages :	100	Copy No.:	N/A
Figures:	67	Tables:	8

*This Report May Not Be Published Wholly Or In Part Without The Written Consent Of The National Research Council Canada*



## **EXECUTIVE SUMMARY**

This report provides a review of aeronautical fatigue and structural integrity work in Canada during the period April 2017 to April 2019. The review is a collection of multiple work summaries that are provided by Canadian industries, universities, and government organizations. All aspects of structural integrity, especially fatigue related work, are covered including: full-scale testing, life assessment and enhancement, load and usage monitoring, structural health monitoring, non-destructive inspection, environmental effects, and new material and manufacturing. This national review will be presented at the 36<sup>th</sup> International Committee on Aeronautical Fatigue and Structural Integrity (ICAF) Conference, which will be held in Krakow, Poland, from June 2<sup>nd</sup> to 7<sup>th</sup>, 2019.



# TABLE OF CONTENTS

<b>EXECUTIVE SUMMARY .....</b>	<b>I</b>
<b>TABLE OF CONTENTS .....</b>	<b>III</b>
<b>1.0 INTRODUCTION.....</b>	<b>1</b>
<b>2.0 FULL-SCALE STRUCTURAL AND COMPONENT TESTING.....</b>	<b>2</b>
2.1 GLOBAL 7500 DURABILITY AND DAMAGE TOLERANCE TESTS .....	2
2.2 BOMBARDIER GLOBAL 7500 FATIGUE TEST CYCLE RATE COMMISSIONING TO ¼ LIFE* .....	8
2.2.1 <i>References</i> .....	10
2.3 F/A-18 FTS2 ARMASUISSE HORIZONTAL STABILATOR FATIGUE TEST (NRC/ARMASUISSE/RUAG).....	10
2.4 F/A-18 AILERON FATIGUE TEST (NRC/RCAF/L-3 MAS).....	13
2.5 CF-188 HORIZONTAL STABILATOR TEAR-DOWN ANALYSIS POST LIFE EXTENSION FATIGUE TEST.....	15
2.6 FATIGUE STRUCTURAL TESTING ENHANCEMENT RESEARCH (FASTER).....	18
2.6.1 <i>References</i> .....	19
2.7 STRUCTURAL ANALYSIS FOR CH-146 AIR TRANSPORTATION KIT PALLET ASSEMBLY .....	19
<b>3.0 FATIGUE LIFE ASSESSMENT AND MANAGEMENT .....</b>	<b>22</b>
3.1 CP-140 (P-3) 7249 DAMAGE TOLERANCE ANALYSIS (DTA) UPDATES .....	22
3.2 CF-188 AIRCRAFT STRUCTURAL INTEGRITY PROGRAM (ASIP) AND AIRCRAFT LIFE EXTENSION (ALEX) PROGRAM .....	23
3.2.1 <i>ELE Extension and New BOS Initiative</i> .....	24
3.2.2 <i>Flight Control Surfaces (FCS) Life Extension</i> .....	25
3.3 F-18 AIRCRAFT INTERNATIONAL SUPPORT .....	27
3.3.1 <i>Fastener Life Improvement Techniques – Coupon Testing</i> .....	27
3.4 CT-114 (TUTOR) AIRCRAFT STRUCTURAL INTEGRITY PROGRAM (ASIP).....	30
3.5 CC-150 POLARIS FLEET IN-SERVICE SUPPORT AND FLEET MANAGEMENT .....	31
3.5.1 <i>Obsolescence and ageing aircraft management</i> .....	31
3.5.2 <i>CC-150T MRTT Mission Mix Study</i> .....	31
3.5.3 <i>CC-150 Estimated Life Expectancy (ELE) Study</i> .....	32
3.6 CH-148 MARITIME HELICOPTER AIRCRAFT STRUCTURAL INTEGRITY PROGRAM (ASIP) .....	32
3.7 DEMONSTRATION OF AN AIRFRAME DIGITAL TWIN FRAMEWORK USING A CF-188 COMPONENT TEST *.....	34
3.7.1 <i>References</i> .....	35
<b>4.0 FATIGUE LIFE ENHANCEMENT TECHNOLOGIES.....</b>	<b>36</b>
4.1 SHOT PEENING TO EXTEND FATIGUE LIFE OF MILITARY AIRCRAFT .....	36
4.2 LIFE IMPROVEMENT QUANTIFICATION OF FASTENER MODIFICATIONS .....	37
4.2.1 <i>References</i> .....	37
4.3 HOLE COLD EXPANSION PROCESS PLASTICITY MODELLING.....	38
4.4 MEASUREMENT OF RESIDUAL STRESSES RESULTING FROM COLD EXPANSION.....	39
4.5 FATIGUE LIFE PREDICTION AT COLD EXPANDED FASTENER HOLES WITH FORCEMATE BUSHINGS*.....	42
4.5.1 <i>Reference</i> .....	43
4.6 FATIGUE PERFORMANCE EVALUATION OF BLIND FASTENERS FOR CP-140 VERTICAL STABILIZER REPAIRS .....	43
<b>5.0 LOAD, USAGE, AND STRUCTURAL HEALTH MONITORING .....</b>	<b>46</b>
5.1 HELICOPTER LOAD AND USAGE MONITORING RESEARCH IN 2017-2019 .....	46
5.1.1 <i>A machine learning approach to load tracking and usage monitoring for legacy fleets [7]*</i> .....	46

5.1.2	Data analytics and predictive maintenance [8].....	47
5.1.3	Usage monitoring using MEMS-IMU sensor system and FDR input data .....	48
5.1.4	Analysis of sensor network data for failure modelling and prediction [9][10][11][12] .....	49
5.1.5	References.....	50
5.2	STRUCTURAL HEALTH MONITORING (SHM) .....	51
5.3	POTENTIAL DAMAGE LOCATION INDICATION DETERMINED USING ACOUSTIC EMISSION DURING CF-188 AILERON FATIGUE TEST .....	52
5.4	REPEATABILITY STUDY OF STRUCTURAL HEALTH MONITORING (SHM) SENSORS AT ROOM TEMPERATURE.....	53
5.5	DAMAGE DETECTION METHODOLOGY BASED ON MULTI-FREQUENCY GUIDED WAVES FOR SHM APPLICATIONS WITH EXPERIMENTAL AND NUMERICAL VERIFICATION .....	55
5.5.1	References.....	57
<b>6.0</b>	<b>NON-DESTRUCTIVE EVALUATION.....</b>	<b>58</b>
6.1	DETECTION OF LOW-VELOCITY IMPACT DAMAGE IN CARBON FIBER SANDWICH PANELS USING INFRARED THERMOGRAPHY* .....	58
6.2	INDUCTION THERMOGRAPHY OF STEEL COUPONS WITH CRACKS .....	60
6.2.1	References.....	60
6.3	RELIABILITY ASSESSMENT OF PULSED THERMOGRAPHY AND ULTRASONIC TESTING FOR IMPACT DAMAGE OF CFRP PANELS .....	61
6.3.1	References.....	61
6.4	AUTOMATED DYNAMIC INSPECTION USING ACTIVE INFRARED THERMOGRAPHY .....	62
6.4.1	References.....	62
6.5	EMBEDDED ELECTROMAGNETIC SENSORS FOR NDE AND SHM .....	62
6.5.1	References.....	64
6.6	TECHNICAL JUSTIFICATION OF ULTRASONIC INSPECTION PROCEDURE FOR HELICOPTER COMPONENTS* .....	64
6.6.1	References.....	67
6.7	EQUIVALENT PENETRATOR SENSITIVITY (EPS) FOR PERFORMANCE EVALUATION OF COMPUTED RADIOGRAPHY (CR) SYSTEMS .....	67
6.7.1	References.....	69
<b>7.0</b>	<b>ENVIRONMENTAL EFFECTS ON FATIGUE AND STRUCTURAL INTEGRITY.....</b>	<b>70</b>
7.1	CORROSION DAMAGE ATLAS FOR AIRCRAFT CORROSION MANAGEMENT AND STRUCTURAL INTEGRITY ASSESSMENT .....	70
7.1.1	References.....	73
7.2	EFFECT OF ALTERNATIVE PAINT STRIPPING PROCESSES ON THE FATIGUE PERFORMANCE OF ALUMINIUM ALLOYS* .....	73
7.2.1	References.....	75
<b>8.0</b>	<b>FATIGUE AND STRUCTURAL INTEGRITY OF COMPOSITES.....</b>	<b>76</b>
8.1	SURFACE DAMAGE EVALUATION OF TEXTURED ALUMINIUM HONEYCOMB SANDWICH PANELS .....	76
8.1.1	References.....	78
8.2	NUMERICAL MODELLING OF COMPOSITE MATERIAL AND STRUCTURAL FAILURE BEHAVIOURS.....	78
8.2.1	Cohesive Zone Modeling of a Unidirectional CFRP DCB Test on Progressive Failure [27].....	78
8.2.2	Progressive failure of a bonded 3D composite section [28].....	79
8.2.3	References.....	80
<b>9.0</b>	<b>FATIGUE AND STRUCTURAL INTEGRITY OF NEW MATERIAL AND MANUFACTURING.....</b>	<b>81</b>
9.1	MEASUREMENT OF THE RESISTANCE TO FRACTURE OF 7249-T76511 ALUMINIUM EXTRUSION .....	81

9.1.1 *References*.....82

9.2 APPLICATION OF MULTIFUNCTIONAL MECHANICAL METAMATERIALS .....82

9.2.1 *References*.....83

9.3 DURABILITY AND DAMAGE TOLERANCE OF ADDITIVE MANUFACTURING POLYMER PARTS FOR AEROSPACE APPLICATION\* .....84

9.3.1 *References*.....86

9.4 CASE STUDY: IN-SERVICE USE OF ADDITIVELY MANUFACTURED AIRCRAFT STRUCTURAL COMPONENTS FOR REPAIR PURPOSES .....86

9.5 DEFORMATION AND EVOLUTION OF LIFE IN CRYSTALLINE MATERIALS – AN INTEGRATED CREEP FATIGUE THEORY.....87

9.5.1 *Reference* .....89

**10.0 ACKNOWLEDGEMENTS.....90**



## 1.0 INTRODUCTION

Canadian industries, universities and government agencies were solicited for information describing their fatigue technology and structural integrity related activities over the period April 2017 to April 2019. This review covers work performed or being performed by the following organizations (including some collaborative organizations):

- Bombardier Aerospace (BA)
  - Bombardier Aerospace Experimental Department (BAEX)
- IMP Aerospace (IMP)
- L-3 Communications (Canada) Military Aircraft Services (MAS)
- Rolls-Royce Deutschland
- Siemens AG
- Siemens Canada
- Carleton University
- Concordia University
- McGill University
- Université Laval
- Department of Mechanical & Aeronautical Engineering, Clarkson University
- Engineering, Harvard University
- Department of National Defence (DND)
  - Defence Research and Development Canada (DRDC)
  - Director of Technical Airworthiness and Engineering Support (DTAES)
  - Quality Engineering Test Establishment (QETE)
  - Royal Canadian Air Force (RCAF)
  - Royal Military College of Canada (RMC)
- Royal Australian Air Force (RAAF)
- United States Navy (USN)
- National Research Council Canada, Aerospace Research Center (NRC Aerospace)

Names of contributors (where available) and their organizations are included in the text of this review. Full addresses of the contributors are available through the ICAF Canadian National Delegate at:

Min Liao, Ph.D., Principal Research Officer

Group Leader - Structural Integrity  
Aerospace, National Research Council Canada  
1200 Montreal Road, Building M14  
Ottawa, ON, K1A 0R6, Canada  
Tel: 1-613-990-9812;  
Email: [Min.Liao@nrc-cnrc.gc.ca](mailto:Min.Liao@nrc-cnrc.gc.ca)

## 2.0 FULL-SCALE STRUCTURAL AND COMPONENT TESTING

### 2.1 Global 7500 Durability and Damage Tolerance Tests

Arkady Alperovitch, Product Development Engineering, Bombardier Aerospace

The Global 7500 Complete Aircraft Durability and Damage Tolerance (DADT) Test started in November 2017 at BAEX (Bombardier Aerospace Experimental Department) in Montreal, Canada, shown in Figure 1.



**Figure 1 Global 7500 durability and damage tolerance tests in Montreal, Canada  
(Note: Bombardier Aerospace has changed the name of the Global 7000 ultra-long range aircraft to the Global 7500 thanks to performance improvements that continue to surpass expectations)**

The main objective of the test is to demonstrate the damage tolerance and fatigue characteristics of the metallic components of the Global 7500 airframe as well as to demonstrate no Widespread

Fatigue Damage (WFD) over the Design Service Goal of 17,000 flights. Other objectives include validation of:

1. Crack growth models for primary metal structure,
2. Inspection techniques and intervals, and
3. Typical repairs and allowable damage limits.

The main components covered by the Complete Aircraft DADT Test: complete fuselage, wing, engine mounts, vertical stabilizer and metallic parts of the horizontal stabilizer. It also covers all doors, landing gear interfaces, as well as the control surface and high lift device attachments and backup structures within the wing box and empennage boxes, as shown in Figure 2.

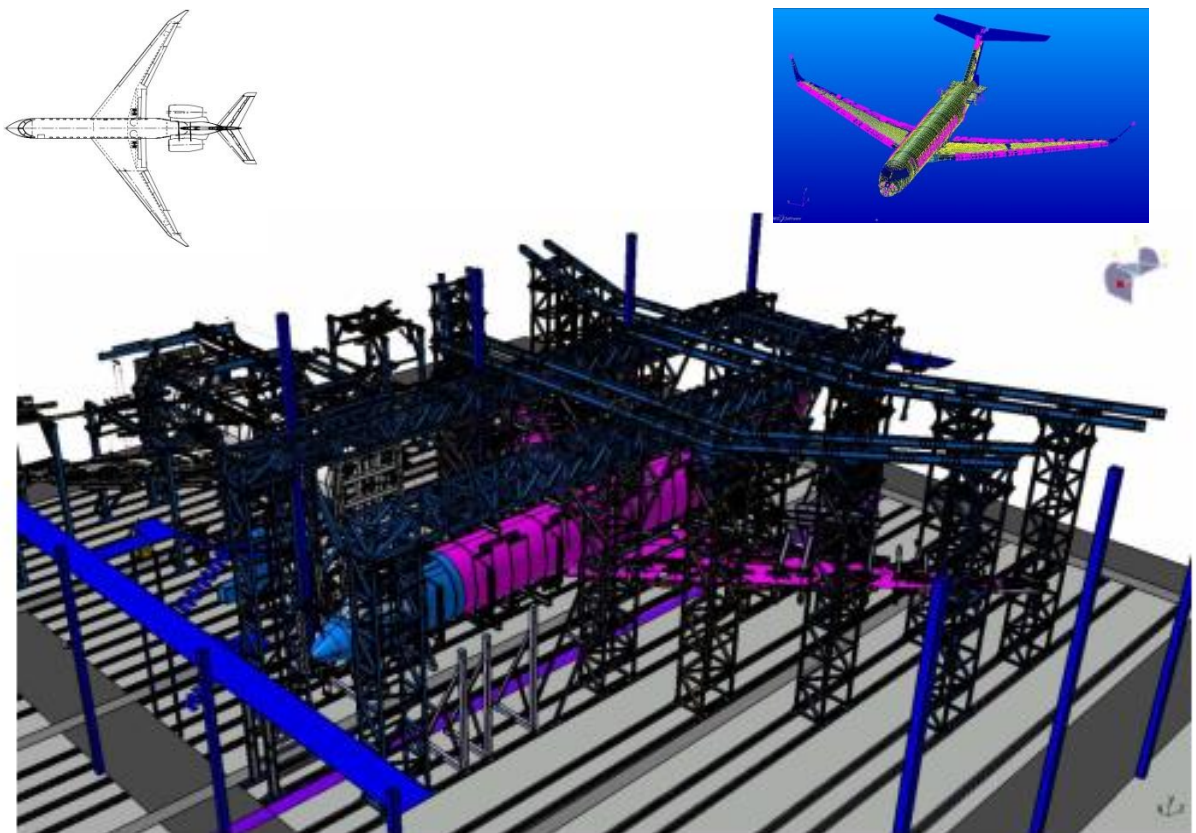


**Figure 2 Overall setup of the Global 7500 complete aircraft DADT test**

The aircraft structure will be subjected to a total of 51,000 flight cycles, which represent three times the Design Service Goal (DSG) of the aircraft. The test program is divided into 3 phases of testing and a final phase for teardown inspection:

1. Phase 1 – Durability testing: Two DSG of flight cycles (34,000 total flights) will be applied to the test article which includes typical manufacturing and in-service damage and repairs (completed).
2. Phase 2 – Damage Tolerance Testing: One DSG of flight cycles (17,000 flights for a total accumulated count of 51,000 flights) will be applied to the test article with the presence of artificial damage at specific primary structural element (PSE) locations.
3. Phase 3 – Residual Strength Testing: A series of residual strength tests will be applied to the test article to demonstrate the structural integrity of standard repairs, confirm the critical crack lengths of the Damage Tolerance Analysis and demonstrate freedom from Widespread Fatigue Damage (WFD).
4. Phase 4 – Teardown inspection.

Close-ups of the wing and fuselage tests are shown in Figure 3 and Figure 4 respectively.

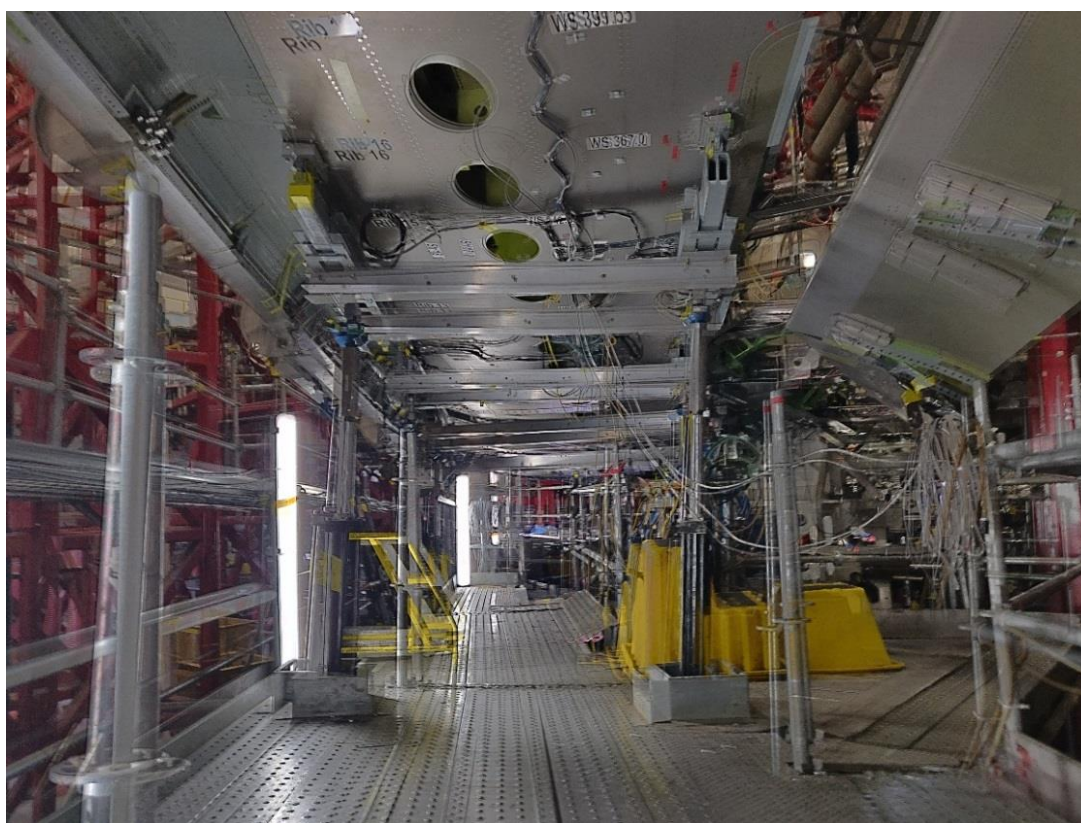


**Figure 3 Close-up of wing test setup**



**Figure 4 Close-up of fuselage test setup**

Three missions with four flight types are applied to the test article. These missions were reduced and truncated to an equivalent of 199 end points, on average, per flight. Number of cycles required for Entry-Into-Service (EIS) was reached at end of Dec 2017. It completed two (2) lifetimes (34,000 flights) of cycling in February 2019.

In addition, there are multiple Durability and Damage Tolerance (DADT) Bench Tests for components not covered on the Complete Aircraft DADT Test. Table 1 contains a list of the main rigs. These bench tests had been currently tested for 51,000 flight cycles and follow the same testing program as the Complete Aircraft DADT Test.

Both Inboard and Outboard flap Durability and Damage Tolerance Tests are performed at BAEX in Montreal, Canada, shown in Figure 5 and Figure 6. Both flaps are moving to various deployment angles during flight-by-flight spectrum to more accurately match interface loads.

**Table 1 List of subsequent metallic test rigs**

TEST RIG (Metallic)
ENGINE MOUNTS (FWD AND AFT) AND THRUST FITTING DADT TESTS
SECONDARY HSTA FITTING DT TEST
ELEVATOR METALLIC COMPONENTS AND REAR SPAR FITTINGS DADT TEST
RUDDER METALLIC DADT TEST
INBOARD FLAP DADT TEST
OUTBOARD FLAP DADT TEST
SLAT DADT TEST
AILERON METALLIC PARTS DADT TEST
SPOILER DADT TEST
WINGLET ROOT JOINT DADT TEST

**Figure 5 Inboard flap test rig**



**Figure 6 Outboard flap test rig**

As the Global 7500 structure is fabricated utilizing various metal alloys as well as Carbon Fiber Reinforced Plastic (CFRP) for its primary structure, other test rigs are being used to evaluate the durability and damage tolerance characteristics of the composite structures. These rigs are following a different testing program. A list of the main test rigs is provided in Table 2.

**Table 2 List of composite test rigs**

TEST RIG (Composite)
AILERON STATIC AND COMPOSITE DADT TEST
ELEVATOR STATIC AND COMPOSITE DADT TEST
RUDDER STATIC AND COMPOSITE DADT TEST
HORIZONTAL STABILIZER AND HSTA ATTACHMENTS STATIC AND COMPOSITE DADT TEST



In anticipation of this aggressive testing milestone, the Bombardier test team employed several new techniques to the full scale test that had not been applied in previous Bombardier fatigue tests. The intent of these extensive preparations was to reduce the amount of ‘on-rig’ learning curve time that was required to reach the optimum performance of the DADT test hardware, such that the schedule risk during commissioning could be minimized. A technical liaison from the National Research Council Canada (NRC) was also on-site prior to and during commissioning activities to support Bombardier’s efforts.

These techniques included: judicious data-informed hydraulic and pneumatic hardware selections; informed design choices to minimize mass and actuator count; hydraulic and load controller training and procedure generation on a dedicated independent test platform; extensive hardware-in-the-loop tuning to maximize performance; and using the global finite element model (GFEM) of the test article, coupled with a simple pneumatic model to better estimate test load transition times. An image of the test setup is shown in Figure 8.



**Figure 8 Global 7500 DADTT test setup (view AFT on LHS)**

These techniques were successfully employed to meet the required certification target schedule, and surpassed the original estimate, as shown in Figure 9. A more fulsome explanation of these techniques is included in a paper in the ICAF2019 conference proceedings [1].

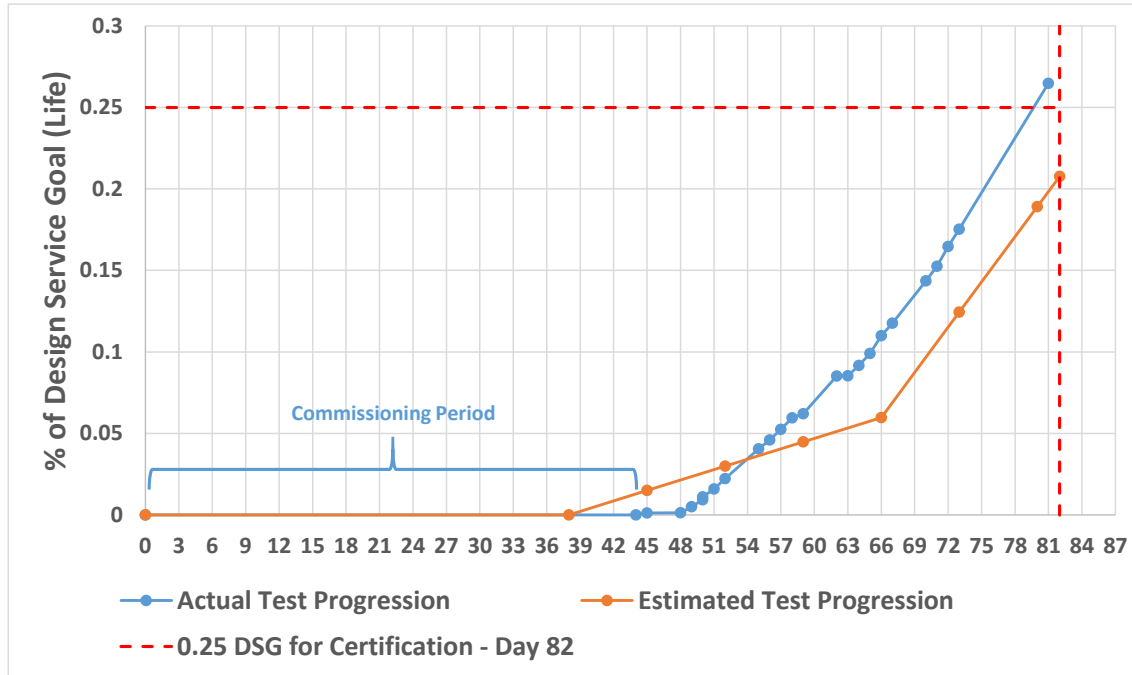


Figure 9 Global 7500 test schedule to certification milestone

### 2.2.1 REFERENCES

- [1] C. A. Beltempo, A. Beaudoin, R. Pothier, “Bombardier Global 7500 Fatigue Test Cycle Rate Commissioning to ¼ Life”, The 30th International Committee on Aeronautical Fatigue and Structural Integrity (ICAF) Symposium, June 2-7, Krakow, Poland, 2019.

## 2.3 F/A-18 FTS2 Armasuisse Horizontal Stabilator Fatigue Test (NRC/armasuisse/RUAG)

R.S. Rutledge, NRC Aerospace

The National Research Council Canada (NRC) completed a fatigue test for the Swiss Air Force (SAF) to evaluate an F/A-18 horizontal stabilator under Swiss Air Force usage. The test was a fatigue durability test of a United States Navy (USN) horizontal stabilator (H-stab), serial number (S/N) A20 2970P test article, using an in-service SAF fatigue test spectrum. To be consistent with previous armasuisse F/A-18 structural test designations, the test article is referred to as the Fatigue Test Swiss 2 (FTS2) H-stab. The FTS2 H-stab test article was manufactured with a 3.1 PCF (pounds per cubic foot) aluminium core and is consistent with the armasuisse fleet configuration.

The NRC Aerospace Research Centre used the same test rig that was used to test the Royal Canadian Air Force (RCAF) H-stab, designated FT905, to fatigue test the armasuisse test article to extend its original certified life. The test setup is shown in Figure 10.



**Figure 10 FTS2 test article with optical marker tracking at actuator locations**

The original plan was to test to 120% of the original certification life, i.e., a life extension of 20% additional usage. However, by the end of testing NRC had applied 144% of the original certification life. Since the Swiss loading spectrum was three times more severe than the RCAF spectrum, depending on which critical location is being evaluated, the Swiss test had a Service Goal (SG) that was much more severe than the RCAF H-stab test completed previously. To illustrate the increased severity between the two spectra, the sum of actuator distance travelled by each actuator during each block is shown in Figure 11.

For the FTS2 test, the loading was introduced using 14 hydraulic actuators, all attached at the bottom surface of a left hand side (LHS) H-stab, as shown in Figure 12. All actuators were at the same locations and whiffle tree configurations as the RCAF test. The test involved a strain survey pre-test and the application of a total of six lifetimes of armasuisse fatigue/durability cycling on the H-stab. All loads were applied on the in-service component to prove that existing component damages and armasuisse magnitude loads will not compromise the required H-stab performance during its desired service life.

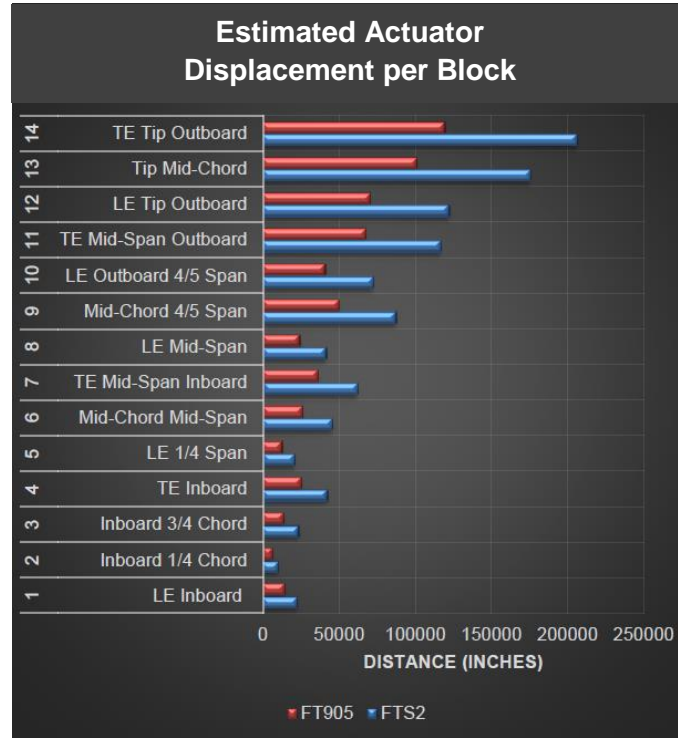


**Figure 11 Fatigue testing actuator travel displacement, a comparison between FT905 (RCAF) and FTS2 (SAF)**

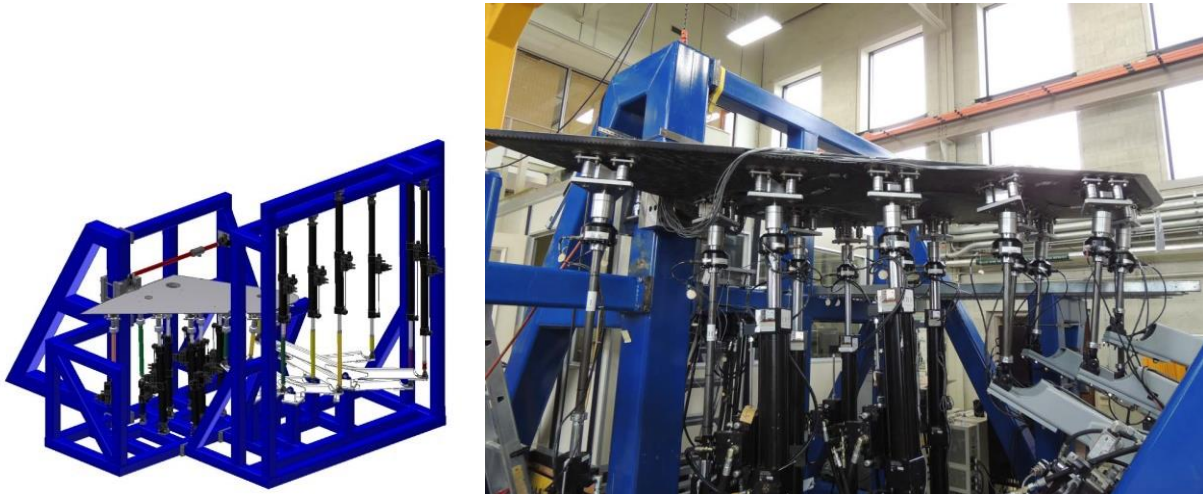


**Figure 12 Fatigue testing FTS2 test configuration**

Testing was carried out at the NRC Structural Integrity Laboratory, building M-14, located at the NRC Montreal Road Campus in Ottawa, Ontario and was completed in November 2018.

## 2.4 F/A-18 Aileron Fatigue Test (NRC/RCAF/L-3 MAS)

R.S. Rutledge, NRC Aerospace

The NRC Aerospace Research Centre completed fatigue durability, damage tolerance and residual strength testing for the Royal Canadian Air Force (RCAF) in 2018. The test was designated FT370 based on the aileron serial number (S/N) A18 0370 test article. The FT370 aileron test article contains aluminium core with pushed fasteners due to hinge modifications carried out during its usage. The intent was to test the durability and damage tolerance of the current configuration RCAF CF-188 aileron in order to extend its life to 133% of its original certification. The test article was made available to NRC by the RCAF and by the end of testing NRC had applied approximately 157% of its original certification on the component and 143% on the hinges that were modified.

NRC had an existing F/A-18 wing test rig that contained a test article that was used to evaluate structural health monitoring techniques. Since this test article had existing damages the wing was replaced and the rig was modified to accommodate the installation of an aileron with additional actuators. This specifically designed and built test rig was used to apply loads normal to the aileron and outer wing using 11 hydraulic actuators, all attached to the bottom surface of a right hand side (RHS) aileron, wing, outboard leading edge flap and dummy wing tip missile through a missile launcher. A picture of the test article in the test rig is shown in Figure 13.



**Figure 13 Aileron test (FT370) article and test rig**

The testing work included: a strain survey pre-test; and the application of five (5) lifetimes of fatigue cycling on the aileron. Note that the test article had 90% of its original fatigue life expended prior to test start. Testing on the in-service component was intended to prove that existing component configuration and damages will not develop to failure and that these damages can be found with the current maintenance procedures. During testing, NRC monitored the entire structure and carried out inspections. Periodic X-ray inspections were carried out at the pushed fastener locations that were created when the hinges were modified. An example of an X-ray inspection is shown in Figure 14.

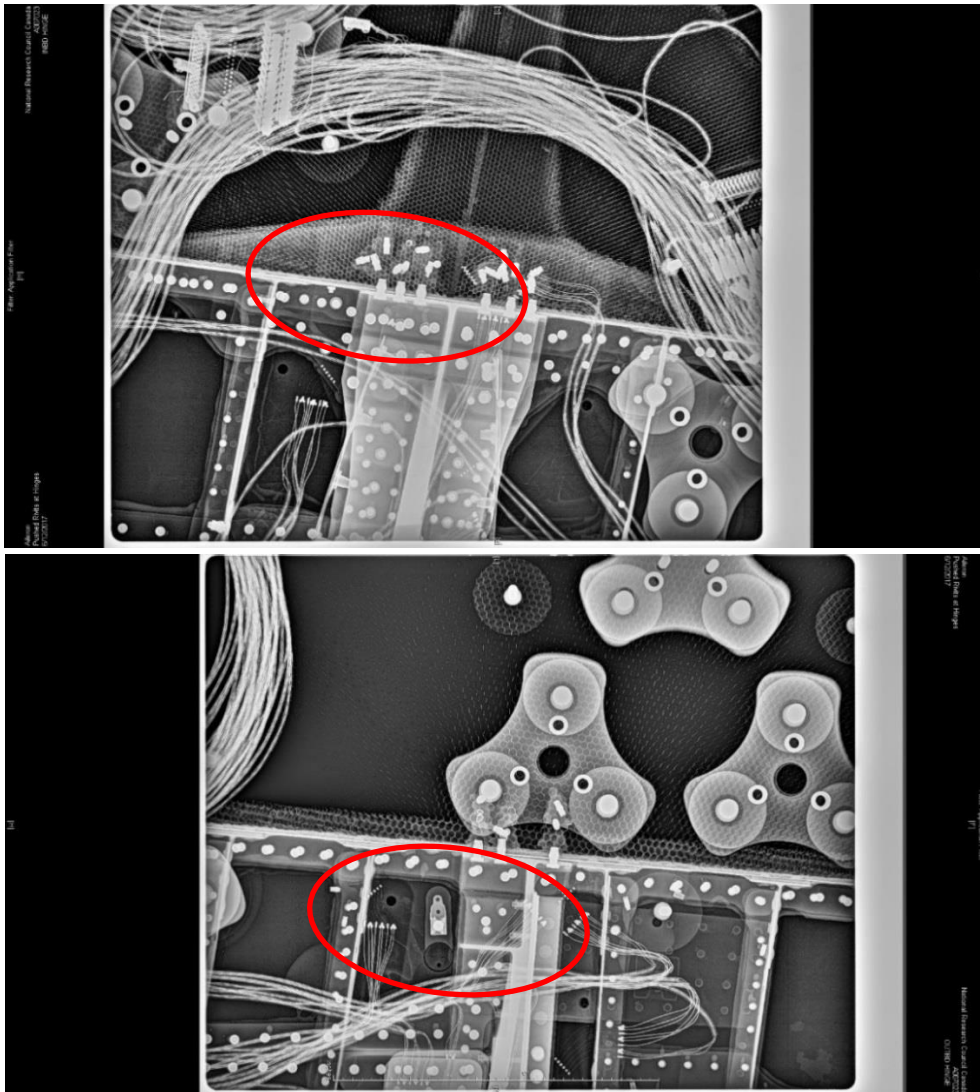


Figure 14 Aileron test (FT370) X-ray inspection showing pushed fastener locations

Following test load cycling, proof residual strength test (RST) loads were applied. Simulated original equipment manufacturing cases were applied to 120% design limit load (DLL). These load cases were re-applied to 133% DLL. Then an additional eight spectrum envelope load cases were applied with the highest load case applying an environmentally factored load case equivalent to 165% DLL. The proof load tests to 120% DLL provided experimental evidence that permanent detrimental deformations of the aileron should not occur during average normal operation, and the RST cases at the higher loads with the environmental factor proved that catastrophic component failure will not occur. NRC is now completing a teardown inspection of the aileron.

All testing was carried out at the Structural Integrity Laboratory, Building M-14, NRC Aerospace Research Centre, Montreal Road Campus in Ottawa, Ontario, Canada.

## **2.5 CF-188 Horizontal Stabilator Tear-Down Analysis Post Life Extension Fatigue Test**

C.A. Beltempo, R.S. Rutledge, NRC Aerospace

In 2015, the Royal Canadian Air Force (RCAF) contracted the National Research Council Canada (NRC) to conduct a life extension test of the CF-188 horizontal stabilator (H-stab) to support the extension of the Canadian CF-188 Estimated Life Expectancy (ELE). This test, referred to as FT905, was conducted in order to avoid costly and time consuming procurement of additional parts. The F/A-18 horizontal stabilator is composed of graphite / epoxy composite skins enclosing an aluminium honeycomb core. Test objectives included determining the durability of the aluminium core in the presence of substantial damage, investigating suitable inspection techniques for this type of damage, and determining suitable inspection intervals if required. The test consisted of five (5) lifetimes of durability cycling, followed by damage introduction, five lifetimes of damage tolerance testing, and then residual strength testing (RST), with the residual strength loads incorporating an environmental load factor to account for the service environment (for more details please refer to ICAF 2017 Proceedings, F-18 Flight Control Surface Life Extension Testing - CF-188 Horizontal Stabilator, C.A. Beltempo et al). Pulse flash thermography was found to be effective in characterizing honeycomb core damage, as shown in Figure 15, where induced damages in three (3) critical areas are presented.

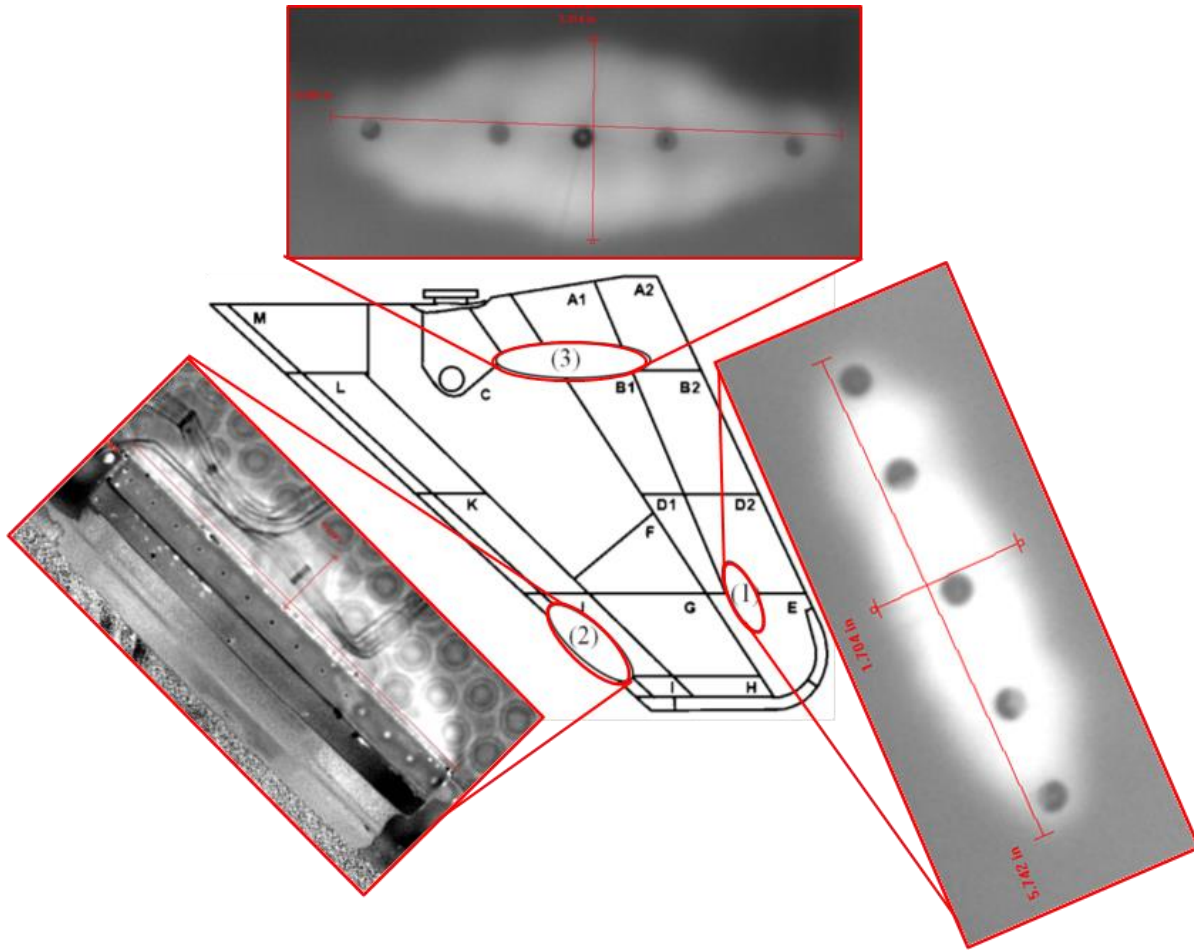


**Figure 15 CF-188 FT905 H-Stab Induced Damages taken by Pulse Flash Thermography**

During the test, periodic X-ray, through transmission ultrasonic C-scan, and pulse flash thermography inspections were carried out, but revealed no damage growth. The test was completed successfully in 2017, and the test article was sectioned in 2018 for post-test non-destructive inspection (NDI). The post-test NDI also did not reveal any damage growth of the induced damages, nor any indications that were not caused by loading system failures or were not already present in the test article. As a result of the NDI null findings during the test, the tear-down sectioning was primarily focused on the three (3) induced damage areas and a fourth area of concern near the tip, to determine whether the induced damages had grown via fatigue cycling. The initial sectioning of the part is shown in Figure 16.



**Figure 16 CF-188 FT905 H-Stab following initial sectioning for tear-down inspection**

The teardown inspection confirmed the NDI findings and also validated pulse flash thermography as an acceptable inspection technique for honeycomb core subsurface damage. The large damages introduced to the honeycomb core had not grown during the damage tolerance cycling of the FT905 test, nor had they changed during residual strength test (RST) load applications. A sample of a final section cut in the aft area is shown in Figure 17. As a result of the teardown inspection, the CF-188 H-stab was certified a life extension of 1.5 times the original certification, with a single comprehensive inspection at 2/3 of the new baseline lifetime usage.



**Figure 17 CF-188 FT905 H-Stab lengthwise section cut showing induced damage with no growth at edges**

## 2.6 Fatigue Structural Testing Enhancement Research (FASTER)

C. A Beltempo, NRC Aerospace

R. Fortune, J.R. Forbes, McGill University

NRC has a long and rich history of carrying out full-scale structural tests on fixed- and rotary-wing aircraft. These tests can be extremely complex from a control systems viewpoint, due to the large number of actuators and the many factors affecting the response of each actuator. In the past decades, the Structures and Materials Performance Laboratory (SMPL) at NRC has undertaken several efforts to improve the manner in which full-scale tests are conducted for our clients. This work ranges from developing reduced structural mass test loading systems to the development of cross-coupled compensation (CCC, or C3 used by MTS as a utility of MTS AeroPro™ Control and Data Acquisition Software ([http://www.mts.com/en/forceandmotion/aerospacetesting/MTS\\_4026296?article=1](http://www.mts.com/en/forceandmotion/aerospacetesting/MTS_4026296?article=1)) technology to obtain higher performance and faster test speeds. Further efforts are on-going to continue to develop the NRC advanced control technologies to improve how full-scale structural tests are run.

The Structural Integrity group at NRC-SMPL had a test rig setup for experimental purposes, shown in Figure 18. This test set up was based on a need to apply bending and torsion loading to a structure for previous Structural Health Monitoring (SHM) sensor and algorithm development. The set up consisted of two (2) identical cantilevered beams on which two (2) actuators were mounted at each end, in order to apply bending and torsion loads to the testing structure in the middle (Figure 18). NRC has recently engaged in a research project in collaboration with McGill University to conduct a variety of control system trials in order to better understand the control problem. The project centered around various activities, including methods for proportional-integral (PI) gain estimation, investigating System Identification approaches to accurately predict plant (complete system) dynamics, developing both single-input single-output (SISO) and multiple-input multiple-output (MIMO) dynamic feedforward (DFF) controllers based on identified plant models, and finally implementing H-infinity controller synthesis methods to assess their performance for force-controlled fatigue test. Although these methods require substantial additional knowledge, preliminary results indicate the application of DFF or H-infinity methods, or a combination of the two, yield lower errors and potential increases in test cycling rate. The preliminary results were also submitted to the proceedings of the 21st International Federation of Automatic Control (IFAC) Symposium on Automatic Control in Aerospace, (ACA 2019) [2]

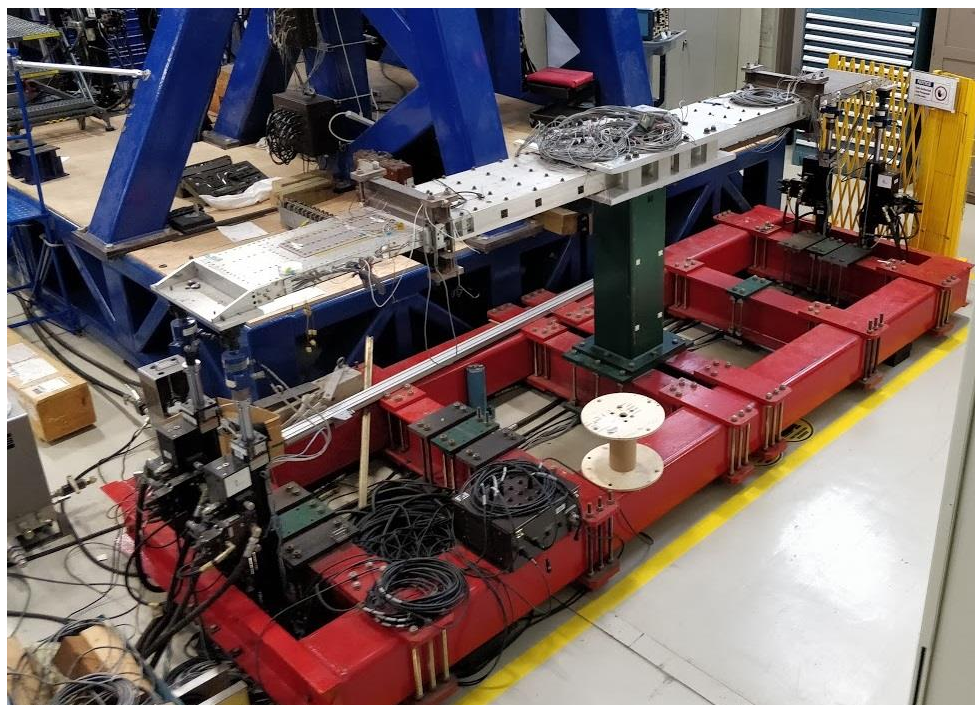


**Figure 18 Test rig setup for FASTER structural fatigue testing research**

### 2.6.1 REFERENCES

- [2] R. Fortune, C. A. Beltempo, James Richard Forbes, System Identification and Feedforward Control of a Fatigue Structural Testing Rig: The Single Actuator Case, submitted to 21st International Federation of Automatic Control (IFAC) Symposium on Automatic Control in Aerospace, Submitted for Review, March 2019.

## 2.7 Structural Analysis for CH-146 Air Transportation Kit Pallet Assembly

G. Qi, G. Li, G. Renaud, J. Rogers, and R. Amos, NRC Aerospace

As a utility tactical transport helicopter, the versatile CH-146 Griffon is used by the Royal Canadian Air Force (RCAF) in a wide variety of missions, such as troop transport, search and rescue, casualty evacuation, and humanitarian relief operations both at home and abroad. In practice, the CH-146s sometimes have to be loaded on a large CC-177 Globemaster III to meet the mission requirements. However, the current CH-146 design is not supportive to this operation, because:

- (1) In order to be loaded into a CC-177, the main rotor of the helicopter must be removed and a flight test is required after it is re-installed, which delays the time the CH-146 becomes available;

- (2) The CC-177 must stay on the ground for a long period of time, waiting for the CH-146 to be loaded and tied down to it. This process is very labour intensive and prone to damage the aircraft by overloading one of the many attachment lugs; and
- (3) Each time only three CH-146s can be loaded into a CC-177.

To improve this operation, the National Research Council Canada (NRC) is currently developing a Palletized Griffon-Air Transportation Kit (PG-ATK). The proposed PG-ATK will be used to load a CH-146 with the main rotor attached into a CC-177. This kit allows transportation of the helicopter without rotor removal, rotor re-installation and a follow-up flight test. The current tedious tie-down process in the CC-177 will be eliminated by pre-mounting the helicopters to a PG-ATK pallet assembly. Thus a CH-146 can be quickly loaded in a CC-177, allowing a rapid turnaround. Furthermore, the PG-ATK will also enable the RCAF to load four helicopters into a CC-177. Therefore, the PG-ATK system can significantly improve the operational efficiency and reliability, and thus have great impact on the future CH-146 Griffon mission capabilities.

As the key component of the PG-ATK system, the pallet support structure assembly must meet all the strength, stiffness and weight requirements, while ensuring the structural integrity of the entire aircraft system. Therefore, a detailed structural analysis is mandatory. Based on the NASTRAN linear elastic finite element (FE) analyses of two preliminary designs, the current analysis is being conducted using ABAQUS/Standard to continually support the on-going design improvement (a prototype of the design is shown in Figure 19). The latest analysis includes elastic-plastic material properties and comprehensive part interactions (see Table 3) to present precisely the load paths and achieve sufficiently accurate stress solutions at all critical locations. A finite element mesh of the pallet support structure assembly is shown in Figure 20. In addition, the fastener related strengths were examined, which are the crucial considerations for the design configuration. Based on the analysis results, a refined design is being carried out.

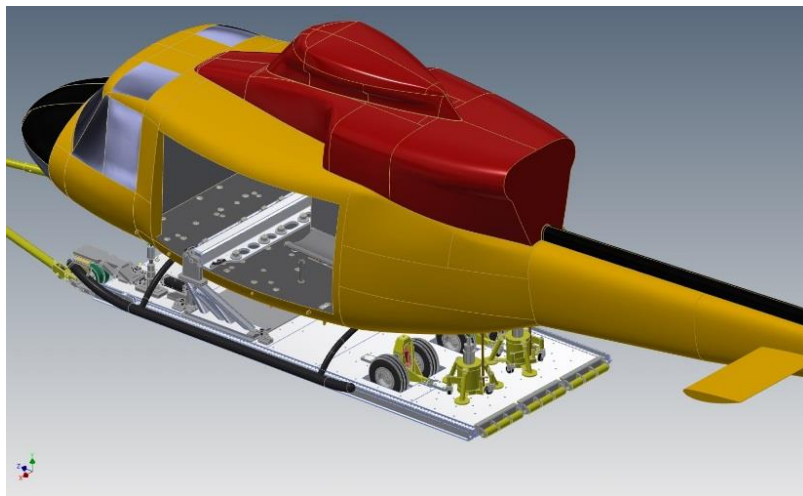


**Figure 19 A prototype of the PG-ATK system**

**Table 3 Pallet FE model assembly interactions**

Category	FE model Assembly Interactions	Subtotal	In total
<b>Coupling</b>	Fastener points (25+13) with fastener holes	53	57
	Aft-Block hole, Fwd-Block hole	2	
	Aft-Lug hole, Fwd Lug hole	2	
<b>Contact</b>	Plate to Aft-Block	1	7
	Plate to Fwd-Block	1	
	Plate to Left-Block	1	
	Plate to Support Assembly	1	
	Support Assembly to Left-Block	1	
	Support Assembly to Aft-Block	1	
	Support Assembly to Fwd-Block	1	
<b>Tie Constraint</b>	Support Assembly tie to Aft-Lug	1	2
	Support Assembly tie to Fwd-Lug	1	
<b>Connector</b>	Loads point with Fasteners (Beam Connector)	13	15
	Aft-Block with Aft-Lug (Hinge Connector)	1	
	Fwd-Block with Fwd-Lug (Hinge Connector)	1	

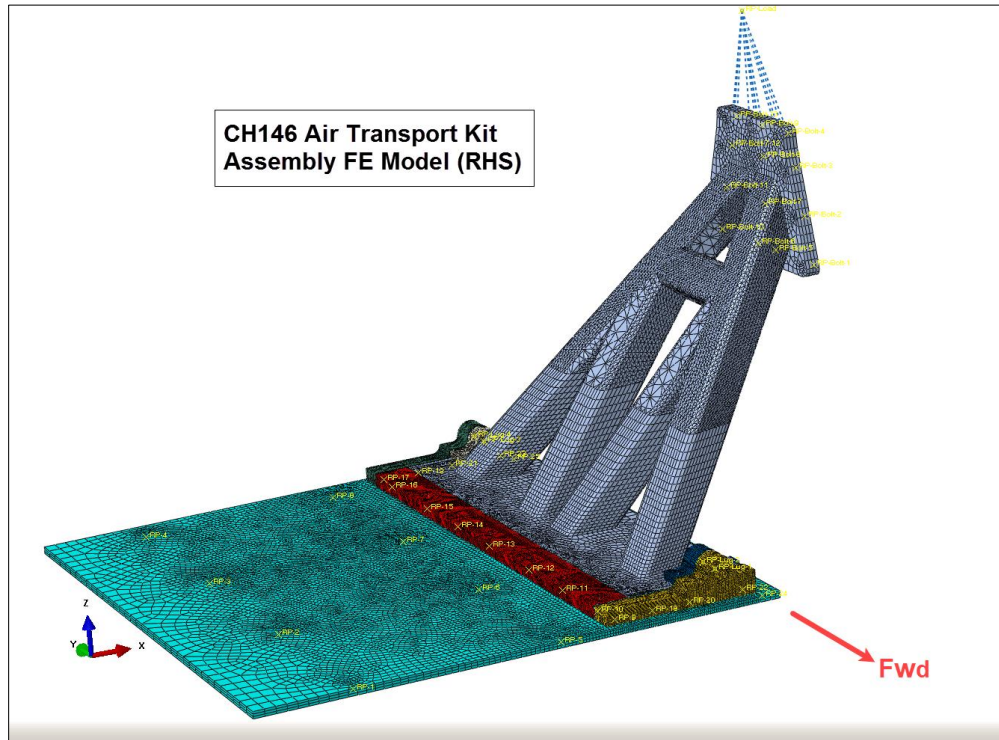


**Figure 20 A finite element mesh of the pallet support structure assembly, right hand side (RHS)**

## **3.0 FATIGUE LIFE ASSESSMENT AND MANAGEMENT**

### **3.1 CP-140 (P-3) 7249 Damage Tolerance Analysis (DTA) Updates**

A.M. Brown, IMP Aerospace

The Canadian CP-140 Aurora (Figure 21), a variant of the P-3 Orion, is completing a fleet mid-life upgrade in the form of the Aurora Structural Life Extension Program (ASLEP). The ASLEP replaces the wings and horizontal stabilizers (H-Stab) on the aircraft and includes design changes intended to address fatigue-prone areas, as identified through previous service experience. In addition to the design changes, the former stress corrosion cracking (SCC)-susceptible 7075-T651 wing and H-Stab material has been replaced by the SCC resistant 7249-T76511. This material change should greatly reduce the occurrences of SCC on the wing and H-Stab and addresses a significant issue with the previous material (7075).

With the material and design changes, it was necessary to update the DTA for all of the tracked structurally significant items (SSI) on the aircraft. This DTA is conducted in combination with individual aircraft tracking (IAT) to support structural usage monitoring and maintenance on the fleet. Aircraft usage is recorded via strain gauges installed on the wings and H-Stab.

FASTRAN is the tool used to perform SSI crack growth predictions on the CP-140 fleet and requires calibration to the applied spectrum. For this it was necessary to perform a series of 7249 coupon tests with representative spectra. Some of the tests were completed at the National Research Council Canada (NRC). The FASTRAN re-calibration efforts showed that 7249-T76511 was much less sensitive to retardation than 7075-T651. This characteristic was not observed until the spectrum coupon testing for the CP-140 was performed, since prior to this, all data were from constant amplitude tests. The sensitivity to retardation resulted in a reduction in inspection intervals for some critical SSI by approximately 50%.

To help counteract the reduced 7249 SSI inspection intervals, additional crack growth paths were added where possible, and beta factors were refined through the use of finite element modelling (FEM).

Further characterization of the material was performed by NRC through fracture toughness testing. Testing results from NRC correlated with earlier fracture toughness results produced by Netherlands Aerospace Laboratory (NLR) that were considered strange. It was found that, for the limited number of thicknesses tested, the fracture toughness of 7249 increased with thickness. This is counter to the behaviour of 7075. However, with correlation of the results from the two independent organizations (NRC and NLR), the 7249 fracture toughness results were incorporated into the updated CP-140 SSI DTA.

While corrosion is much less of a concern on the new wings and H-Stab, efforts are ongoing to mitigate the reduced SSI inspection intervals as a result of the switch from 7075-T651 to 7249-T76511. These include the incorporation of cold-working residual stresses in the DTA as well as the development of non-invasive NDI techniques that could be used on a more frequent basis (e.g. non-invasive inspection every depot versus invasive inspection every 2nd or 3rd depot).



Figure 21 CP-140 Aurora (<http://www.rcf-arc.forces.gc.ca/en/aircraft-current/cp-140.page>)

### **3.2 CF-188 Aircraft Structural Integrity Program (ASIP) and Aircraft Life Extension (ALEX) Program**

L-3 Communications (Canada) Military Aircraft Services (L3 MAS)

L3 MAS, a wholly owned subsidiary of L3 Technologies, is among Canada's leading In-Service Support (ISS) integrator, offering military and commercial customers a full range of modifications and sustainment solutions, in support of their aircraft and ship fleets. L3 MAS employs over 900 people in its main facility in Mirabel, Quebec and in other operating centers throughout Canada (Bagotville, Cold Lake, Halifax, Shearwater, Comox, Pat Bay, Greenwood, Gatineau, Ottawa, Toronto, Trenton and Petawawa).

Since 1986, L3 MAS performs the in-service support of the Royal Canadian Air Forces (RCAF) CF-188 (Boeing F/A-18) fleet as part of System Engineering Support Contract (SESC). This contract includes the conduct of all aspects of the Aircraft Structural Integrity Program (ASIP) and of related depot level structural maintenance. L3 MAS also fulfils similar roles in support of the CT-114 (Canadair CL-41) Tutor aircraft, a fleet that the RCAF currently employ for their Snowbirds aerobatic team and the CC-150 Polaris aircraft (Airbus A310). As a key partner to Lockheed Martin in the Maritime Helicopter Program (MHP), L3 MAS also performs ASIP functions on the CH-148 (Sikorsky S-92) helicopter. L3 MAS also provides engineering services to international F/A-18 operators such as the US Navy, armasuisse and Finnish Air Force.

L3 MAS conducts a full-fledged ASIP program on the CF-188 fleet on behalf of the RCAF. Above and beyond usage and structural condition monitoring activities mandated by MIL-STD-1530, the program has effectively extended the life of the aircraft by approximately 50% via the life extension program (ALEX). ALEX is comprised of over 250 items total, approximately 60% of which has been executed at depot (third line) level of maintenance in Mirabel, in three major phases. The last phase, control point phase 3 (CP3), is in production since 2012. The rest of the ALEX program is synchronized with the periodic maintenance, which occurs at every 600 airframe hours and is executed primarily at the base, as far as inspections and modifications are concerned. Some of the corrective maintenance, primarily on wing components and flight control surfaces, entails re-induction at depot, on a case-by-case basis and, exceptionally, mobile repair parties or fly-in into third line (depot) when the fuselage is affected.

The fatigue life of the airframe is managed primarily via the Fatigue Life Expended Index (FLEI) (computed at the wing root) as part of the Individual Aircraft Tracking (IAT) program. Other areas on the airframe are certified with higher scatter factors to account for other load influences that are not tracked by the wing root index and/or dynamic loading. The so-called Tracking Factor is embedded in the lifing in order to obtain a similar level of safety for all areas of the aircraft. Landing gear components are managed via manoeuvre counts (essentially landings and retraction cycles) and flight control surfaces are managed by component cumulative flight hours (CFH).

### **3.2.1 ELE EXTENSION AND NEW BOS INITIATIVE**

In 2017, the RCAF has expressed the need to extend the Baseline life of the CF-188 to support an Estimated Life Expectancy (ELE) up to the 2030-2032 timeline. This has induced an increase of 8% in the wing root FLEI limit to accommodate fleet leaders and similar increases in the required number of airframe hours and landings, compared to previous ELE scenario which was 2025-2030. In parallel, the RCAF is also acquiring 18 aircraft from the Royal Australian Air Force (RAAF) in order to reduce the yearly flying rates (YFR) on the current fleet and to meet increasing operational requirement inside the country and to fulfil its obligations with NATO and NORAD. L3 MAS is

currently assisting the RCAF to assess and increase the fatigue life of these aircraft which were initially planned for an early retirement as part of the RAAF fleet.

In the effort to re-assess all critical areas (over 1,000 locations with potential fatigue issues at the onset) in support of the 8% FLEI increase and to cover the usage characterization of selected critical locations by L-3 MAS, an automated, but also more refined, lifing and failure rate calculation methodology, based on the New Baseline Operational Spectrum (BOS), was developed. The New BOS is a multi-phase spectrum derived from actual fleet usage, developed in the late 2000s, and it differs significantly from the original BOS that was developed and used during the follow-on testing efforts in the 1990s. This new approach uses the New BOS multiple phases, representative of distinct usage periods, to properly characterize the cumulated fatigue damage at specific locations and to obtain projected trends. Given the current life extension scenario, the New BOS showed that while for some locations, the loading seems to be less severe than anticipated, other locations seem to accumulate fatigue damage faster than expected with the original BOS, locations affected by Negative Nz (i.e. up to -3g) for example. The latter would affect the fatigue lives of locations such as wing spar upper flanges, fuselage lower longerons, etc. The impact of this finding on the life of the critical locations of the aircraft is currently under assessment.

### **3.2.2 FLIGHT CONTROL SURFACES (FCS) LIFE EXTENSION**

Up until the late 2000s, the Flight Control Surfaces (FCS) of the CF-188 had not been considered systematically and holistically as part of the Aircraft Structural Integrity Program (ASIP) effort. One of the key reasons is that FCS are easily swapped from one aircraft to another and that, as a result, preventive modifications or refurbishment are not tied directly to the ALEX CP1-CP2-CP3 framework.

The RCAF had previously adopted an interim position to use the OEM-recommended inspections at 6000 CFH, which provides an extension to 7000 CFH; however, even this effort is not adequate to meet RCAF fleet requirements. Supporting the fleet until an ELE of 2028-2032, with due consideration for non-repairable damages (primarily due to environmental induced damages on honeycomb core and/or bonded joints) and limited additional provisions for further extensions ELE, has led to a need to certify FCS for up to 9000 CFH.

Previously, a somewhat conservative assumption had been made that the FCS had to be certified to the original BOS. In reality, the New BOS, is less critical than the original BOS at the wing root and aircraft will be allowed to operate for up to 9000 to 10000 hours. Hence, the current plan is to certify FCS to the New BOS instead, for consistency.

The certification strategy is primarily based on full scale component testing of the horizontal stabilator (H-stab), the aileron, the inboard leading edge flap (ILEF) and the trailing edge flap

(TEF). L3 MAS and the National Research Council Canada (NRC), the test agency, are working in close collaboration on these programs. Further details are provided below:

- Horizontal Stabilator (H-stab) test

This quasi-static test had the objectives of evaluating the life of the honeycomb core (3.1 PCF (pounds per cubic foot) configuration) under repeated loading for 9000 CFH and also to demonstrate the damage tolerance capability with either fatigue damage or induced damage. The test started in March 2015 and cycled for 50,000 SFH (simulated flight hours) of fatigue cycling (including a 10,000 SFH of damage tolerance). Using a total scatter factor of 5, the test has shown a Safe Life Limit (SLL) of 10,000 CFH (50,000 SFH/5).

At the end of the fatigue cycling, the test article went successfully through a residual strength test (RST) during which it was submitted to a total RST factor of 120% Design Limit Load (DLL) with Environmental Factor (EF). Data gathered following the teardown of the test was used to certify the critical locations on the H-stab.

- Aileron test

Similar to the H-stab, the quasi-static aileron test has the objectives of evaluating the life of both aileron attachment hinges and the surrounding honeycomb core under repeated loading for 9,000 CFH and also to demonstrate the damage tolerance capability with core induced damage during maintenance. The test has successfully completed fatigue cycling (41,728 SFH), residual strength test (RST) and ultimate static test. Data gathered following the teardown of the test was used to certify the critical locations on the aileron. More test setup and details can be found in Section 2.4 in this National Review.

- Trailing edge flap test

Similar to the aileron, the Trailing Edge Flap (TEF) attachment hinges do not meet the ELE target of 9000 CFH. Due to the urgency of certifying these hinges, two separate tests will be carried out in two different phases. Phase 1 is near test start and is aiming at certifying the life extension modifications of the outboard hinge (oversize, coldwork of lug hole, blend and shot peen surface area), while Phase 2 (a separate test) is aiming at certifying the OEM inboard hinge. Data gathered following the teardown of these tests will be used to certify the critical locations on both hinges.

- ILEF component fatigue test.

The ILEF fatigue life is assumed to be 7,000 CFH until a demonstration of a life extension to 9,000 CFH is done through a component test. The main objective of the test is to certify the life extension modifications (blend and shot peen) of the ILEF attachment transmission lugs to the wing. It is a quasi-static test, and both the test life target and test set-up are currently under evaluation. Once completed, the ILEF would be able to reach its required ELE.

### **3.3 F-18 Aircraft International Support**

L-3 Communications (Canada) Military Aircraft Services (L3 MAS)

Over the years, L3 MAS has performed several fatigue life assessments and/or development of modifications (and inspections) for other F/A-18 operators, namely the Royal Australian Air Force (RAAF), United States Navy (USN), armasuisse and the Finnish Air Force. The locations addressed via these efforts are often the same or similar in terms of configuration to those covered in the CF-188 Aircraft Life Extension Program (ALEX) program. The other key reason why these operators have come to L3 MAS for assistance is because of the unique capability that the company has developed for in-situ robotic applications, namely machining and shot peening. In 2017, L3 MAS reported herein on the comprehensive experimental program that it conducted on behalf of the USN on these types of robotic applications. In a similar fashion, coupon testing was also conducted recently at NRC, in support of fastener life improvement techniques.

#### **3.3.1 FASTENER LIFE IMPROVEMENT TECHNIQUES – COUPON TESTING**

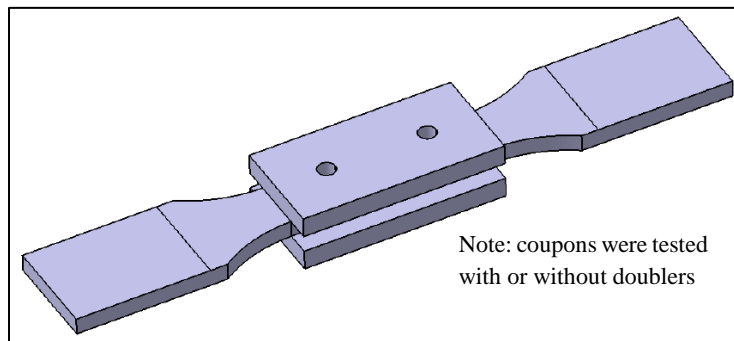
The fatigue performance resulting from the use of blind interference fit ground shank fasteners (I/F GS) were compared with that of legacy clearance fit blind fasteners with ring pad coining (RPC), that needed to be replaced, and with interference fit Hi-Lok fasteners (I/F HL) that can be used for locations that are accessible from both sides. These comparisons were required to assess retrofit modifications for which several fasteners had to be replaced and/or fastener holes had to be reworked, either for life improvement or for access purposes. However, the life improvement factor (LIF) of the I/F GS fasteners to be installed was limited by the fleet operator to 2.0. This suggested that the analytical crack initiation (CI) life benefit that could be claimed from the use of these fasteners was lower than that of the RPC or I/F HL, which had an approved LIF of 3.0.

In cases where the local peak stress at the hole is more than 150% of the yield strength ( $1.5 \times F_{ty}$ ), the fleet operator was attributing a LIF of 1.0. However, this sudden shift from a LIF of 3.0 (or 2.0) to 1.0 when crossing the stress limitation was seen as arbitrary and not representative of the actual performance of these fastener systems. Further, assuming the same LIF before and after the modification appeared potentially un-conservative if the I/F GS fastener holes truly have a shorter life than that of the I/F HL or the RPC fasteners. For these reasons, a coupon test program was developed to evaluate the relative difference in LIF between the three fastener systems. The characteristics considered in this program are summarized in Table 4.

**Table 4 Parameters considered in fastener tests**

Characteristics	Test Values Considered
Material	Aluminium plate, 6-in thick
Stress level	1.5×Fty (93 ksi) and 2.0×Fty (124 ksi)
Hole diameter (in)	0.25
Surface finish	Etched
Targeted C/F	0.0015-0.0020”
Targeted I/F	0.0020-0.0025”
Pitch and e/D	6D and 1.5D
Stress state	Through and bearing loads: no- and high- load transfer
Grain direction	LT
Marker bands	Added in spectrum (bar code type)
Spectrum	Military Wing Root bending Moment spectrum
Spectrum truncation	30%

Twelve mandatory and two conditional series of seven coupons were defined to cover baseline cases (open holes) and fastener configurations with and without load transfer. Moreover, each coupon allowed life determination from two identical holes. The geometry of the fastener test coupons is illustrated in Figure 22.

**Figure 22 Geometry of fastener test coupons (with doublers).**

The results are shown in Table 5 (unfactored) and Table 6 (factored) below. The series with HL and load transfer was not conducted as being optional (to save test cost and duration). The results confirmed that the LIF associated with I/F GS is effectively lower than RPC and I/F HL. A very high scatter was observed for the I/F GS with no load transfer series, which generated a LIF as low as 2.06. However, as part of an on-going follow-on coupon test on fatigue damage removal, the same hole assembly was tested, but with an e/D (hole edge distance/hole diameter) of 1.77 (instead of 1.5) and showed a much smaller scatter (Log 10 std. dev.= 0.091) and a LIF of 4.37. This suggests that with e/D closer to blue print values, the GS LIF would perform much better.

This test program identified two interesting collateral findings. First, the LIF is not reduced when the stress level exceeds 1.5×Fty. In fact, it increases in all cases except for the RPC holes with load transfer. Secondly, the LIF on crack growth (CG) life is significant, and even higher than on CI life for the I/F GS and more or less than that of the CI life for other Life Improvement Techniques (LIT). Note that these coupons have an e/D of 1.5 only, so the CG being relatively short, is more affected by the LIT than if the plate would have been wider. Further testing/evaluation of these collateral findings is yet to be conducted.

**Table 5 Unfactored results**

Unfactored Lives (Log-Average / Median of lognormal fit)							Unfactored		
Group	Fastener	Load Transfer	Peak Stress	CI	Total	CG	LIF CI	LIF Tot	LIF CG
1A	Open hole	N/A	93	5033	9162	4028			
1B			124	1255	2570	1302			
2A	C/F blind + RPC	Yes	93	54547	81108	26109	10.84	8.85	6.48
2B			124	8606	21076	12345	6.86	8.20	9.48
2C		No	93	35741	52498	16489	7.10	5.73	4.09
2D			124	13574	22222	8073	10.81	8.65	6.20
3A	Hi-Loks	Yes	93						
3B			124						
3C		No	93	69147	122770	48874	13.74	13.40	12.13
3D			124	23238	37926	12313	18.51	14.75	9.46
4A	I/F blind	Yes	93	47179	114543	65728	9.37	12.50	16.32
4B			124	20284	44736	24287	16.16	17.40	18.65
4C		No	93	33632	61952	31321	6.68	6.76	7.77
4D			124	12856	25242	11720	10.24	9.82	9.00

**Table 6 Factored results**

Factored Lives (CDF = 1/1000 on lognormal fit)							Factored			
Group	Fastener	Load Transfer	Peak Stress	CI	Log10 std dev on CI	Total	CG	LIF CI	LIF Tot	LIF CG
1A	Open hole	N/A	93	3269	0.0613	7615	2137			
1B			124	882	0.0501	2359	935			
2A	C/F blind + RPC	Yes	93	32145	0.0751	46752	10847	9.83	6.14	5.08
2B			124	4814	0.0825	15546	8489	5.46	6.59	9.08
2C		No	93	25967	0.0454	44919	10334	7.94	5.90	4.84
2D			124	7783	0.0790	19239	2921	8.82	8.15	3.12
3A	Hi-Loks	Yes	93							
3B			124							
3C		No	93	17520	0.1949	46831	14593	5.36	6.15	6.83
3D			124	7290	0.1646	29967	3149	8.26	2.70	3.37
4A	I/F blind	Yes	93	10674	0.2110	29410	15217	3.27	3.86	7.12
4B			124	11263	0.0835	28382	14966	12.77	11.03	16.01
4C		No	93	6734	0.2265	20234	13303	2.06	2.66	6.23
4D			124	4695	0.1430	17447	6102	5.32	7.39	6.53

### 3.4 CT-114 (Tutor) Aircraft Structural Integrity Program (ASIP)

L-3 Communications (Canada) Military Aircraft Services (L3 MAS)

L3 MAS conducts a full-fledged ASIP program on the CT-114 fleet on behalf of the RCAF. Aircraft usage monitoring is achieved by collecting, evaluating and processing the Operational Loads Monitoring (OLM) system data. Periodically, collected aircraft usage data is validated and accumulated fatigue damage is calculated for major aircraft components. In addition, remaining life for every major aircraft component is calculated based on predicted aircraft usage by using the software tool GIFTS. The monitoring program findings and L3 MAS recommendations are reported to DND on a monthly basis.

L3 MAS was mandated to extend the service life of the Tutor fleet to 2030. This resulted in the review of teardown inspection results, identification of additional SSI requiring inspection/rework, electrical / mechanical systems obsolescence and the development of a fleet strategy to manage the rotation of service aircraft with those in storage in order to meet the new planned retirement date.

In addition, airworthiness risk assessments and damage tolerance analyses were performed on some locations identified from the review of teardown inspection results. L3 MAS recommendations resulted in new inspections, modification and repair development. Work is in-progress on the modification and repair development. DND is in-progress of reviewing its maintenance manual to incorporate the new inspections.



Figure 23 CT-114 Tutor (Snowbird, <http://www.rcaf-arc.forces.gc.ca/en/aircraft-current/ct-114.page>)

## **3.5 CC-150 Polaris Fleet In-Service Support and Fleet Management**

L-3 Communications (Canada) Military Aircraft Services (L3 MAS)

As part of the Polaris Program, L3 MAS is mandated to provide in-service support for the operations of the five CC-150 Polaris aircraft (Figure 24) (Airbus A310-304) of DND. L3 MAS develops and maintains an A310 maintenance schedule to satisfy 180 minutes Extended range Twin-engine Operations (ETOPS) and CC-150 specific modifications. L3 MAS also provides engineering support to satisfy Canadian Forces operational requirements and the configuration control of the CC-150 Polaris (A310 Airbus) fleet.

### **3.5.1 OBSOLESCENCE AND AGEING AIRCRAFT MANAGEMENT**

L3 MAS provides assistance for the management and resolution of technical challenges associated with maintaining ageing aircraft with diminishing manufacturing sources. L3 MAS is responsible to develop plans, forecast maintenance and engineering activities, and to provide advice on upcoming changes to Airworthiness regulatory framework that could affect the fleet, and medium/long term obsolescence issues affecting aircraft components and missions systems on both MRTT (Multiple Role Transport Tanker) and non-MRTT aircraft. Maintenance Monitoring Program - L3 MAS performs Reliability Monitoring based on Airworthiness Manual Advisory AMA 571.101/1 to monitor the effectiveness of the CC-150 maintenance program.

### **3.5.2 CC-150T MRTT MISSION MIX STUDY**

L3 MAS was mandated to perform an engineering study on CC-150 MRTT Mission Mix. Two out of five CC-150 aircraft were modified as Multi Role Transport Tanker by Airbus. As the structure and mission type of the A310 MRTT is different than the basic A310 aircraft, Airbus published a Supplemental Airworthiness Limitation Item (S-ALI) for all MRTT variances regarding this modification. Amongst documented differences, the S-ALI introduces an updated Limit of Validity (LOV) for the structural maintenance program and a specific flight profile limiting the expected mission mix distribution. Several actions were then required to allow continued operation of the fleet up to the current ELE of 2025/2026, they are:

- Confirmation of mission roles versus aircraft configuration;
- Review of CC-150T utilization to evaluate the impact of mission type on life expectancy;
- Mechanism set-up to track future utilization of MRTT (role and flight profile);
- Airbus assignment to obtain adjustment factors to evaluate the margins of operational MRTT aircraft life (life expended values per aircraft zone);
- MRTT maintenance program adjustment (mainly flight controls and engine mounts), and
- Structural components replacement to meet current fleet life expectancy.

### 3.5.3 CC-150 ESTIMATED LIFE EXPECTANCY (ELE) STUDY

The main purpose of this tasking was to help DND identify all technical activities required to maintain the CC-150 fleet up to the Estimated Life Expectancy (ELE). The scope was also to outline the technical impacts to be managed for various ELE scenarios (FY 25/26, FY 26/27 and FY 27/28) on the CC-150 platform (tanker and non-tanker).



Figure 24 CC-150 Polaris in tanker configuration (<http://www.rcfa-arc.forces.gc.ca/en/aircraft-current/cc-150.page>)

## 3.6 CH-148 Maritime Helicopter Aircraft Structural Integrity Program (ASIP)

L-3 Communications (Canada) Military Aircraft Services (L3 MAS)

As part of the Maritime Helicopter Program (MHP), L3 MAS is mandated to conduct an ASIP program on the S-92, designated as CH-148 by the RCAF. Usage monitoring is enabled via the S-92 Health and Usage Monitoring System (HUMS). The HUMS has the capability to recognize regimes/manoeuvres via recorded flight parameters and sensor data. This data is processed by the Usage Comparison and Reporting Tool (UCART) that computes fatigue damage rates at selected locations for each individual aircraft and compares them to the design spectrum according to the requirements of MIL-STD-1530.

In 2018, algorithms for fatigue damage rate derivation in UCART from the HUMS regime and event data were completed. Filtering of the captured regime data was implemented in order to provide realistic usage data and avoid multiple triggering of the regime recognition when aircraft is operating close to the defined thresholds. These filtering algorithms are currently validated and improved through flight testing.

The other major component of the CH-148 ASIP Program is the Structurally Significant Item (SSI) database. The SSI database records all the relevant information about each SSI, also known as Primary Structural Element (PSE), from the design phase and into the in-service phase in order to enable ASIP analysts to monitor structural damages and, when needed, recommend changes to the maintenance program or modifications to the helicopter.

Usage monitoring and structural condition monitoring are now well implemented and periodic reporting is now available. The captured usage data is compared with the design spectrum to identify any potential discrepancies.



**Figure 25 CH-148 Cyclone helicopter (<http://rcf-arc-images.forces.gc.ca/gallery/caf/detail/?filename=HS28-2016-0001-011&assetId=410>)**

### **3.7 Demonstration of an Airframe Digital Twin Framework using a CF-188 Component Test \***

G. Renaud, M. Liao, and Y. Bombardier, NRC Aerospace

\* Paper being presented at ICAF2019

The airframe digital twin (ADT) framework is a potential game-changing fleet management concept recently proposed by the United States Air Force (USAF) to allow proactive and cost-effective decisions on an individual aircraft basis. The National Research Council Canada (NRC) is currently demonstrating the ADT framework using a CF-188 full-scale component test to assess the adaptability of this approach for the Royal Canadian Air Force (RCAF) fleets [3].

The major advantage of the ADT approach is that it provides a probabilistic representation of individual aircraft tracking (IAT) and inspection data. However, the fact that some inputs, such as crack findings, are initially very scarce makes the determination of a probability of failure (POF) very challenging. The Bayesian inference method is therefore employed to address this shortcoming by updating prior modelling assumptions to increase the reliability of the predictions as new information becomes available, throughout the service life of the aircraft. An in-house analysis tool is being developed to perform quantitative risk assessment (QRA) based on the Bayesian inference method using individual aircraft tracking and non-destructive inspection data. The modular components of the ADT tool include load and crack size distribution updating, material initial discontinuity state, residual stress effects, load transfer functions, crack tip stress intensity factor calculations, and crack growth predictions. Development and validation of the modular components of the ADT analysis tool have already highlighted the benefits of Bayesian updating for realistic test cases that combined uncertain material initial states with scarce inspection results.

In parallel, NRC has developed a demonstration case, illustrated in Figure 26 that utilizes an ongoing CF-188 inboard leading edge (ILEF) full-scale life extension test to simulate a flying aircraft. The tested ILEF is a retired component from the RCAF with a repair history representative of the current fleet and the loading test spectrum is representative of current and future CF-188 fleet usage. The ILEF transmission lugs, the actual RCAF life limiting items, are the main focus of this full-scale component test and of the ADT demonstration. The objectives of the demonstration are to compare the ADT framework with the current lifing and fleet management practices, and to provide recommendations for the RCAF aircraft fleets.

Short-term benefits are expected from this demonstration for the improvement of existing RCAF fleet management. First, it allows for improving IAT system and data, with quantification of variability and correlation of IAT accuracy with risk. Second, it can improve fatigue life estimation

for more efficient structural life management. In a longer term, a higher return on investment could be possible, with benefits that include better decision-making, increased fleet availability, and reduced total ownership costs.

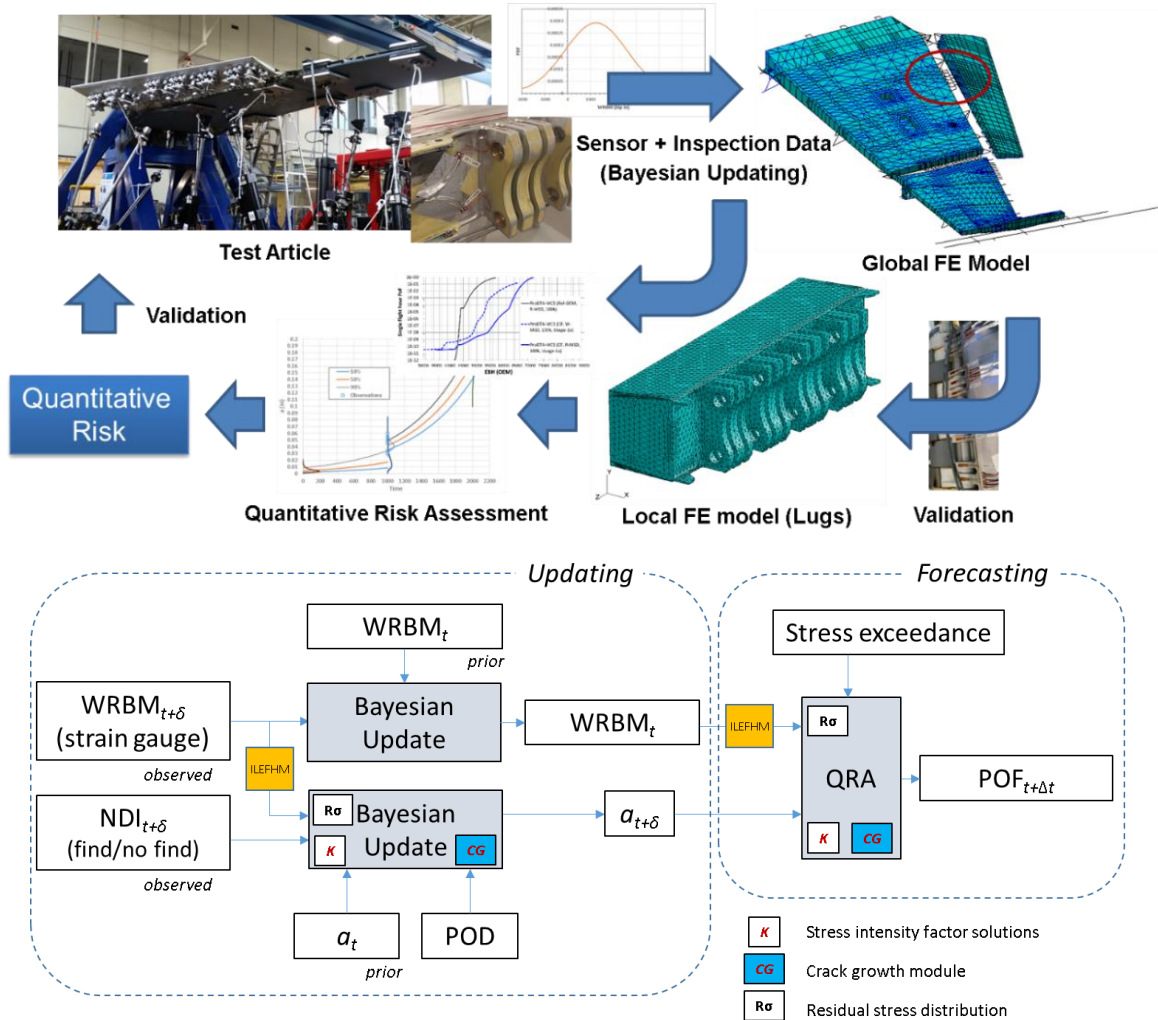


Figure 26 ADT framework demonstration using the CF-188 ILEF component test

### 3.7.1 REFERENCES

- [3] M. Liao, G. Renaud, and Y. Bombardier, “Airframe Digital Twin (ADT) Technology Adaptability Assessment and Technology Development Roadmap”, NRC Laboratory Technical Report, LTR-SMM-2018-0063, March 2018.
- [4] G. Renaud, M. Liao, and Y. Bombardier, “Demonstration of an Airframe Digital Twin Framework using a CF-188 Component Test”, Proceedings of the International Committee on Aeronautical Fatigue and Structural Integrity (ICAF 2019), Krakow, Poland, Jun 2019.

## 4.0 FATIGUE LIFE ENHANCEMENT TECHNOLOGIES

### 4.1 Shot peening to extend fatigue life of military aircraft

L-3 Communications (Canada) Military Aircraft Services (L3 MAS)

The shot peening of aluminium parts as a retrofit to extend fatigue life of military aircraft has already been used for about two decades in the Canadian aircraft industry. For the applications performed at L3 MAS, the required Life Improvement Factor (LIF) was generally not higher than 1.5. Based on limited coupon testing performed in the late 1990s, engineers were satisfied that manual application of shot peening with a 200% coverage would provide this level of LIF. More recently, robotic systems were developed to perform shot peening in-situ as a Life Improvement Technique (retrofit) to extend the aircraft service life (also see Section 3.3.1). For the more recent applications, the LIF requested from shot peening went up to 3.0.

In that context, a new coupon test program was required to certify that higher LIF target using the robotic system. The application involves Al 7050-T7451 plate, 6" thick with a variable amplitude spectrum (maximum R-ratio of approximately -0.3). The geometries are generally radii at the bottom of machined pockets with stress concentration Kts varying between 1.4 and 1.5 and stresses in vicinity of the yield point. Prior to the shot peening being applied at up to 80% of the baseline unfactored life of the critical hot spot, a light blend of 0.003" to 0.006" was carried out to remove some of the accumulated surface damage. Several test series were defined to address all bulkhead hot spot parameters that could affect the shot peening behaviour (ex. stress level, grain direction, geometry of the critical hot spot, etc.). The effect of performing this retrofit over a 0.015" deep crack was also verified. Besides this latter series, all test series showed LIF significantly above the requirement/expectations, as shown below in Figure 27.

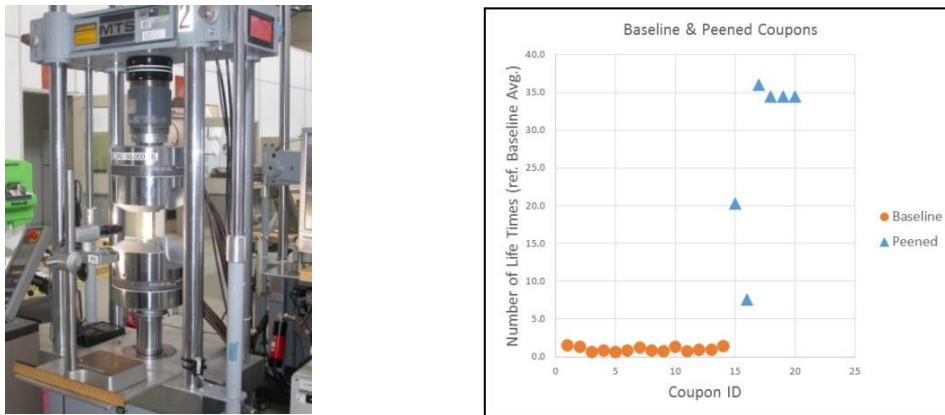


Figure 27 Recent test program at NRC on shot peening

## 4.2 Life Improvement Quantification of Fastener Modifications

G. Renaud and M. Liao, NRC Aerospace

P. Martin, L-3 Communications (Canada) Military Aircraft Services (L3 MAS)

A coupon test program is currently being carried out at NRC to certify fastener modifications that aim at extending the lives of military aircraft components that are short of revised usage goals [5]. The objective of this program is to determine if a life extension penalty should be considered when blind interference fit ground shank fasteners (I/F GS) were to be used instead of clearance fit blind fasteners with ring pad coining (RPC), or interference fit Hi-Lok (I/F HL) fasteners. Further, the life extension performance of these three fastener types are to be evaluated for highly loaded situations. The results obtained from 85 coupons, summarized in [5], suggest that, in general, the I/F GS fasteners do not provide as much life extension as the other two fastener types. Furthermore, contrary to current assumption from the fleet operator, the factored LIF is not reduced when the stress goes from  $1.5 \times F_{ty}$  up to  $2.0 \times F_{ty}$ . In this context, the crack initiation (CI) life is defined at the time to reach a 0.254 mm (0.01 inch) deep crack. A factored life improvement factor (LIF) is defined at the life ratio between the tested case and the equivalent open hole configuration, at a 1/1000 cumulative probability of crack initiation.

**Table 7 Fastener life improvement factor comparison**

Fastener Type	Load Transfer	Local Stress ( $\times F_{ty}$ )	Factored CI LIF	Scatter Factor
RPC	Yes	1.5	9.83	1.70
		2.0	5.46	1.79
	No	1.5	7.94	1.38
		2.0	8.82	1.74
I/F HL	No	1.5	5.36	3.95
		2.0	8.26	3.19
I/F GS	Yes	1.5	3.27	4.42
		2.0	12.77	1.80
	No	1.5	2.06	4.99
		2.0	5.32	2.74

Additional coupons (58) are currently being tested to quantify the effect of fatigue damage removal, for a nominal to next size fastener typical for these locations, and the effect of an I/F bushing modification. Results obtained to date suggest that hole oversizing resets the fatigue life.

### 4.2.1 REFERENCES

- [5] G. Renaud, P. P. Martin, and M. Liao, "Experimental Life Improvement Quantification of Shot Peening and Fastener Modifications", 12<sup>th</sup> International Fatigue Congress, May 27 – June 1 2018, Poitiers, France.

### 4.3 Hole Cold Expansion Process Plasticity Modelling

G. Renaud, G. Li, M. Liao, NRC Aerospace

Cold expansion (Cx) of fastener holes has been used for decades to enhance the fatigue lives of critical airframe structures. Although the benefits of this technology are undeniable, current requirements for structural life extension and inspection scheduling remain very stringent. Research at the National Research Council Canada (NRC) aims at developing physics-based analytical methodologies and tools to calculate life improvement factors from Cx residual stresses. As part of the international Engineered Residual Stress Implementation (ERSI) workgroup sponsored by the USAF, NRC is actively working for improving hole Cx process simulation to generate reliable residual stress distributions that can be used for accurate crack growth analysis. One of the recent focuses of the NRC effort was to characterize material properties of 2024-T351 plate material for Cx residual stress distributions measured experimentally by the contour method. The objective was to determine characteristics that are typically not included in Cx process models and assess their impacts on the predicted residual stresses. These characteristics include tension-compression behaviours, anisotropic hardening, and reverse yielding. Then, a thorough calibration was carried out to identify best practices for Cx process modelling using von Mises, Chaboche and Barlat plasticity models. For example, the stress-strain curves obtained in different directions for a  $\pm 1.5\%$  compression-tension strain cycle are presented in Figure 28 a), and a comparison of mid-thickness residual stress curves is presented in Figure 28 b). Overall, the best results were obtained when anisotropic properties were considered. Additional tests and calibration exercises, focusing on additional parameters, were proposed.

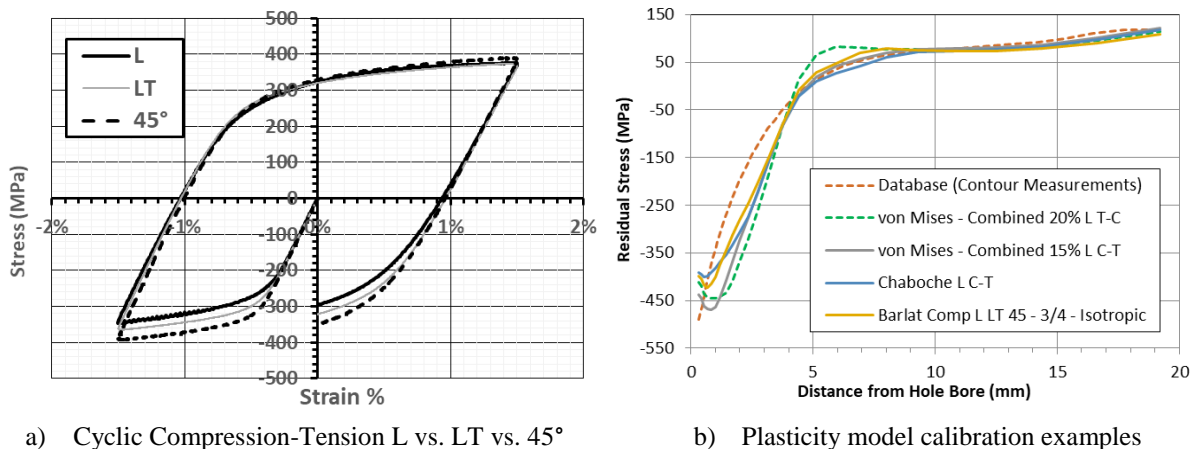


Figure 28 Hole cold expansion process modelling from material characterization

## 4.4 Measurement of Residual Stresses Resulting from Cold Expansion

D. Backman, G. Renaud, NRC Aerospace

In support of a research program focussed on incorporating residual stresses into finite element simulations of the cold expansion process, accurate experimental measurements of the residual stress field around cold expanded holes using X-ray diffraction (XRD) analysis was performed. The following two tasks were addressed in more detail:

- Determining X-ray elastic constant for 7075-T6 aluminium
- Residual stress measurements of cold expanded holes

To obtain the most accurate residual stress measurements possible, an initial investigation was undertaken to determine the correct X-ray elastic constant (XEC) for the material. The XEC is related to the elastic modulus, and is used to convert changes in the crystallographic lattice spacing (i.e., strain changes) into residual stress results. The changes in lattice spacing are analogous to the changes in displacement one measures using conventional strain measurement techniques, such as strain gauges.

For this test, a thin strip of 7075-T6 aluminium was instrumented with a conventional strain gauge on one face and centered in a four-point bend fixture. The four-point bend fixture was used to apply known displacements on the thin strip, for which strain was measured by strain gauges on one face and residual stress was measured by XRD on the other. The strain gauge reading was then converted into applied stress which is plotted against the XRD residual stress in Figure 29.

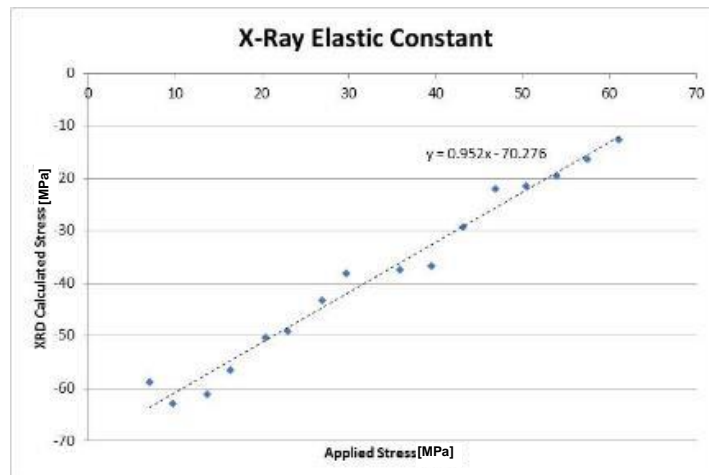
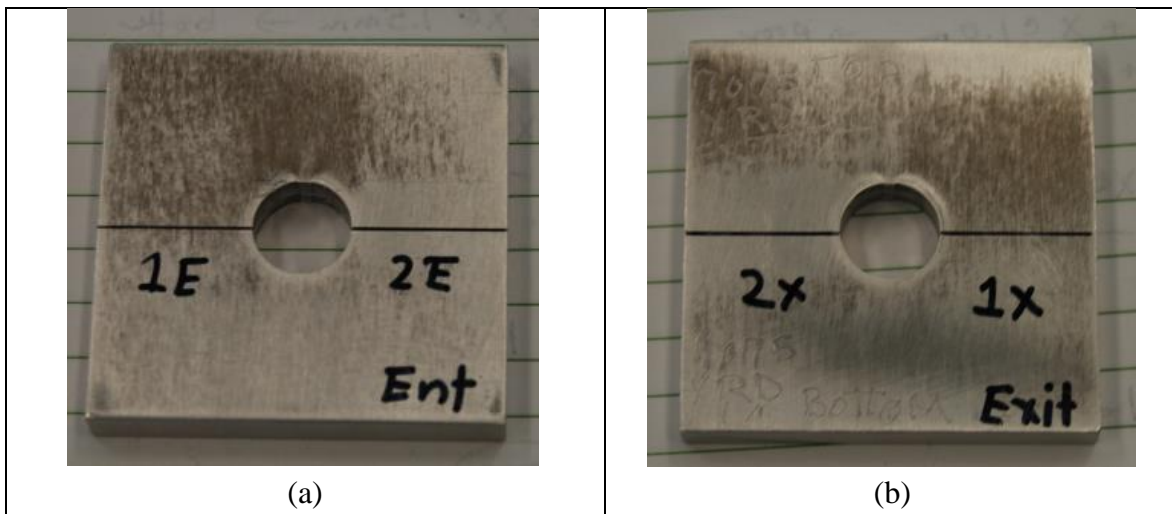


Figure 29 X-ray elastic constant determination

By determining the relationship between the mechanical Elastic Modulus and the estimated XEC, an XEC correction factor can be determined. From the initial XEC estimate for generic aluminium alloy of  $18.89 \times 10^{-6} \text{ MPa}^{-1}$ , a more refined determination of the XEC specifically for 7075-T6 was calculated as  $17.99 \times 10^{-6} \text{ MPa}^{-1}$ .

Two coupons were provided for XRD analysis, with each coupon having a central hole which had been cold expanded using standard FTI (Fatigue Technology Incorporated) tooling (16-1-N). The residual stress was measured on both the left and right sides of each hole (see Figure 30 and Figure 31) and on both the entry and exit faces. The dark line on Figure 30 denotes the region where XRD measurements were made.



**Figure 30 (a) Coupon H1 Entry face (b) Coupon L1 Exit face**

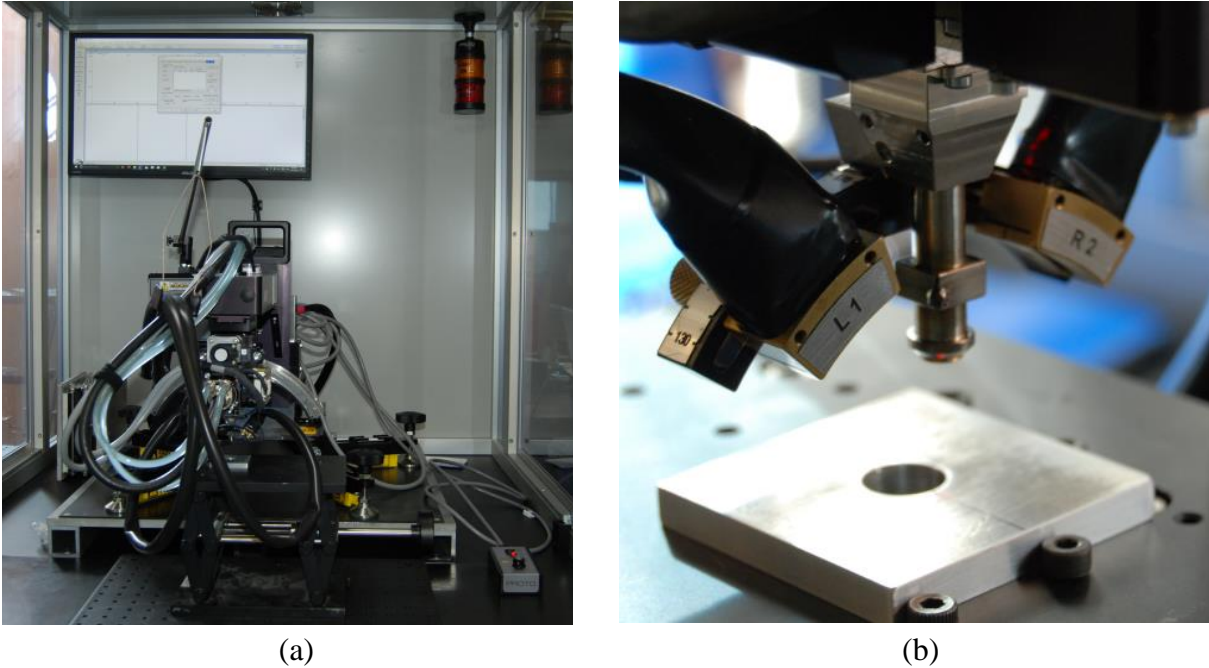


**Figure 31 (a) Overall view of XRD machine (b) Detail view of XRD aperture, left and right detector and coupon**

All XRD measurements were made using a 2 mm diameter aperture, with a measurement spacing of 0.25 mm. The results from the left and right side of each coupon face were averaged together, with the overall line profile of the residual stresses provided in Figure 32 and Figure 33 below.

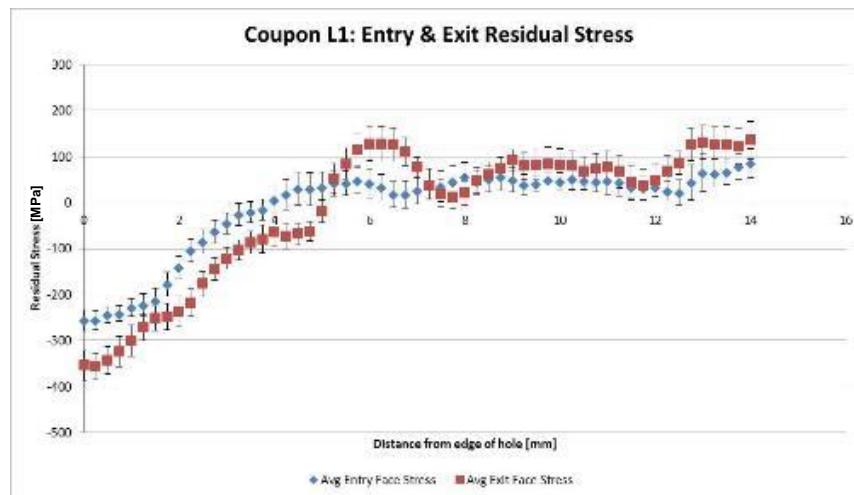


**Figure 32 Entry and exit face residual stress results for coupon L1**

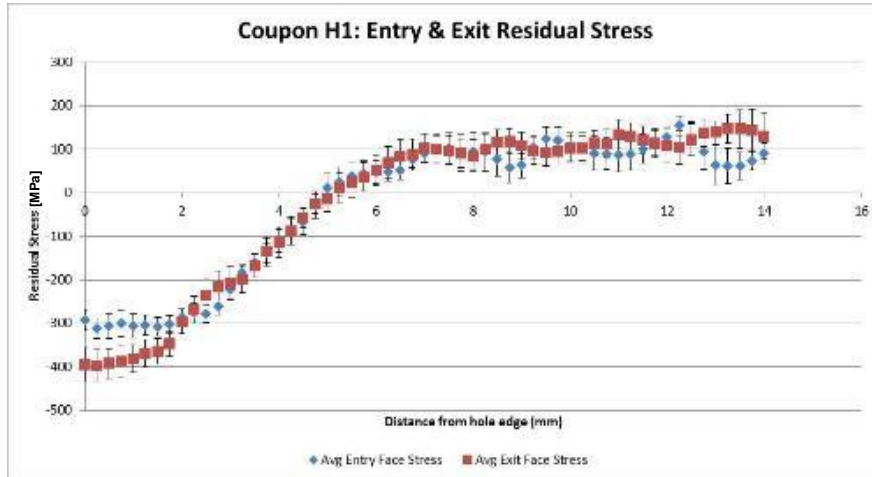


**Figure 33 Entry and exit face residual stress results for coupon H1**

The results for both coupons show that in the region next to the hole edge, the residual stresses were higher on the exit face than on the entry face. This result appears to be consistent with data from the open literature.

#### **4.5 Fatigue Life Prediction at Cold Expanded Fastener Holes with ForceMate Bushings\***

Y. Bombardier, G. Li, and G. Renaud, NRC Aerospace

\* Paper being presented at ICAF2019

ForceMate high interference fit expanded bushings, made by Fatigue Technology Inc. (FTI), are used by aircraft designers and maintainers to improve the fatigue and wear resistance of holes. While the fatigue life improvement factor (LIF) resulting from the installation of ForceMate bushings has been demonstrated experimentally, no analytical methods have been approved to benefit from this technology. To address this gap, a methodology was developed to analytically determine the LIF resulting from the installation of ForceMate bushings by taking into account the residual stresses and the effect of high interference fit bushings. To achieve this, a three-dimensional residual stress field is obtained from finite element analysis of the ForceMate installation; fatigue crack nucleation lives are calculated; crack propagation analyses are conducted to calculate the resulting crack shapes and stress intensity factors, and the crack growth predictions are performed. This methodology was demonstrated on a CF-188 bulkhead at the holes attaching the main landing gear uplock mechanism. Based on this analytical study, a predicted LIF of 6.6 was obtained for crack nucleation and 4.9 for crack growth from a 0.254 mm quarter-circular crack to a through-thickness crack. While there are several aspects of this analytical study that need to

be validated experimentally, the calculated LIF correlates with the LIF typically obtained with the ForceMate system.

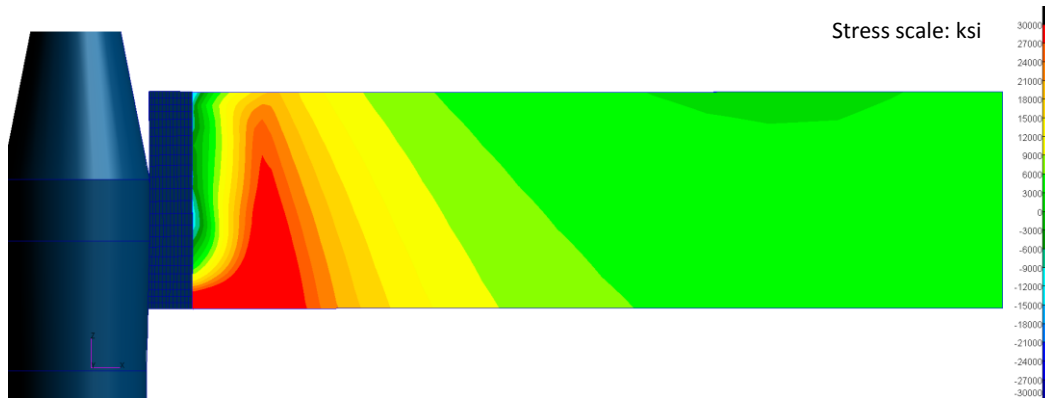


**Figure 34 Calculation of the residual stresses resulting from the finite element simulation of the installation of a ForceMate bushing**

#### 4.5.1 REFERENCE

- [6] Y. Bombardier, G. Li, and G. Renaud, Fatigue Life Prediction at Cold Expanded Fastener Holes with ForceMate Bushings, Proceedings of the International Committee on Aeronautical Fatigue and Structural Integrity (ICAF 2019), Krakow, Poland, Jun 2019.

## 4.6 Fatigue Performance Evaluation of Blind Fasteners for CP-140 Vertical Stabilizer Repairs

Y. Bombardier, NRC Aerospace

The original equipment manufacturer (OEM) of the CP-140 aircraft does not typically endorse the use of blind fasteners for vertical stabilizer skin repairs, as these types of fasteners could reduce the life of the structures by as much as 56%. Due to limited access to the internal structure of the CP-140 vertical stabilizer, these recommendations cannot always be followed by the maintenance, repair, and overhaul (MRO) organizations and blind fasteners sometimes have to be used to execute repairs.

The main objective of this project was to determine the fatigue life reduction factor resulting from the use of blind fasteners in-lieu of solid rivets. To achieve this objective, the National Research Council Canada (NRC) designed a test coupon representative of typical vertical stabilizer skin panel repairs. The specimens were manufactured by IMP Aerospace and Defence to replicate the installation procedures and to be representative of the CP-140 aircraft.

Static and fatigue tests were conducted by NRC on specimens, illustrated in Figure 35 and Figure 36, with three types of fasteners: MS20426AD6 flush-head solid rivets, MS20470AD6 protruding-head solid rivets, and NAS1670-3L blind bolts. The fasteners were tested in a double lap shear configuration to mimic the presence of the stringers that reduce the occurrence of out-of-plane bending. The fatigue lives obtained with MS20470 and NAS1670 fasteners were equivalent and the fatigue failures typically originated from fretting damage around the fastener holes. The fatigue lives obtained for MS20426 flush-head solid rivets were significantly shorter and all fatigue failures originated from the rivet. Further investigation is therefore required to identify the poor performance of the specimens with MS20426 fasteners compared to the two other types of fasteners.

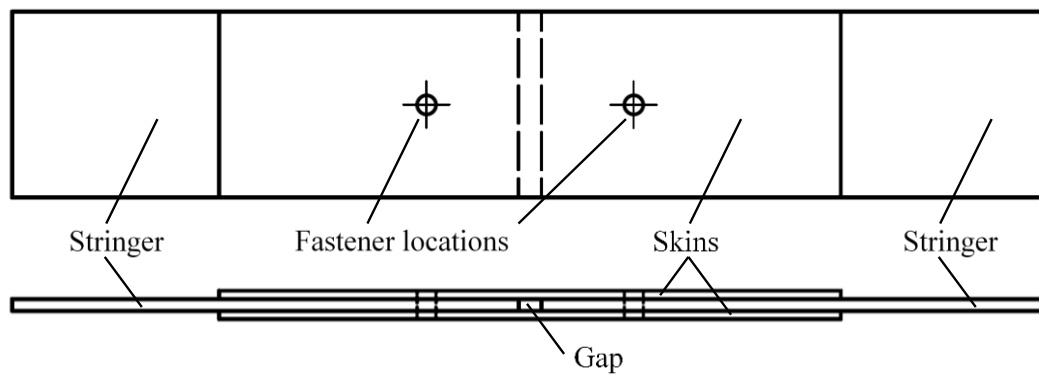


**Figure 35 Double lap shear specimen design**

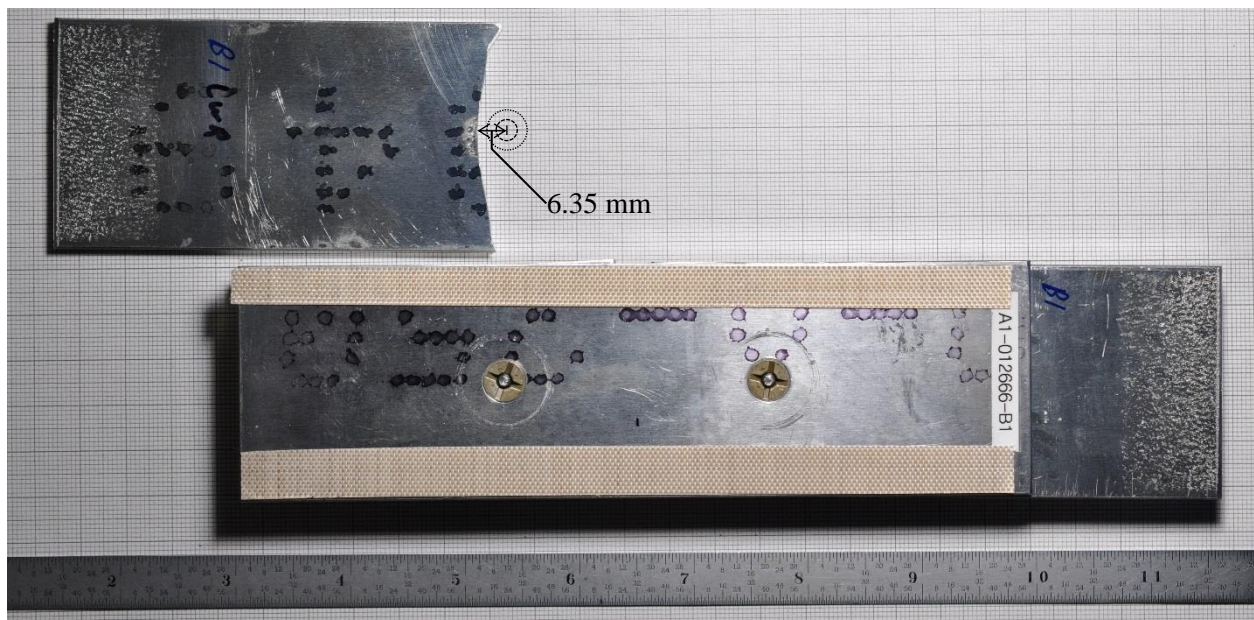


**Figure 36 Typical failure at a NAS1670 blind bolt**

While the preliminary results indicate that the fatigue performance of the tested blind bolt was equivalent to the protruding-head solid rivets, four additional effects need to be investigated to fully quantify the fatigue performance of blind bolts: 1) the effect of secondary bending moments, 2) the effect of a multi-row fastener layout, 3) the effect of clamping force upon installation, and 4) the effect of vibrations. Although all four effects likely play a major role in the fatigue performance of the joints, the clamping load effect is particularly important, as all failures observed for MS20470 and NAS1670 fasteners originated from fretting damage between the layers, whereas the failures observed by the OEM had resulted from fatigue cracks nucleating at the fastener hole.

## 5.0 LOAD, USAGE, AND STRUCTURAL HEALTH MONITORING

### 5.1 Helicopter Load and Usage Monitoring Research in 2017-2019

C. Cheung, NRC Aerospace

#### 5.1.1 A MACHINE LEARNING APPROACH TO LOAD TRACKING AND USAGE MONITORING FOR LEGACY FLEETS [7]\*

\* Paper being presented at ICAF2019

Indirect methods of estimating component loads based on existing aircraft sensor data have been in development using flight data from an Australian Black Hawk (S-70-A-9) helicopter and CH-146 (Bell 412) Griffon helicopter, illustrated in Figure 37. The load and fatigue life results obtained thus far have shown tremendous potential for accurate and consistent estimates using the same methodology on both platforms. Significant upgrades to the computational approach have been undertaken towards improving the efficiency and robustness of the algorithm and code. As a result of these improvements, larger data sets from the two helicopter platforms could be processed to provide a more complete picture of the effect of more accurate load monitoring.

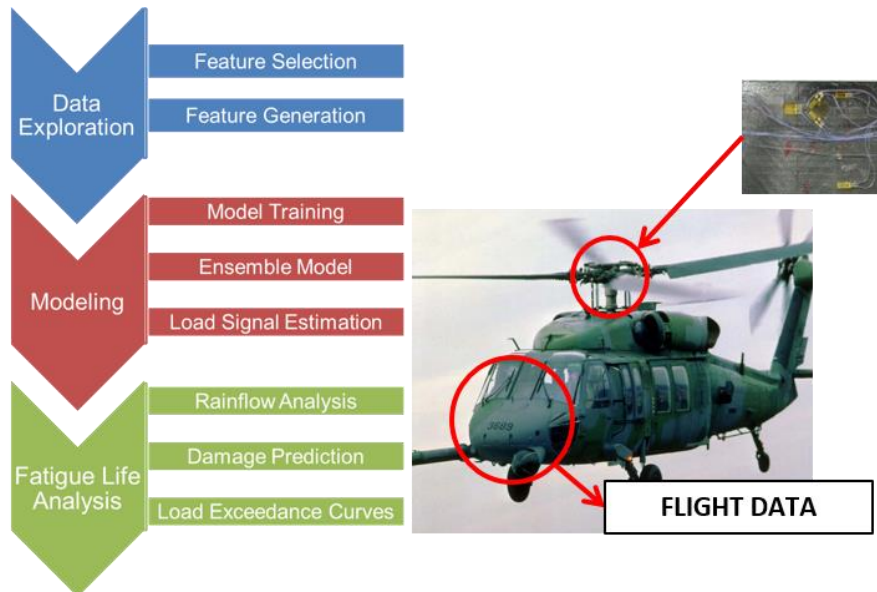


**Figure 37 Illustration of load estimation approach**

Refinements to the machine learning models are ongoing as we continue to explore different types of model architectures and model settings. These models and their results could all be combined in the load estimation framework to provide an ensemble of models, averaging their results.

Accurate load signal prediction enables ongoing load monitoring, allowing for comparisons of load histograms and load exceedance distributions between individual aircraft, time periods, aircraft flying certain missions, regions, squadrons, etc. Mean, maximum and minimum loads can also be compared. These types of comparisons do not rely on any material properties that the OEM may have used in the design process. With access to material data, more accurate fatigue damage accumulation can be monitored based on actual usage. Incorporating ground-air-ground analysis will be addressed in future work.

### 5.1.2 DATA ANALYTICS AND PREDICTIVE MAINTENANCE [8]

The application of predictive analytics to aerospace operational and maintenance data has the potential to further enhance overall aircraft safety and realize significant cost savings for aircraft Original Equipment Manufacturers (OEMs), Maintenance Repair and Overhaul (MRO) organizations and aircraft operators; be they civilian or military. Potential cost savings include, but will not necessarily be limited to, improved operational availability, avoidance of Aircraft-on-Ground (AOG) incidents, avoidance of unscheduled maintenance through timely and proactive intervention and spares provisioning optimization.

Aerospace predictive analytics are such that significant quantities of data are accumulated from each flight. Therefore, the implementation of such a capability requires the application of Big Data Techniques and Technologies. However, although several organizations have tried to apply Big Data Techniques to this data, few, if any, organizations have been able to demonstrate tangible Return On Investment (ROI). This lack of success can be attributed to factors such as lack of appropriate domain expertise integration with the big data techniques, poorly defined requirements, a lack of understanding of the parameters that need to be monitored and the development of appropriate models and analysis techniques for data processing. As part of this effort, NRC has partnered with Celeris Aerospace Canada Inc. to evaluate how large quantities of operational and maintenance data acquired from in-service aircraft can be effectively analyzed and synthesized to provide a truly predictive capability that provides tangible operational and maintenance benefits.

The first part of this process involves obtaining clarity as to the benefits (requirements) aircraft operators, maintainers, OEMs and other stakeholders are seeking to obtain through the collection of this data. To that end an online survey focused on determining the predictive operational and maintenance requirements of the different stakeholders was developed and distributed.

Ongoing advances in technology coupled with the trend to “capture all available data” based on the assumption that one day it may prove valuable, suggests that the number of parameters captured (and the corresponding data file sizes) will continue to increase at almost exponential rates for the foreseeable future. Organizations wishing to derive tangible operational and maintenance benefits from this data-tsunami need to address three main issues. First, they should implement effective

data management and processing strategies to avoid becoming overwhelmed with data, which they cannot process, validate, understand and interpret. Second, they should counter the widely held belief that the more data that is collected, the greater the insight that can be obtained, regardless of whether the rationale for collecting the data is understood or not. Finally, they should evaluate the actual cost-benefit of adding additional parameters and the associated impact on overall system design, implementation and cost. Effective solutions to these issues can only be obtained through a multi-disciplinary approach that evaluates and optimizes the relative merits and implications of proposed solutions from an overall system design perspective, as opposed to an individual constituent “discipline-silo” perspective. Consequently, the successful implementation of an Aircraft Health Monitoring Program that produces tangible operational, maintenance ROI requires a disciplined approach to overall system integration.

### 5.1.3 USAGE MONITORING USING MEMS-IMU SENSOR SYSTEM AND FDR INPUT DATA

To support life extension and usage monitoring efforts in various helicopter fleets with limited to no on-board data logging capability, the National Research Council (NRC) developed a stand-alone sensor system based on micro-electromechanical systems and inertial measurement unit (MEMS-IMU) technology, shown in Figure 38. This work was initiated as a temporary usage monitoring option for an older aircraft fleet, where a standalone system was preferable. This system recorded relevant flight data to be processed by manoeuvre recognition algorithms.

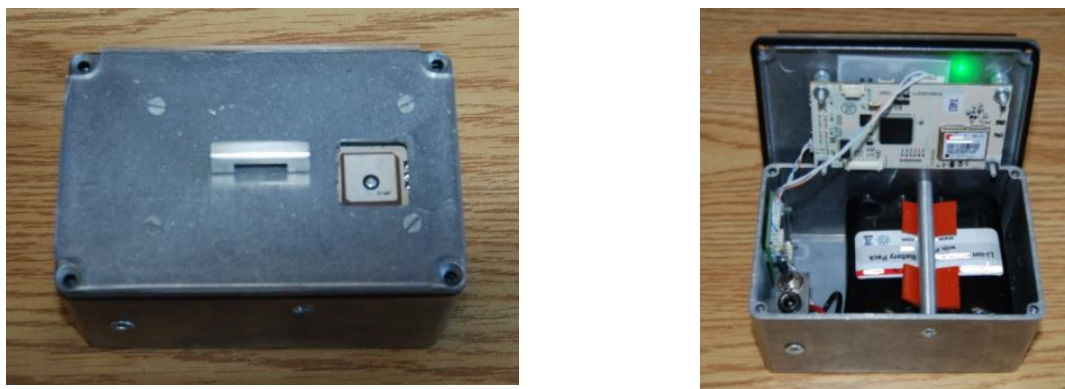


**Figure 38 MEMS-IMU system for helicopter usage monitoring**

An initial flight test of the sensor system was performed on a Bell 206 helicopter. The initial manoeuvre recognition results based on the sensor system measurements were very promising, though limited to only 7 general manoeuvres. More comprehensive in flight testing of the sensor system has recently been carried out on a Bell 412 CH-146 Griffon helicopter. A much broader range of 60 manoeuvres and regimes from the CH-146 usage spectrum were flown. Data was collected for several scripted flights from the MEMS-IMU sensor system as well as the from the

flight data recorder (FDR). Data-driven manoeuvre recognition models based on the recorded data from both data sources were developed and compared.

Continued analysis of the flight test data has included exploring different approaches to training a classification model that performs well when trained and tested on data from a separate flight. The data labels were relabelled to reduce the number of targets from 60 specific flight conditions to 7 general flight conditions.

The data was highly unbalanced as certain manoeuvres were performed many more times than others or were of longer duration than others, thus providing more samples. Thus, to balance the data set, the majority classes were under-sampled randomly so that the manoeuvres had about the same number of occurrences or samples. After training with this under-sampled but more balanced training set, the classification model improved considerably. The testing results indicated that considerable improvements can be obtained by balancing the data using a random under-sampling method. Furthermore, using fewer classes improves the predictive performance of the models. In the future, different data balancing techniques could be explored, such as techniques that generate data of the minority classes. Acquiring more data would also reduce the variance in the model, as the training set would have a more diverse set of manoeuvres. However, without more data the results will only improve through the exploration of new balancing methods.

#### **5.1.4 ANALYSIS OF SENSOR NETWORK DATA FOR FAILURE MODELLING AND PREDICTION [9][10][11][12]**

Rapid developments in sensor technology, data processing tools and data storage capability have helped fuel an increased appetite for equipment health monitoring in mechanical systems. As a result, the number of sensors and amount of data collected for health monitoring has grown tremendously. Developing strategies and capabilities to extract useful information from the tremendous amounts of data collected is a well-known challenge. This information can be used to establish system health indicators and contribute to the implementation of condition-based maintenance. It is hoped that by collecting large quantities of operational data, predictive tools can be developed that will provide operational, maintenance and safety benefits.

Data mining and machine learning techniques are important tools in addressing the ensuing challenge of extracting useful results from the data collected. However, incorporating as much physical domain knowledge to the analysis as possible is also necessary to ensure the results are relevant and practical for the operator and end-user.

This work relates to continued efforts to analyze sensor data for the turbocharger subsystem of a diesel engine system. The engine has hundreds of sensors monitoring both the inputs of the engine operator and the resulting equipment outputs. A turbocharger seizure was recorded by the diesel engine sensor system. While the sudden nature of the turbocharger incident was not a typical

example of a slowly deteriorating mechanical system, the opportunity to build models with a known outcome was still valuable. Therefore, data analysis of this incident including the lead up to the event allows for monitoring and identification of changes in equipment condition indicators with a known outcome.

The objective of the data analysis was to characterize and distinguish the healthy and failed states of the turbocharger seizure as recorded by the diesel engine sensor system. The analysis approach included the mapping of high-dimensional sensor data to a low-dimensional space using a variety of linear and nonlinear techniques in order to highlight and visualize the underlying structure of the information. Figure 39 shows an example of the 3-D visualization of a mapping of the turbocharger data using the Isomap technique. This mapping is overlaid with the Turbo A speed sensor values during the period of data analysis. In addition, data analysis tools were used to characterize the healthy and deteriorated states of the turbocharger system, including various classification and anomaly detection techniques.

Future efforts are aimed at expanding this analysis to data from other diesel engines and other failures in the engine system. Further work to generalize the analysis to a diesel engine system model instead of a turbocharger-specific model is in progress. The development and implementation of these tools should help enable advance indication of a change in behaviour that could be investigated before a major incident.

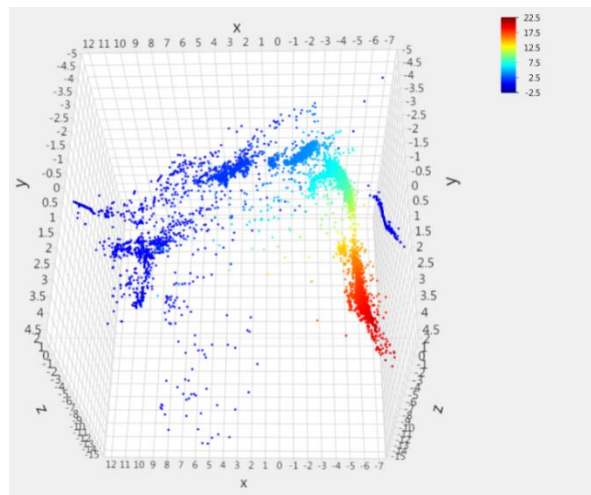


**Figure 39 Turbo A speed sensor value [kRPM] overlay onto Isomap transformation**

#### 5.1.5 REFERENCES

- [7] C. Cheung, S. Sehgal, J.J. Valdés, “A machine learning approach to load tracking and usage monitoring for legacy fleets”, Proceedings of the International Committee on Aeronautical Fatigue and Structural Integrity (ICAF 2019), Krakow, Poland, Jun 2019.

- [8] Stephen R. Hall, Catherine Cheung, and John W.R. Miner, “Considerations for Obtaining Tangible Operational and Maintenance Benefits from Aircraft Health Monitoring Systems in a Big Data Environment”, Proceedings of the 11th DST International Conference on Health and Usage Monitoring Systems (HUMS2019), Melbourne, Australia, Feb 2019.
- [9] C. Cheung, N. Kilfoyle, J.J. Valdés, S. Sehgal, R. Salas Chavez, “Low-dimensional spaces for relating sensor signals with internal data structure in a propulsion system”, Advances in Science, Technology and Engineering Systems Journal, Special Issue on Multidisciplinary Sciences and Engineering, Vol. 3. No. 6, pp. 23-32, 2018.
- [10] C. Cheung, J.J. Valdés, R. Salas Chavez, S. Sehgal, “Failure modelling of a propulsion subsystem: unsupervised and semi-supervised approaches to anomaly detection”, International Journal of Pattern Recognition and Artificial Intelligence, accepted Jan 2019.
- [11] C. Cheung, J.J. Valdés, R. Salas Chavez, A. Lehman Rubio, “Failure modelling and anomaly detection of a propulsion subsystem”, Proceedings of International Conference on Pattern Recognition and Artificial Intelligence (ICPRAI 2018), Montreal, QC, May 2018.
- [12] C. Cheung, J.J. Valdés, A. Lehman Rubio, R. Salas Chavez, C. Bayley, “Low-dimensional spaces for the analysis of sensor network data: Identifying behavioural changes in a propulsion system”, Proceedings of IEEE International Symposium on Robotics and Intelligent Sensors (IEEE IRIS2017), Ottawa, ON, Oct 2017.

## **5.2 Structural Health Monitoring (SHM)**

L-3 Communications (Canada) Military Aircraft Services (L3 MAS)

L3 MAS is an active member of three on-going collaborative R&D initiatives with universities, colleges and industrial partners: CRIAQ (Quebec Aeronautical Industrial Research Consortium), CARIC (Consortium for Aerospace Research and Innovation in Canada) and MICA (Metrology and Inspection of Composites in Aerospace). Internal and collaborative projects that have been completed recently were in the areas of Structural Health Monitoring (SHM), shot peening, robotics and composite materials, as well as software tools in support of fatigue life assessments and in-service monitoring/management, including Artificial Intelligence (AI) initiatives.

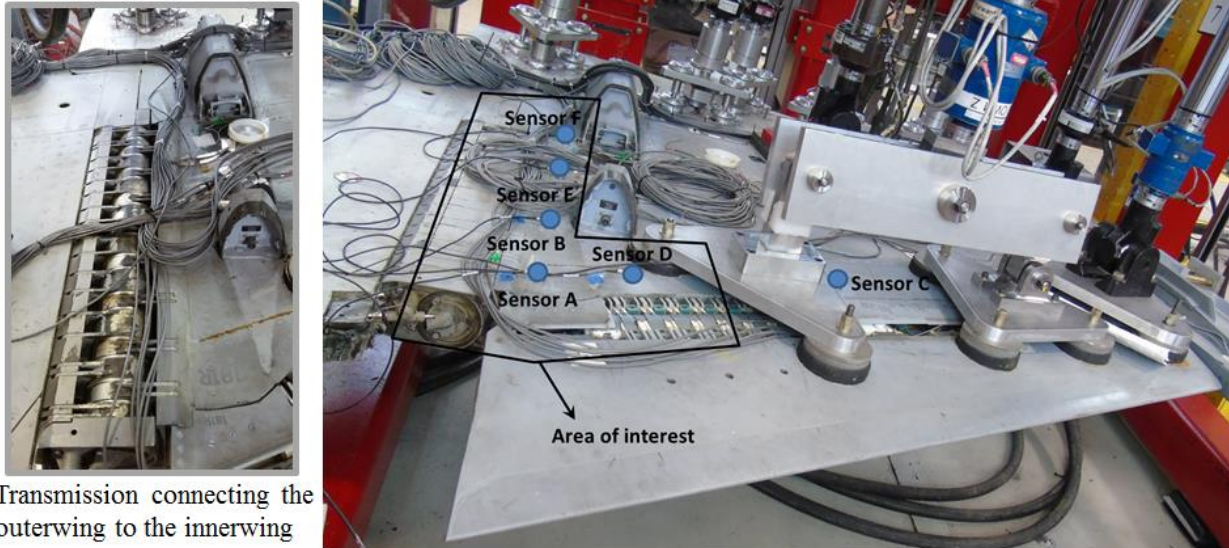
In 2018, L3 MAS and Paradigm Shift Technology (PST) have completed a technology demonstration project funded under the Build-in-Canada Innovation Program (BCIP). The sensor developed by PST, coined Chameleon Skin Gauge (CSG), is a passive, thin, isotropic film, which may be cut and formed in any shape. Once interrogated by the reader and processed through proprietary software, the sensor data provide direct information on the cumulative effect of host structure exposure to stress/strain loads and cracking. The project has evaluated the ability of the Prognostica™ technology to detect structural defects in four different applications deemed

representative of the critical CF-188 locations: fatigue cracks in fastener holes and in fillet radii, disbonds and cracking in underlying structures (detected from the overlaying graphite epoxy skin).

### **5.3 Potential Damage Location Indication Determined using Acoustic Emission during CF-188 Aileron Fatigue Test**

S. Pant, R. Rutledge, NRC Aerospace

A full-scale test of the aileron was conducted at NRC as a part of life extension efforts for all CF-188 flight control surfaces. This testing involved fatigue durability and damage tolerance cycling with static residual strength tests completed at the end of the two cycling test phases. The aileron test article contains aluminium core with pushed fasteners, due to modifications carried out during its usage. The intent is to test the durability and damage tolerance of the current configuration of CF-188 aileron in order to extend its life by an additional one third of a lifetime. During the cyclic testing, loud noises were emanating from the test article. To locate the noise source, the test had to be stopped and the entire area had to be manually searched using a Non-Destructive Evaluation (NDE) technique, such as ultrasonic inspection. These inspections are time consuming and labour intensive, as the entire area had to be inspected. Inspecting the entire test article meant that the test had to be stopped for that duration plus the additional labour hours required for the inspection itself. In order to minimize downtime and determine the location of the noise source, an Acoustic Emission (AE) technique was implemented. The AE system was developed in-house using commercial off-the-shelf (COTS) components and custom post-processing and source location algorithms. The goal was to locate the area of interest to find out if the source creating the noise was also creating significant damage to the test article. For this purpose, six piezoelectric sensors were placed at strategic locations, which were moved throughout the test. Sensors' signal amplitudes, frequencies along with their arrival times were analyzed to narrow down the location of area of interest. This area of interest was found to be the transmission connecting the outer wing to the inner wing, as shown in Figure 40.



Transmission connecting the outerwing to the innerwing

**Figure 40 Area of interest of the noise source determined using Acoustic Emission**

## 5.4 Repeatability Study of Structural Health Monitoring (SHM) Sensors at Room Temperature

S. Pant, D. Backman, P. Keum, and M. Yanishevsky, NRC Aerospace

This work is focused on exploring the repeatability of Structural Health Monitoring (SHM) sensors to detect fatigue cracks emanating from crack-starter notches in 0.063 inches thick, aluminium 7075-T6 panels, measuring 12 by 24 inches in a room temperature environment. Three ( $n=3$ ) panels were tested in total, where each panel had three ( $n=3$ ) 0.25 inches diameter holes, drilled at 3 inches apart along the vertical centre of the plates. Two outer holes had Electrical Discharge Machining (EDM) notches for starting fatigue cracks. Four ( $n=4$ ) different Structural Health Monitoring (SHM) technologies: Acoustic Ultrasonic (AU), National Research Council (NRC) developed Crack Foil Sensor (CFS), resistance wire Strain Gauges (SG), and Thermoelastic Stress Analysis (TSA), were all evaluated for their ability to repeatedly and reliably detect growing fatigue cracks. Repeatability in the context of this work is defined as the ability of a particular sensor technology to successfully detect cracks in multiple holes or on multiple test panels. The repeatability score is simply defined as the number of positive results divided by the total number of trials.

A strain survey was initially performed using Digital Image Correlation (DIC) technique and was corroborated with the numerical model developed in ABAQUS. The panels were cycled in tension-tension fatigue at 5 Hz with a maximum constant sinusoidal load of 8000 lbf at a load ratio of  $R =$

0.1. The experimental setup is shown in Figure 41. Each panel consisted of four AU, eight CFS, and four SG sensors installed at different locations to detect crack growth, as well as a single TSA camera capturing thermal images of the specimen. The test ran until the cracks emanating from the EDM notches propagated through all the installed CFS. Marker band loadings were applied to each specimen during testing to allow for crack growth information to be extracted using quantitative fractography (QF).

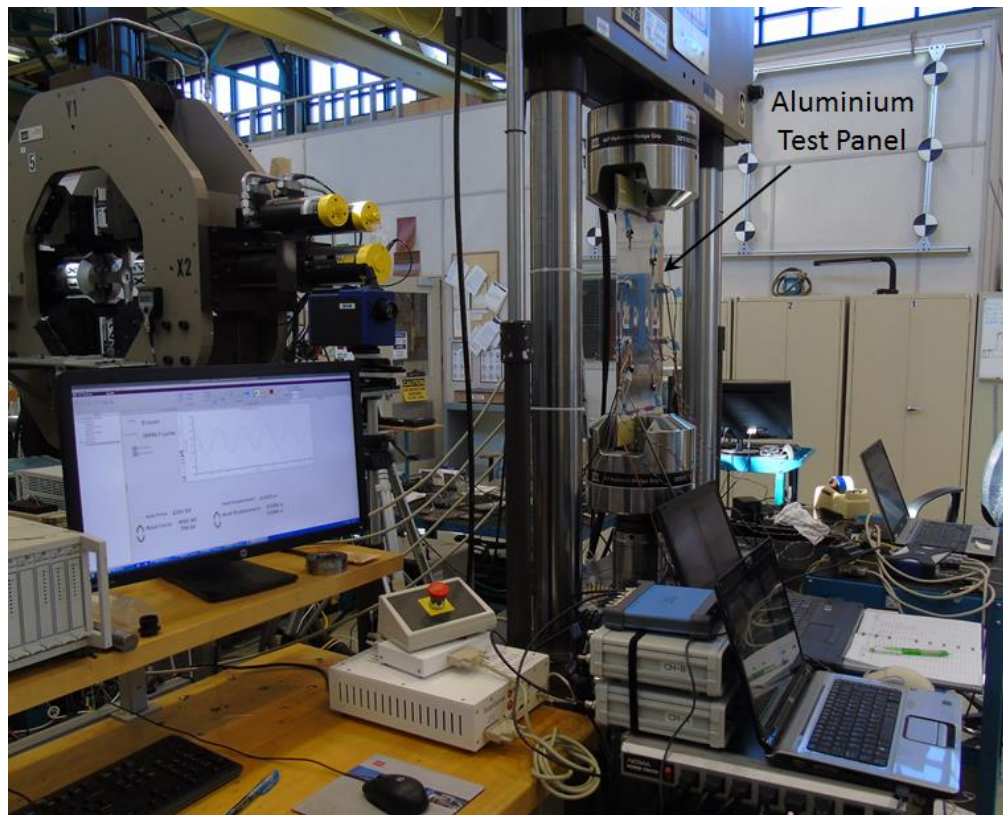


**Figure 41** Experimental setup for a repeatability study of SHM sensors

The results showed that despite all three panels being similar and undergoing the same fatigue loading sequence, cracks grew at a faster rate in some panels versus others, which highlighted the fact that cracks emanating from holes in identical components fabricated from the same material and experiencing the same loading can still behave somewhat differently in fatigue. This emphasised the potential usage of SHM systems to detect and track damages / cracks in individual components to reduce / eliminate unnecessary inspection as a part of aircraft maintenance. As for the different SHM systems that were tested, the repeatability of the AU technique was evaluated for two excitation frequencies of 300 kHz and 350 kHz for a total of 72 paths. Correlation Coefficient (CC), Energy Ratio (ER) and Amplitude Ratio (AR) were compared between the wave signal taken at zero cycles and at different cycles for detecting growing cracks. Overall, there were 12 false calls out of 72 paths, which could be attributed to faulty sensors for an aggregate

repeatability rating of 83% (60/72). Out of twenty-four (n=24) NRC developed Crack Foil Sensors (CFS) that were tested, only one (n=1) was found to be defective. All the functioning CFS tripped when cracks propagated through the sensors, corresponding to a repeatability of 96% (23/24). Twelve (n=12) resistance wire Strain Gauges (SG) were used to monitor crack growth trends, and as expected, increases in strain readings were witnessed by all the twelve SG sensors, when the crack propagated close to the SG, for a repeatability score of 100% (12/12). The Thermoelastic Stress Analysis (TSA) were used to monitor cracks at the two outer holes with the EDM notches for a total of six (n=6) repeats. The TSA was not only able to detect crack formation, but was able to track crack growth in all six cases giving this technology a repeatability score of 100% (6/6).

## **5.5 Damage Detection Methodology based on Multi-frequency Guided Waves for SHM Applications with Experimental and Numerical Verification**

S. Pant, M. Yanishevsky, D. Backman, NRC Aerospace  
M. Martinez, Clarkson University

Even with increasingly sophisticated sensors and damage detection algorithms, Structural Health Monitoring (SHM) systems have not yet achieved widespread acceptance by aircraft operators. One of the challenges includes the ability of SHM systems to provide robust damage detection algorithms to minimize/eliminate false-calls, which can prompt for unnecessary maintenance actions. Therefore, the primary objective of this study is to aid in reducing the false-call rates by using a newly developed Damage Response Factor (DRF) method. This method is based on the use of multi-frequency guided wave excitation for assessing the presence of damage along an actuator - sensor path. In this study, the corresponding change in the cross-correlation (CC), amplitude ratio (AR) and energy ratio (ER) of the wave signal were analysed to detect a growing fatigue crack in a C-Channel type structure made from aluminium alloy 7075-T651 (Figure 42).

A 0.25 mm thick jeweller's saw blade was used to introduce a saw-cut approximately 0.4 mm in length to act as a fatigue crack starter notch at the edge of the 3.2 mm diameter hole. To grow the crack, the C-Channel was loaded in tension-tension fatigue using a sinusoidal waveform at a frequency of 5 Hz with a maximum load of 2500 lbf [11120 N] and a load ratio of  $R = 0.1$ . In addition to the commonly used threshold value, the DRF approach uses the upper and lower bounds of the average DRF value along with the separation of the DRF based on excitation frequency. A combination of all of these criteria, provided an improved means to identify damage rather than the classical sole-threshold method.

It is also well known that increasing the load will enhance crack detection by opening up the crack surfaces. Therefore, instead of using the fatigue cycling data, the load data is used at any given fatigue cycle, i.e. the baseline is taken at the lowest tensile load as a "cycle-free baseline"

technique. The idea behind the “cycle-free baseline” technique is to interrogate the structure during the same cycle, but at different loading conditions. The advantage of using this technique is to minimize the false calls due to sensor degradation caused by fatigue and environmental cycling. The “cycle-free baseline” technique may be beneficial in reducing the false calls associated with sensor degradation as the structure is interrogated using the same sensor state for determining the baseline and the change. This technique also eliminates the requirement to store and process all the data associated with each cycle. However, the downside to this technique is the requirement for applying discrete loads to the structure. For aircraft applications this can be done before and after fueling or before and after loading the aircraft with cargo and/or passengers. Unfortunately, this approach may not be able to detect the damage if it is located on the compressive side of the structure, an issue which will be addressed in future.

The method was verified numerically using ABAQUS. For running ABAQUS, a Windows 7 computer with two Intel Xeon CPU 2650V3 (a total of 20 physical CPUs) running at 2.30 GHz with 128 Gigabytes of RAM was used. Despite the simplistic crack model (extension of a notch), the Finite Element Model (FEM) results displayed that the waves excited at a higher frequency corresponding to smaller wavelength are in fact more reactive to the presence of the damage in their path, as compared to the waves generated at a lower frequency corresponding to a longer wavelength; thereby, verifying the DRF approach [13].

One major issue using ABAQUS was, despite the high computational resource, many of the simulations took over a week to converge for a total time window of only 350 microseconds. Therefore, to improve upon the simulation time, new wave propagation software called Onscale was evaluated and compared against ABAQUS and experiment data. Onscale results were in excellent agreement with the ABAQUS results, while reducing the simulation time from 10 days to less than 3 hours on the same machine. This opens the possibility of generating Model Assisted Probability of Detection (MAPoD) curves. Onscale is currently being used to simulate wave propagation in order to compare the DRF method with the experimental and ABAQUS results [14].

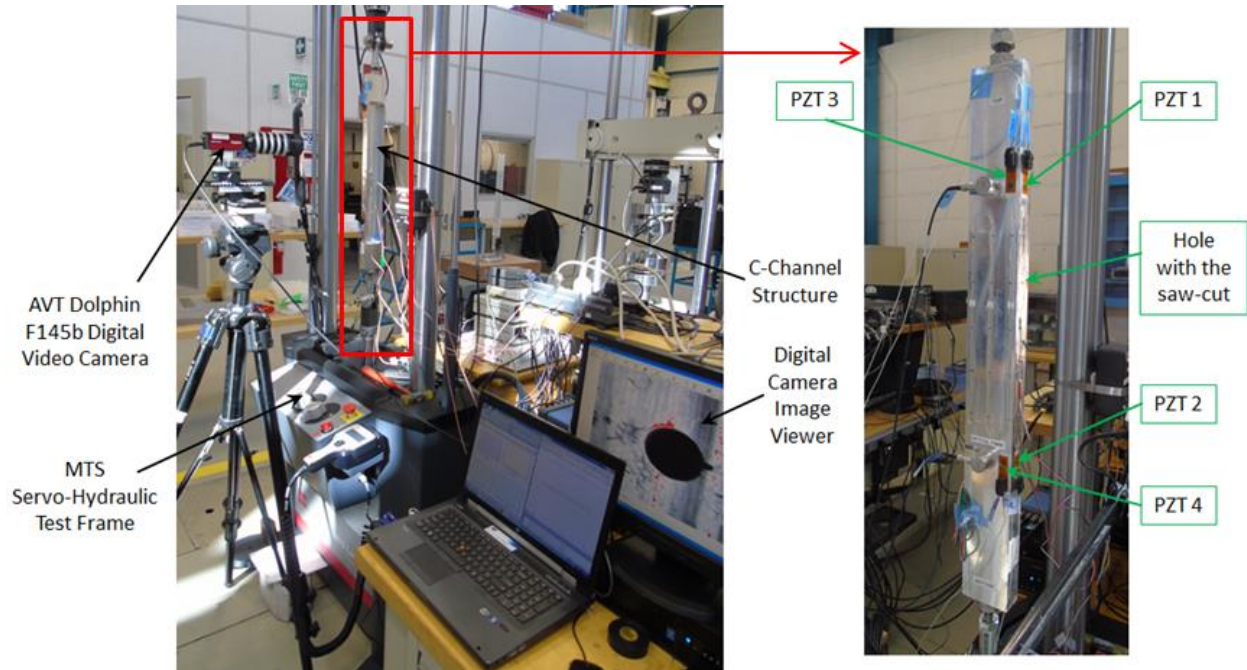


**Figure 42** Experimental setup to grow fatigue crack in C-Channel structure

### 5.5.1 REFERENCES

- [13] S. Pant, M. Martinez, M. Yanishevsky, and D. Backman, "Damage Detection Methodology for Structural Health Monitoring (SHM) Applications based on Multi-frequency Anti-symmetric Guided Waves", 9th European Workshop on Structural Health Monitoring, Manchester, UK, 2018.
- [14] F. Falcetelli, M. B. Romero, S. Pant, M. Martinez, "Time Reversal Technique to model Pencil-Lead Break Acoustic Emission Sources", 18th International Workshop on Holistic Structural Integrity Process (HOLSIP), Utah, USA, 2019.

## 6.0 NON-DESTRUCTIVE EVALUATION

### 6.1 Detection of Low-Velocity Impact Damage in Carbon Fiber Sandwich Panels Using Infrared Thermography\*

T. Rellinger, D. Wowk and T. Krause – Royal Military College of Canada, C. Marsden - Concordia University

\*Masters thesis. Tanner Rellinger, Royal Military College of Canada, January 2019.

Sandwich panels with honeycomb core and composite facesheets are commonly used for aerospace applications, but are susceptible to low-velocity impact events which may result in damage that is difficult to detect. Some of the damage modes that may occur are plasticity of the facesheet, crushing of the core, delamination in the facesheet and disbonding of the adhesive between the facesheet and core. While any form of disbond or delamination is unacceptable, plasticity in the facesheet and crushing of the core may be acceptable, if within allowable limits. It is therefore important to be able to differentiate between the different types of damage. An apparatus using active infrared thermography was designed and used to identify disbonds and measure their diameter.

The apparatus was designed and constructed around a FLIR T620 infrared camera and consisted of two 50 Watt halogen bulbs as a heat source, parabolic reflectors for uniform heating, an Arduino computer and relay board for controlling the heating, and a MATLAB code for post-processing the thermal images. Figure 43 shows some of the key features of the apparatus.

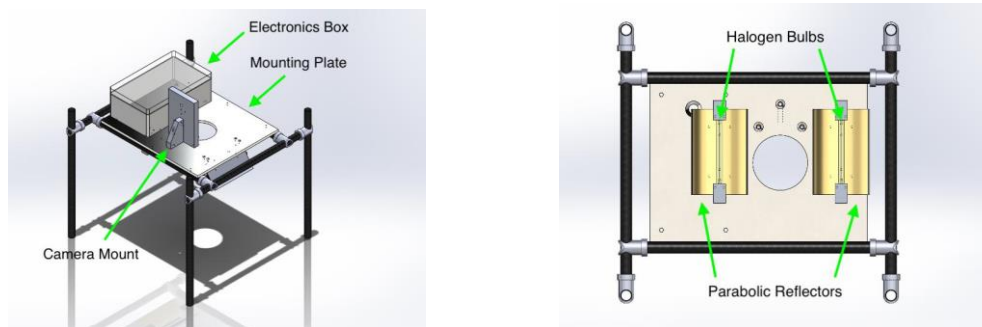


**Figure 43 Infrared thermography apparatus for heating the sample and recording a sequence of images of the surface temperature**

Sandwich panel coupons and laminate facesheets were manufactured in-house using a table-top autoclave. Two different types of impact damage were created in the panels using a drop tower apparatus. The first was a disbond between the facesheet and the core. Following springback of the facesheet, no dent was visible on the surface of the panel although core crushing existed beneath. The second was a dent, where the facesheet stayed depressed and adhered to the core.

This damage mode was created by wet sanding the surface of the laminate facesheet prior to adhering the core.

Thermographic images of the coupon showed higher temperatures in regions where a disbond occurred, because the air gap does not transmit the thermal energy into the core as readily as the intact portion of the panel. Figure 44 a) shows a cross-section of a disbond between the facesheet and the core with the corresponding thermographic image shown in Figure 44 b). The presence of the disbond is identified by the local increase in temperature, and the width of the disbond was measured to within 25% for 9 coupons subject to different impact energies.

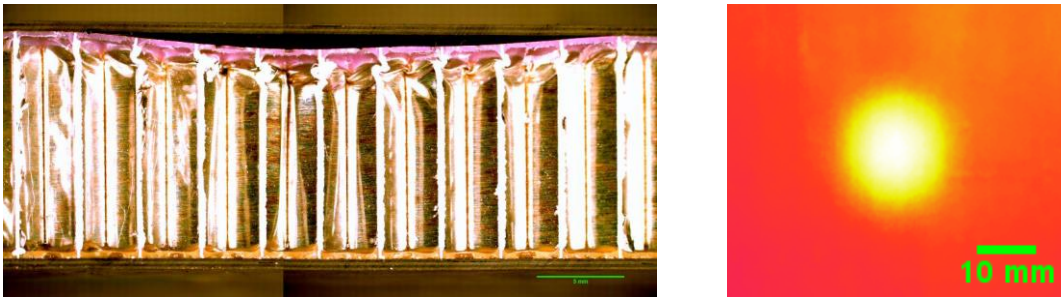


**Figure 44 a) Cross-section of an impact location with an adhesive disbond, b) thermographic image of the surface of the impact region**

Figure 45 a) shows a cross-section of a dent with no disbond and Figure 45 b) shows the corresponding thermographic image. The uniform temperature of the panel indicates that no disbond is present. Even though core crushing and facesheet plasticity exist, they are acceptable damage modes and can be quantified based on the surface dent.



**Figure 45 a) Cross-section of an impact location with an intact adhesive bond, b) thermographic image of the surface of the impact region**

This work has shown that thermography has the potential to identify disbonds in sandwich panels with composite facesheets in regions damaged by low-velocity impacts. The main benefits of this method are that it does not require any specialized training to implement or interpret the results, and it is relatively cost effective and efficient.

## 6.2 Induction Thermography of Steel Coupons with Cracks

M. Genest, G. Li, NRC Aerospace

Induction thermography techniques were assessed experimentally and numerically on notched steel coupons using two coil configurations: straight line and loop conditions. The coupons had different fatigue crack lengths varying from 0.1 mm to 3 mm, shown in Figure 46. The numerical predictions showed that the peak temperature was always located at the crack tip or the notch tip position. The loop coil resulted in higher temperatures than that of the straight line coil. Results showed that the numerical methods effectively supported the application assessment of this non-destructive evaluation (NDE) technique for the steel material, but crack geometry remains a challenge as the exact shape of a natural crack is typically unknown. It is shown that induction thermography can detect cracks as small as 1 mm in the notched steel coupons [15][16].

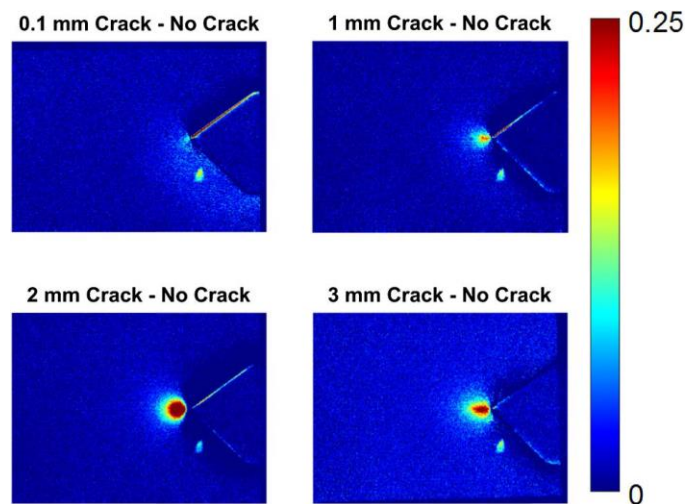


**Figure 46 Temperature difference from the reference sample with the 50A current at time 100 ms heating time**

### 6.2.1 REFERENCES

- [15] M. Genest, G. Li, “Induction Thermography for Detection of Cracks in Steel Publication Number, Advanced Infrared Technology and Application (AITA 2017)”, Quebec City, QC, 27 -29 September 2017.
- [16] M. Genest, G. Li, “Induction thermography of steel coupons with crack, Applied Optics”, Vol. 57, No 18, June 20, 2018 | Advanced Infrared Technology and Applications 2018, pp. D40-48.

### 6.3 Reliability Assessment of Pulsed Thermography and Ultrasonic Testing for Impact Damage of CFRP Panels

Université Laval and NRC Aerospace

In order to quantitatively compare the reliability of pulsed thermography (PT) and ultrasonic testing (UT) techniques, a set of thirty-five carbon fiber reinforced plastic (CFRP) composite panels with impact damages from some aerospace engine nacelles are inspected by PT and UT. Comparative experimental results and Probability of Detection (PoD) analysis results are presented. The quantitative comparison shows that PT has smaller defect size at 90% PoD with 95% confidence level, i.e.  $a_{90/95}$  values than UT for the parameters and setup used in the inspections of these thirty-five CFRP composite panels. PoD curves from PT and UT indicate that PT has a higher inspection reliability than UT for the parameters and setup used in these inspections. The intent of this research was to increase the acceptance of infrared thermography NDT & E techniques beyond the laboratory, especially in the aerospace industry. While, currently, PT is used as a complement or alternative to UT inspection technology in some practical applications, it is shown that it could become the inspection method of choice depending on the critical flaw size.

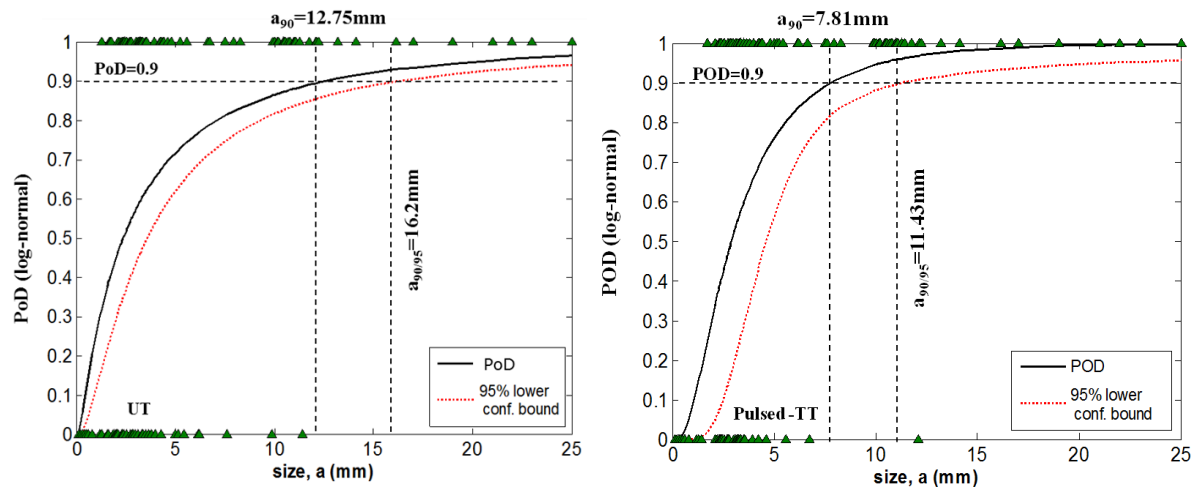


**Figure 47 Log-normal PoD curve and the corresponding 95% lower confidence bound for UT (left) and pulsed thermography (right) [17]**

#### 6.3.1 REFERENCES

- [17] Y. Duan, H. Zhang, X. Maldague, C. Ibarra-Castanedo, P. Servais, M. Genest, S. Sfarra, and J. Meng, "Reliability Assessment of Pulsed Thermography and Ultrasonic Testing for Impact Damage of CFRP Panels", *NDT & E International*, Volume 102, Pages 77-83, March 2019.

## **6.4 Automated Dynamic Inspection Using Active Infrared Thermography**

Université Laval and NRC Aerospace

Active thermography is a proven technology used in a wide variety of applications. In the most common approach using a static configuration, the elements involved in the inspection do not move. This presents serious drawbacks when it is applied to the inspection of large products and machines. An alternative approach is dynamic inspection, which enables the inspection of large and complex products with better resolution, but it is also extremely challenging as data reconstruction is necessary. This work analyzes two methods for dynamic inspection using active infrared thermography: the thermal photocopier and the line scan. Automatic robust methods are proposed to calculate the temperature–time history, producing a pseudostatic sequence that can be further processed using advanced data processing algorithms to improve defect detection. Results demonstrate the robustness of the proposed methods and the ability to inspect large products with excellent results [18].

### **6.4.1 REFERENCES**

- [18] R. Usamentiaga, M. Y. Mokhtari, C. Ibarra Castanedo, M. Genest, and X. Maldague, “Automated dynamic inspection using active infrared thermography”, *IEEE Transactions on Industrial Informatics*, Volume 14 , Issue 12 , 5648 – 5657, 2018.

## **6.5 Embedded Electromagnetic Sensors for NDE and SHM**

C. Mandache, NRC Aerospace

Under a project supported by Defence and Research Development Canada (DRDC), thin, surface-conformable copper coils are proposed as in-situ eddy current sensors for detection of fatigue cracking developed from fastener holes in aircraft metallic structures. In this technique, eddy currents are induced into metallic structures via a time-changing magnetic field created by the coil. Their flow is disturbed by the presence of a crack. The same coil, or a separate, sensing device, detects the change in the magnetic flux due to the presence of a discontinuity. The development and potential broad use of these coils are motivated by a few consistent arguments: (i) inspection of structures of complicated geometries and hard to access areas, that often require disassembly; (ii) alternative to regular inspection actions that are known to introduce inadvertent damage; (iii) inspection of structures that have short inspection intervals; and (iv) inspection of repaired structures where fastener holes contain bushings and prevent further bolt-hole inspections. The specimen used for demonstration purposes is shown in Figure 48, where the fatigue cracks are imitated by through-wall electrical discharge machining (EDM) notches of various lengths.

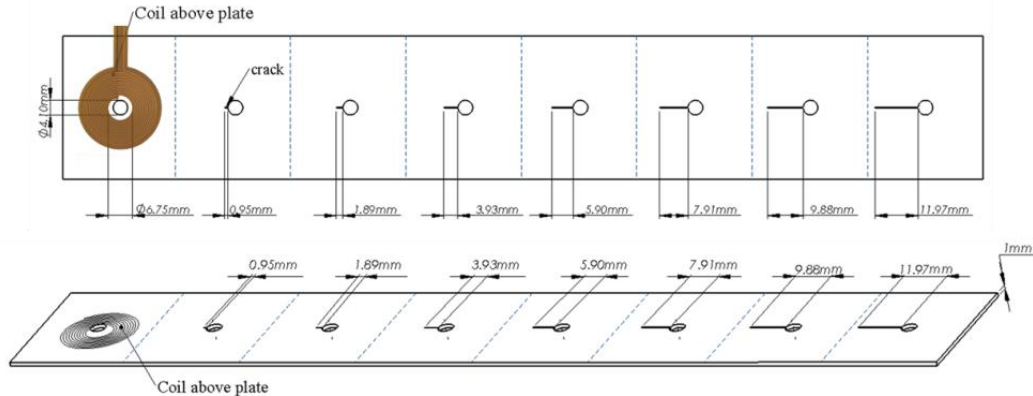


**Figure 48 Spiral coil centred around a fastener hole, on the back side of a mock-up specimen**

In this study, thin copper circuits, printed on polyimide film substrates are used as surface conformable eddy current transducers that could be permanently mounted on or between the layers of metallic aircraft structures. High and low frequency applications in absolute and transmit-receive modes, respectively, are shown in the next figures (Figure 49 and Figure 50).

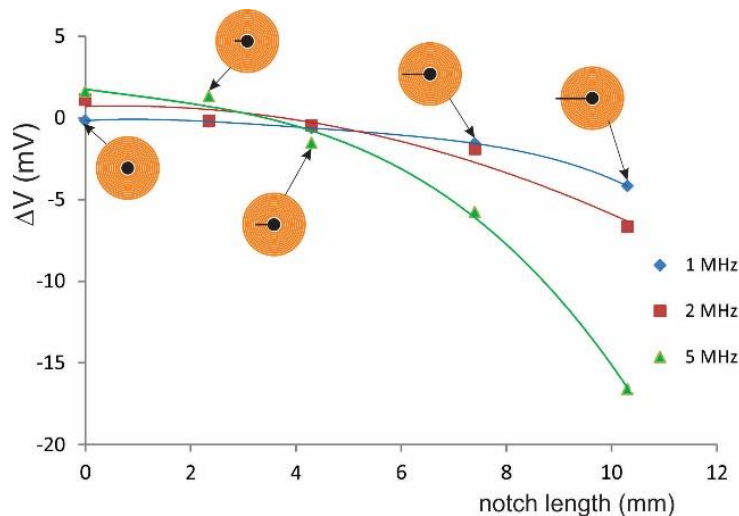


**Figure 49 High frequency application: voltage variation with respect to the notch length when the coil is used in absolute mode**

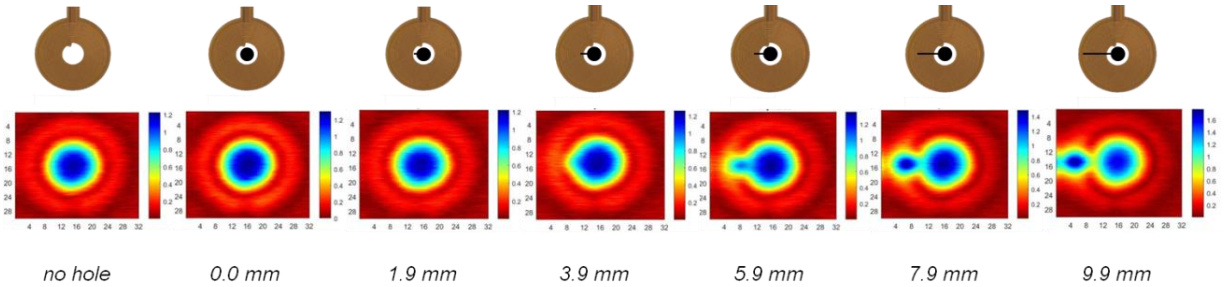


**Figure 50 Low frequency application: area scan with a Hall sensor, when the coil is used as a driver in a transmit/receive mode**

The work is still at an early stage of in-situ NDT development, but the simplicity of the approach and the preliminary results are showing great promise. The introduction of capable and durable eddy current coils adjacent to faying surfaces in multi-layer metallic structures can detect fatigue cracks. Printed conductive traces or coils, of silver or copper, on flexible polyimide film substrates are suitable for permanent attachment and integration into the part/structure to be monitored. Issues with sensor durability and degradation, as well as coil-structure bonding need to be included in future work. The environmental temperature is another parameter that needs to be investigated before these types of sensors are moved towards applications in a simulated operational environment.

### 6.5.1 REFERENCES

- [19] Mandache C., Pant S., Khan M., Genest M., “Structure conformable eddy current coils for in-situ crack detection”, NATO AVT-305 Research Specialists’ Meeting on Sensing Systems for Integrated Vehicle Health Management for Military Vehicles, Athens, Greece, December 10-14, 2018.
- [20] Mandache, C., “Characterization and optimization of spiral eddy current coils for in-situ crack detection”, Proc. SPIE 10599, SPIE Smart Structures and Materials + Nondestructive Evaluation and Health Monitoring, Denver, Colorado, 4-8 March, 2018.

## 6.6 Technical Justification of Ultrasonic Inspection Procedure for Helicopter Components\*

M. Khan, NRC Aerospace

\* Paper being presented at ICAF2019

For many Non-Destructive Evaluation (NDE) applications, traditional Probability of Detection (POD) assessments are impractical because of the cost, time, and complexity associated with

manufacturing and preparing the required specimens representative of in-service conditions. Various alternative methods have been developed to reduce the number of test specimens required for the reliability estimation.

Technical justification (TJ) is a process that includes analytical and experimental evidence, physical reasoning, summary and recommendation. Those are gathered and compiled in a structured format to verify that the targeted inspection technique, equipment and written procedure conform to the requirements and can meet its stated objective. Inspection qualification through technical justification minimizes the reliance on the manufacturing of test pieces and their time consuming inspection trials. In this paper, this promising approach in accordance with the European Network for Inspection and Qualification (ENIQ) guideline is applied to demonstrate the reliability of an ultrasonic NDE procedure for the inspection of a helicopter upper tail-cone assembly. It is intended to provide comprehensive evidence for determining whether the minimum detectable discontinuity size by an ultrasonic inspection procedure for a helicopter upper tail-cone assembly can be reduced from 1.27 mm (0.050 inches) to 0.64 mm (0.025 inches), without compromising the current level of confidence [21].

The main elements of TJ are relevant input information (component, defects, and required inspection objectives), identification and analysis of influential parameters, physical reasoning (qualitative evaluation), experimental evidence, recommendation and conclusion summary. The input information data is all related information regarding the area or component to inspect, type and features of expected defects, and qualification objectives. Input information (including essential parameters describing the component, material, discontinuities etc.) has to be available prior to the start of the process of inspection qualification.

For ENIQ based inspection qualification, all parameters suspected of influencing the capability and reliability of the NDE procedure are termed as influential parameters. Influential parameters need to be identified and documented. The natural variability and the ranges of each parameter are also required. Essential parameters are a subset of influential parameters, whose change in value would actually affect reliability of a particular inspection in such a way that the inspection can no longer meet its defined objectives. The calibration requirements of the inspection procedure need to ensure that such parameters are verified at appropriate intervals, to ensure that they remain within the specified tolerance.

The input group contains the parameters that define the particular inspection problem, including test objects, discontinuities and environments. The list of input group (material and discontinuities) parameters identified for the selected ultrasonic inspection procedure are: pylon lug material (steel 4340), stress (if residual stress exists), pylon lug geometry, thickness of pylon lug (essential parameter), surface roughness, surface coatings, couplant condition, temperature, material homogeneity, etc. Discontinuity group influential parameters include: damage types (fatigue or

stress corrosion cracks), sizes and orientations of the discontinuity, crack closure/tip radius, opening or orientation, surface roughness of reflecting surface, tilting/skewing angle of discontinuity. Many of the above parameters (material, homogeneity, etc.) are assumed to remain unchanged during the product life-cycle. Influential parameters from procedure group include: ultrasonic transducer, transducer frequency, sound wave speed, wave length/mode, reference calibration discontinuity notch, beam angle ( $37^\circ$ ), surface distance, scanning direction etc. The equipment influential parameters contain: ultrasonic testing instrument, analog/digital resolution, dynamic range, sampling rate, cables, transducer type (essential parameters), crystal size of transducer (essential parameter) frequency range, resolution, etc.

The physical reasoning section describes the rationale for selecting the procedure for this inspection. Of the available ultrasonic techniques, the pulse-echo ultrasonic technique in angle beam is most suitable for ensuring full volumetric coverage for discontinuity detection. The selection of a  $37^\circ$  angle was determined by a combination of Snell's Law, bench trials and the critical location as the most probable angle for the required inspection. The generally accepted lower limit of detection (rule of thumb approximation) is that a discontinuity (biggest dimension) must be larger than one-half the wavelength for a reasonable chance of being detected. Following this equation, using a 5 MHz shear wave angle beam ultrasonic technique, the estimated detectable discontinuity length would be 0.33 mm (0.013 inches), which is almost half of the target detectable length of 0.64 mm (0.025 inches).

The CIVA ultrasonic simulation software was used to model the sound beam pressure, beam propagation and its interaction with discontinuities using the geometry of the specimen coupled with the as-built probe and wedge (Figure 51 (a)). Parametric studies were performed using CIVA modelling tools to help evaluate the signal response from a crack-like indication. CIVA modelling demonstrated that tilt of the indication was found to be an influential parameter, but not considered to be an essential parameter. Sample thickness variations and variations in probe positioning were found to be essential parameters. Both the LogLog and Logit PoD models produced an  $a_{90/95}$  area value of  $0.16 \text{ mm}^2$ . This would correlate approximately to a 0.4 mm (0.016 inches) by 0.4 mm (0.016 inches) simulated EDM notch.

The technical issues surrounding the reduction of the minimum detectable crack size were investigated. The CIVA simulation results yielded an  $a_{90/95}$  value lower than 0.64 mm (0.025 inches targeted value) (Figure 51 (b)). Despite the simulation and physical reasoning suggesting a little improvement in the detection capability, there is a lack of supportive experimental evidence to confidently support lowering the detectable flaw size of the current inspection procedure. Also there are a number of influencing factors that have not been assessed yet, and these factors can have detrimental effects on the inspection results.

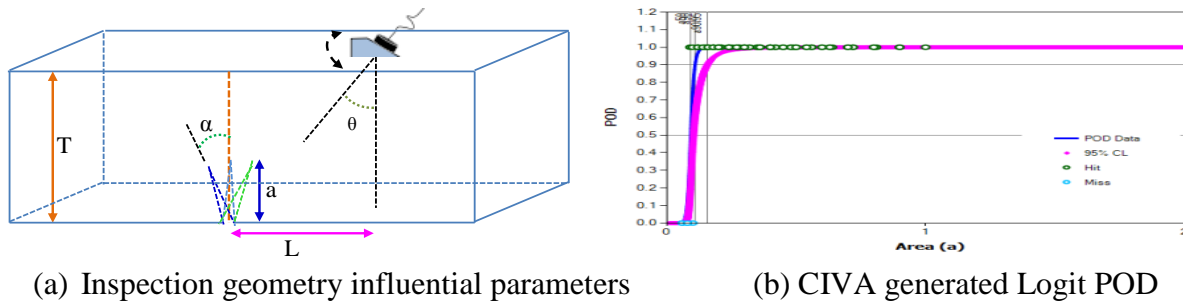


**Figure 51 Inspection geometry and simulation**

### 6.6.1 REFERENCES

- [21] M. Khan, "Technical Justification for an Ultrasonic Inspection Procedure Applied to a Helicopter Component", Proceedings of the International Committee on Aeronautical Fatigue and Structural Integrity (ICAF 2019), Krakow, Poland, Jun 2019.

## 6.7 Equivalent Penetrameter Sensitivity (EPS) for Performance Evaluation of Computed Radiography (CR) Systems

M. Khan, M. Brothers, NRC Aerospace

To obtain radiographic images which are adequate for non-destructive inspection requirements, methods are required to evaluate the performance of the imaging technique. Although visual observation of radiographs can meet part of the quality assessment of radiographic technique, this method is neither a sufficient nor a reliable way for quantitative assessment of image quality. Image quality indicators (IQI) are used in film-based industrial radiography as means to determine if the quality of the radiographic technique is satisfactory. Visualization of a specific IQI in a production radiograph measures the sensitivity or effectiveness of a radiographic technique in detecting small density changes in the evaluated specimen. The sensitivity of radiographic technique is usually represented by its ability to visualize a percentage change of some parameters with respect to the test piece thickness, where a smaller percentage means better radiographic sensitivity.

For computed radiography (CR), the primary metrics for establishing the performance are signal-to-noise ratio (SNR), contrast-to-noise ratio (CNR), and basic spatial resolution ( $SR_b$ ). However, SNR, CNR or  $SR_b$  do not provide enough information for a quick quantitative performance evaluation of the CR technique. Moreover, in CR, often the required IQI hole can be seen in the radiograph even when the computed radiography system's performance, in terms of SNR or CNR,

is inadequate for the application. To address these limitations, the concept of equivalent penetrameter sensitivity (EPS) is being used in CR. The EPS is a measure of the intrinsic (inherent) contrast sensitivity of an imaging system and gives an indication of how well small density changes in objects can be detected at a given exposure level. Instead of a single IQI hole, an EPS test requires a plate with a series of holes and evaluates the number of holes visible using the CR technique. Although the EPS test is subjective, it is considered to be a reliable means to establish and monitor a critical performance metric of CR systems. A case study was performed during the qualification of a CR system, using the EPS concept to demonstrate the concept as a way of reliable means to establish and monitor a critical performance metric of computed radiography systems [22].

The EPS value is defined for hole type IQIs in ASTM E1025-11 as:

$$EPS (\%) = \frac{100}{t_{material}} \sqrt{\frac{T_{IQI} d_{hole}}{2}} \quad (1)$$

Where, EPS - Equivalent penetrameter sensitivity in % of material thickness

$t_{material}$  - Thickness of penetrated material

$T_{IQI}$  - Thickness of IQI,

$d_{hole}$  - Diameter of IQI hole

The purpose of the EPS testing is to determine the exposure levels (exposure charts for CR in analogy to film radiography) necessary to ensure an adequate SNR. The EPS process control tests check the present plateau and compare it with the baseline plateau to ensure that it is stable over time and to determine if a system is getting “noisier” with age. Therefore, it is not only the contrast, but also noise and EPS could be considered as an alternative way to measure SNR.

Although the EPS test standard contains holes similar to a standard hole-type penetrameter, by incorporating multiple holes over an area, the effect of image noise is more robustly assessed. For systems with a linear relationship between pixel value and exposure received, improved visibility corresponds to a low EPS: so in essence a low EPS is analogous to a high SNR and CNR. Although the identification of the number of visible holes is subjective to the judgement of the viewer, this practice is generally accepted in industrial radiography and has been demonstrated to be a reliable means to establish and monitor a critical performance metric of computed radiography systems.

The primary purpose of the EPS test is to find the start of its plateau and the acceptable gray value working range of the CR system and imaging plate combination and was found in this study. EPS plaques are used because they allow the radiographer to discern subtle differences in image quality

as radiographic parameters are changed, and also because they provide an acceptable exposure range for CR imaging plates (Figure 52).

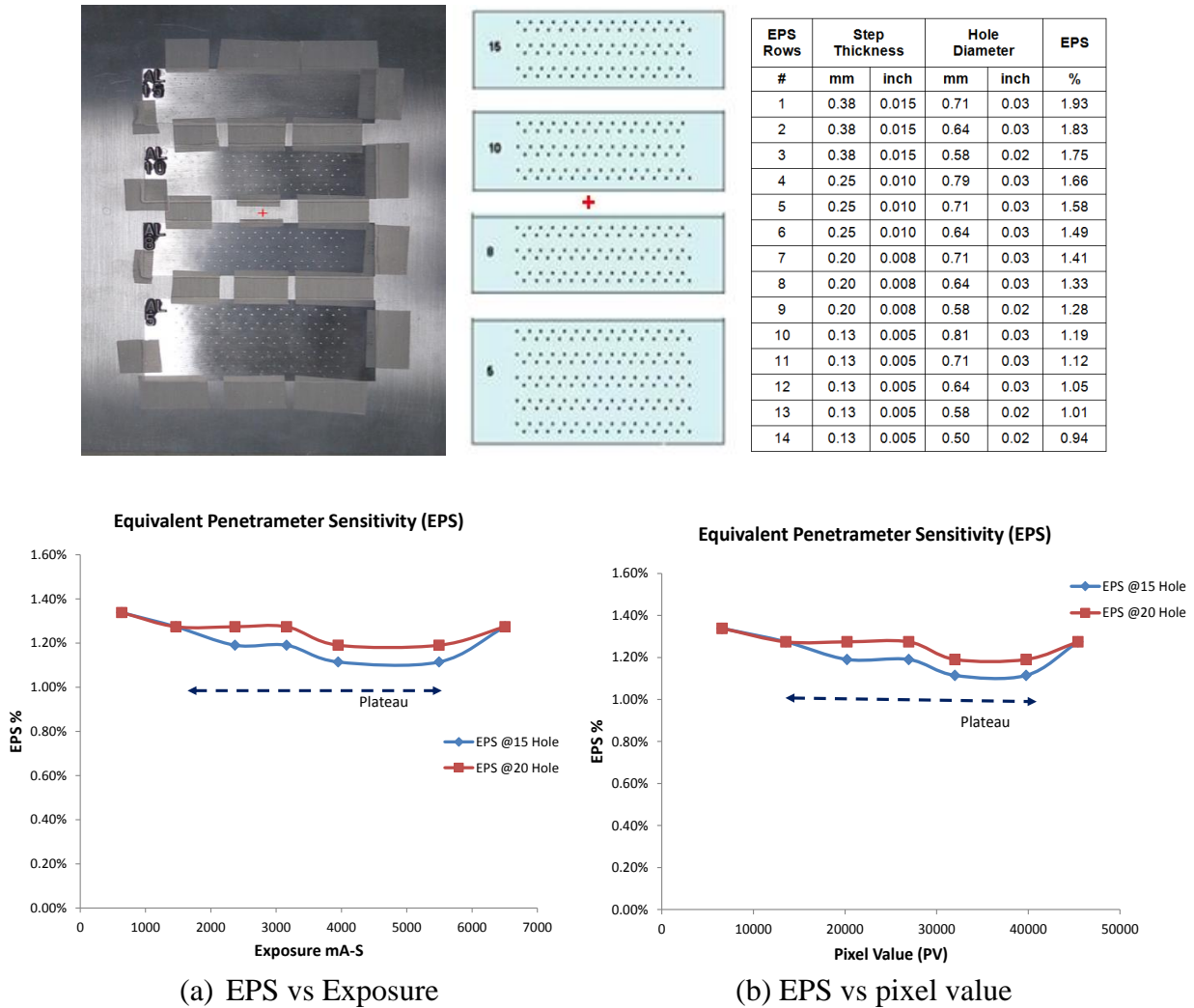


Figure 52 EPS and aluminium (Al) absorber plate setup and EPS curve

6.7.1 REFERENCES

[22] M. Khan, M. Brothers, “Equivalent Penetrator Sensitivity for Performance Evaluation of Computed Radiographic Systems”, 12th European Conference on Non-Destructive Testing, Gothenburg, Sweden, November, 2018.

## **7.0 ENVIRONMENTAL EFFECTS ON FATIGUE AND STRUCTURAL INTEGRITY**

### **7.1 Corrosion Damage Atlas for Aircraft Corrosion Management and Structural Integrity Assessment**

M. Liao, NRC Aerospace

As military aircraft fleets continue to age, most often beyond their original design life, they become more susceptible to the time-dependent effects of corrosion. Corrosion has significant impacts on maintenance cost and fleet availability. For example, the corrosion costs for all aviation and missiles of the United States Department of Defense are \$8.97B in FY17 and \$10.18B in FY18 (LMI annual report on Estimated Impact of Corrosion on Cost and Availability of DoD Weapon Systems), which includes the Air Force costs of \$5.325B (FY17) and \$5.669B (FY18, i.e., 23.6% of total maintenance cost). In addition, corrosion can affect structural integrity by accelerating the time to fatigue crack development and stress corrosion cracking for those safety-of-flight structural locations. Therefore a corrosion assessment is required under the Task II of the United States Air Force (USAF) Aircraft Structural Integrity Program (MIL-STD-1530).

To improve the Royal Canadian Air Force (RCAF) CPCP (corrosion prevention and control plan) program, NRC was tasked by RCAF to carry out CPCP review and assessment for all the RCAF air fleets in 2009-2011. The activities included reviewing the CPCP documents for all fleets to identify common issues/concerns and revising the Canadian Forces Technical Order (CFTO) C-12-010-040-TR-021 that is governing fleet wide corrosion prevention plan.

A team of NRC researchers first reviewed various CFTOs for four fixed wing aircraft (CC-130, CP-140, CF-188, CC-177), two fixed wing lighter aircraft (CC-115, CT-142/Dash-6/7/8) and one rotary wing aircraft (CH124). Then a focused review was conducted on a general document C-12-010-040-TR-021, i.e., *Aircraft Cleaning and Corrosion Control Exterior and Interior*, 1997-04-30, Ch/Mod 5-2008-01-16 (referred as TR021-97/08 in this paper), which aims at all RCAF fleets, especially a few fleets which do not have specific corrosion documents. The C-12-010-040-TR-021 is equivalent to the USAF Technical Manual, TO-1-1-691, i.e., *Cleaning and Corrosion Prevention and Control Aerospace and Non-Aerospace Equipment*. Based on the review and extensive discussion with the RCAF fleet ASIP manager, NRC summarized a number of findings and recommendations including:

- revise/add corrosion definitions in TR021-97/08; provide more realistic corrosion examples/photos (corrosion damage atlas) for the CFTOs, especially TR021-97/08;
- update the outdated (1990s) list for corrosion prevention compounds (CPCs)/corrosion inhibiting compounds (CICs) in the CFTOs following the common MIL standards;

- reassess three levels of corrosion (light, moderate, severe) associated with the non-destructive inspection (NDI) capability and their impacts on structural integrity and fleet management; and
- develop research projects to study topics such as corrosion growth rate for corrosion prognostics and effect of CPC/CIC on new materials used in the new aircraft structures (ex. aluminium alloy 7249 in the new CP-140 wings).

Among the above items, it was strongly recommended that a corrosion damage atlas be developed, which would include images of different types of corrosion and their severity levels. In 2015, NRC developed an aircraft corrosion damage atlas, including additional inputs from The Technical Cooperation Program (TTCP) nations. In 2016, DND issued an updated C-12-010-040-TR-021 (herein referred as TR021-2016), which incorporated some of results and recommendations from the NRC CPCP assessment project.

At the NATO AVT-303 Corrosion Management workshop, NRC presented a paper [23] which summarized some results of the NRC developed corrosion damage atlas with “real-world” examples of various types of corrosion that have been found in military aircraft fleets. Eight forms of corrosion are documented, i.e. 1) Pitting corrosion; 2) Intergranular corrosion (IGC); 3) Exfoliation corrosion; 4) Crevice corrosion; 5) Filiform corrosion; 6) Galvanic corrosion; 7) Stress corrosion cracking; and 8) Fretting corrosion. The damage atlas includes images from destructive and non-destructive inspections (NDI) of corrosion-damaged areas. For comparison, this paper also presents some corrosion sketches updated in TR021 (Figure 53) and explains why and how to use the damage atlas example (Figure 54) together with TR021 for more accurate damage characterization, and for further analyses of corrosion effects on structural integrity.

In particular, the NRC paper [23] highlighted some examples (pitting, IGC, exfoliation) from the damage atlas, and demonstrated that the NRC corrosion damage atlas can be used in conjunction with the RCAF corrosion control manuals (ex. C-12-010-040/TR-021) to improve corrosion level/severity evaluation. The presented corrosion examples were used for assessing their effects on structural integrity in order to assure aircraft safety and continued airworthiness. One of the case studies is presented in Figure 55. In the end, this paper discussed a major gap/need on corrosion growth rate material model and data. This paper suggests to continue updating the NRC corrosion damage atlas by collecting more real-world examples from service and including new materials (ex. 7249 versus 7075, as shown in Figure 56). As a result, it is expected that operators can continue improving military aircraft corrosion management with reduced cost and improved availability.

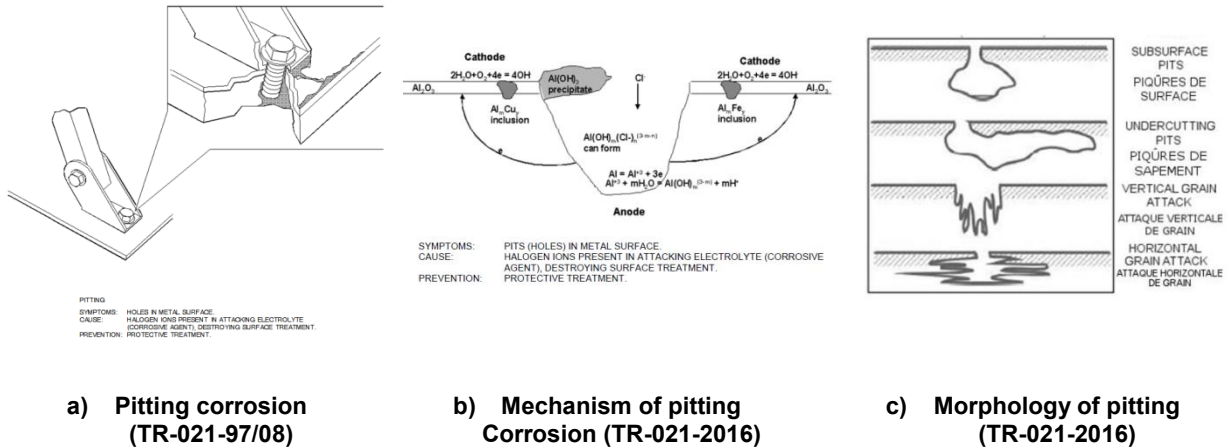


Figure 53 Pitting corrosion sketch and updates in DND C-12-010-040-TR-021

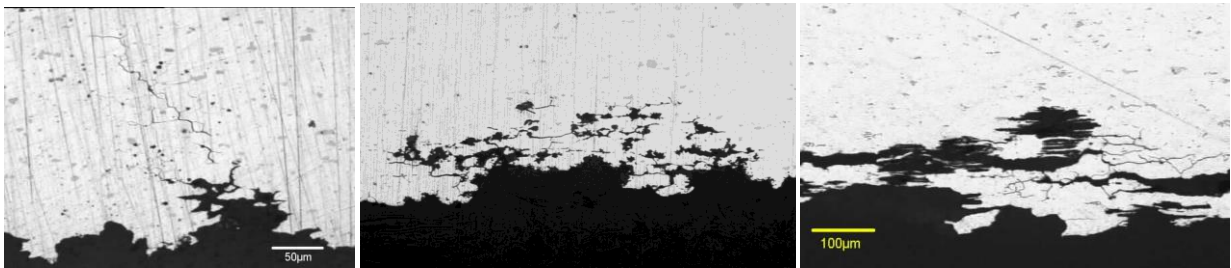


Figure 54 Optical micrographs showing additional damage at base of pits found on the faying surface of a 2024-T3 fuselage lap joint

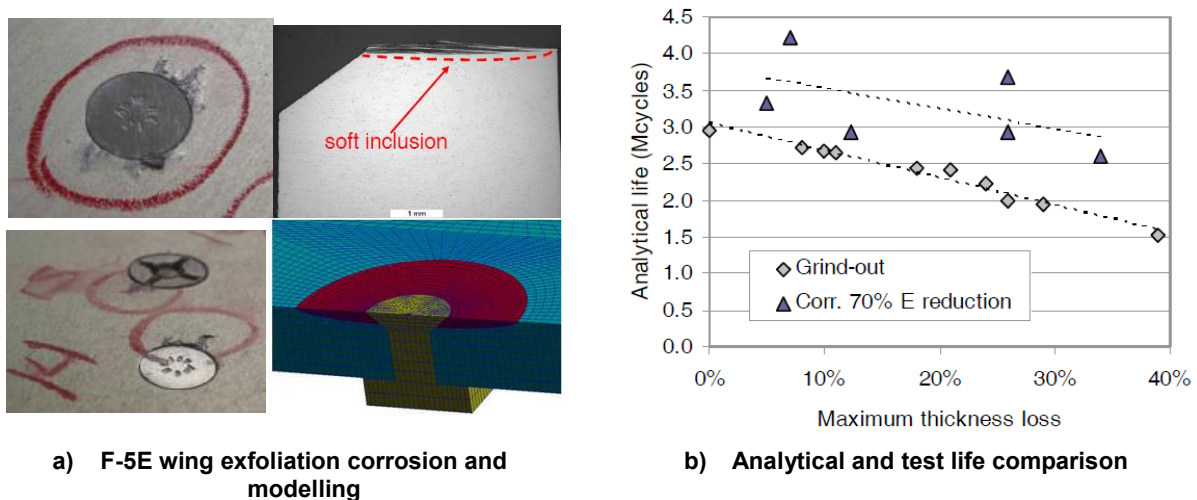
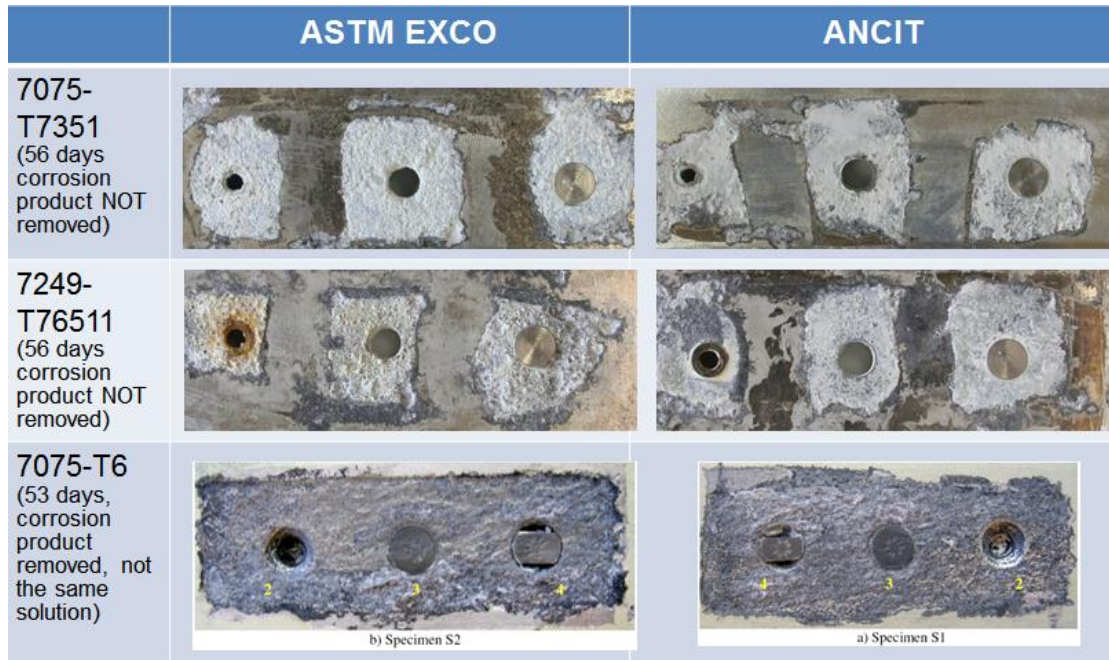


Figure 55 Modelling of exfoliation corrosion effect on F-5E upper wing (7075) structural integrity



**Figure 56 Accelerated corrosion tests for aluminum alloys, 7075-T7351, 7249-T76511, and 7075-T6**

### 7.1.1 REFERENCES

- [23] M. Liao, "Corrosion Damage Atlas for Aircraft Corrosion Management and Structural Integrity Assessment", Proceedings of the NATO AVT-303 Corrosion Management Workshop (STO-MP-AVT-303), Athens, Greece, December 2018. ISBN: 978-92-837-2208-3, DOI: 0.14339/STO-MP-AVT-303-07-PDF  
(<https://www.sto.nato.int/publications/STO%20Meeting%20Proceedings/STO-MP-AVT-303/MP-AVT-303-07.pdf>)

## 7.2 Effect of Alternative Paint Stripping Processes on the Fatigue Performance of Aluminium Alloys\*

A. Merati, M. Yanishevsky, and Y. Bombardier, NRC Aerospace

\* Paper being presented at ICAF2019

As reported in the last ICAF symposium, NRC has been tasked to investigate the potential of the novel de-painting technologies; Atmospheric Plasma (AP) and Laser Ablation (LA). Typically, aircraft paint schemes lose their effectiveness for corrosion protection as well as cosmetic

appearance every three to five years. As such, an aircraft will usually undergo at least five paint / de-paint cycles in their lifetime. The conventional methods for removing paint employed throughout the Canadian Forces mainly include environmentally unfriendly chemical stripping and abrasive media blasting. These processes yield high amounts of volatile organic compounds and generate large quantities of waste which requires proper disposal / treatment. Concern over environment, safety and worker health with current paint removal processes has resulted in the enactment of new alternative removal processes during the past several years.

In this study, the effectiveness of the novel AP and LA systems are compared to a chemical solution and Type VII starch-acrylic media blasting stripping processes. The fatigue behaviour on both the paint-stripped and unstripped sample/region were measured and compared. The graphs in Figure 57 compare each crack on the stripped region to its mirrored crack in the unstripped region, seen in Figure 58.

So far fatigue testing and crack length measurements revealed that the novel paint stripping processes, similar to the traditional processes, were neither detrimental nor beneficial to the fatigue properties of the aluminium substrates. In all cases, regardless of paint colour, substrate thickness or aluminium alloy, the averages of the crack lengths in the paint stripped regions were approximately equivalent to the lengths in the unstripped regions.

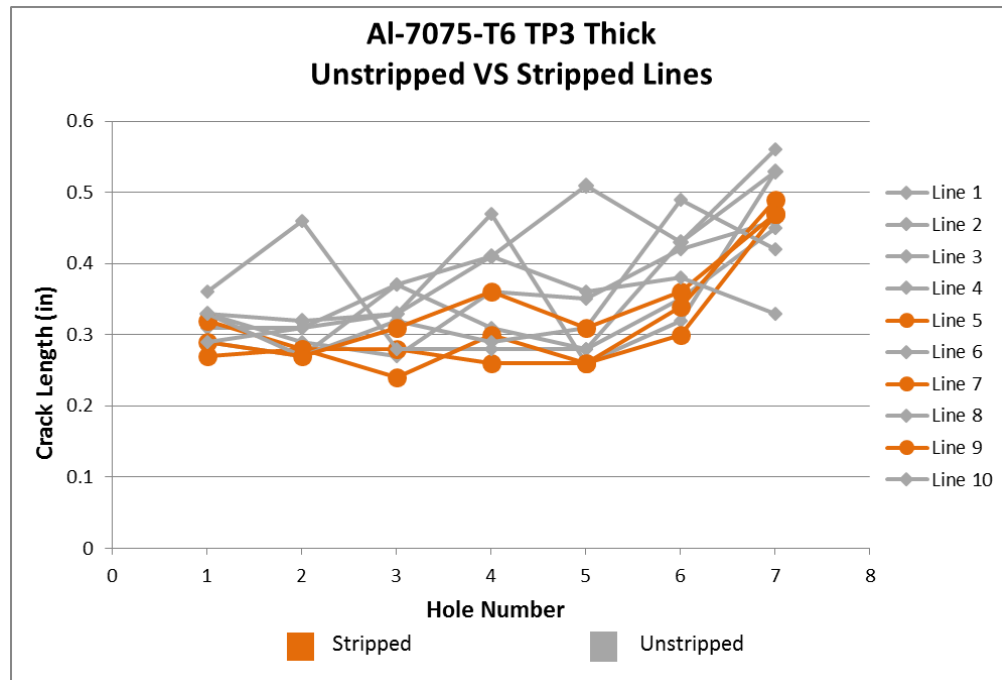


**Figure 57 Al-7075-T6 TP3 full crack length results and comparison between all lines on the test panel**

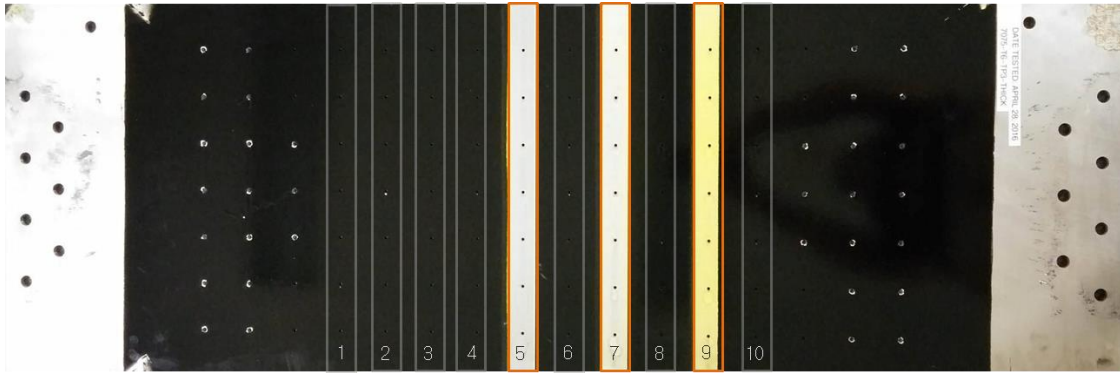


**Figure 58 Panel layout showing stripped and non-stripped lines in Figure 57.**

#### 7.2.1 REFERENCES

- [24] A. Merati, M. Yanishevsky, T. Despinic, P. Lo, V. Pankov, “Alternate Environmentally Friendly De-Painting Process for Aircraft Structures - Atmospheric Plasma”, JA-SMM-2017-0038, Journal of Minerals and Materials Characterization and Engineering (JMMCE), Vol. 5, July 2017, pp. 223-235.
- [25] M. Yanishevsky, A. Merati, Y. Bombardier, “Fatigue Testing of Baseline and Atmospheric Plasma Treated 2024-T3 Aluminium Alloy Sheet”, NRC, Laboratory Technical Report, LTR-SMM-2017-0130, November 2017.

## 8.0 FATIGUE AND STRUCTURAL INTEGRITY OF COMPOSITES

### 8.1 Surface Damage Evaluation of Textured Aluminium Honeycomb Sandwich Panels

J. Sun and D. Wowk - Royal Military College of Canada, C. Marsden – Concordia University

3D laser scanning has been proposed as an efficient tool for evaluating surface damage in aerospace sandwich panels. This method has been proven to provide accurate and repeatable measurements for dents in flat and moderately curved panels, but has not yet been applied to textured floor panels [26]. The current study examines the use of laser scanning for quantifying the depth, area and diameter of dents in flat honeycomb sandwich panels with a raised textured pattern. This pattern is typical of the non-slip surface for exposed floor panels (Figure 59 a)), but creates challenges with the identification and measurement of dents. In the proposed method, the textured pattern is removed from the fits of the damaged and undamaged surfaces to allow for a deviation analysis to be performed.

The entire floor panel is scanned using a FARO® ScanArm apparatus mounted to a lab workstation to generate a point cloud of 3D scan data. A preliminary analysis is performed on the entire floor panel in order to identify the locations and approximate sizes of the dents. A deviation analysis was used to measure the distance between the raw point cloud data that includes the textured pattern and an idealized flat undamaged surface. Figure 59 b) shows approximations of the dented regions in the panel identified in yellow. The red circles are the tie downs.

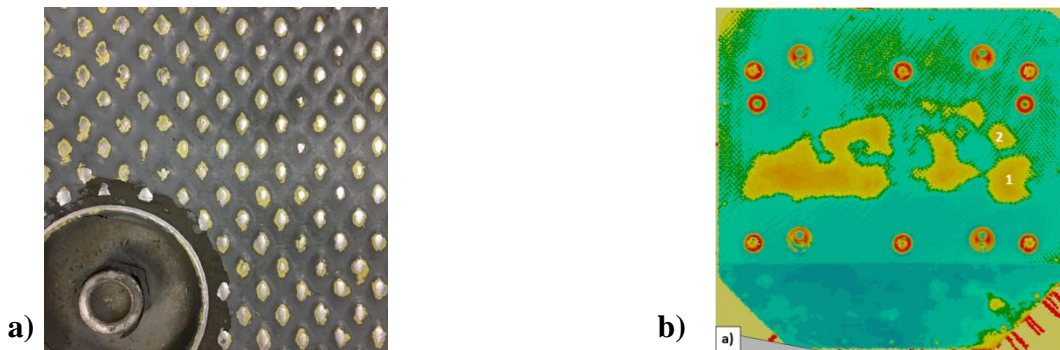


**Figure 59 a) Close-up of the textured tread pattern on the floor panel, b) preliminary deviation analysis of the entire floor panel with the dented regions shown in yellow**

A more detailed analysis is then performed for each identified dent individually on a smaller 110 mm by 135 mm area of the panel. A mesh fit of the undamaged surface was created by defining

control regions in between the protrusions. The control regions were only defined in the region surrounding the dent (Figure 60 a)), as identified from the preliminary analysis. Being able to accurately recreate the undamaged panel surface is a key step in the process, as the original geometry of the panel is typically not available to the inspection personnel. A mesh fit of the damaged surface was created by defining control regions between every protrusion, including within the dent region (Figure 60 b)). Surfaces are fit through these control regions, and defining the control regions between the protrusions has the effect of removing the texture from the surface fits.

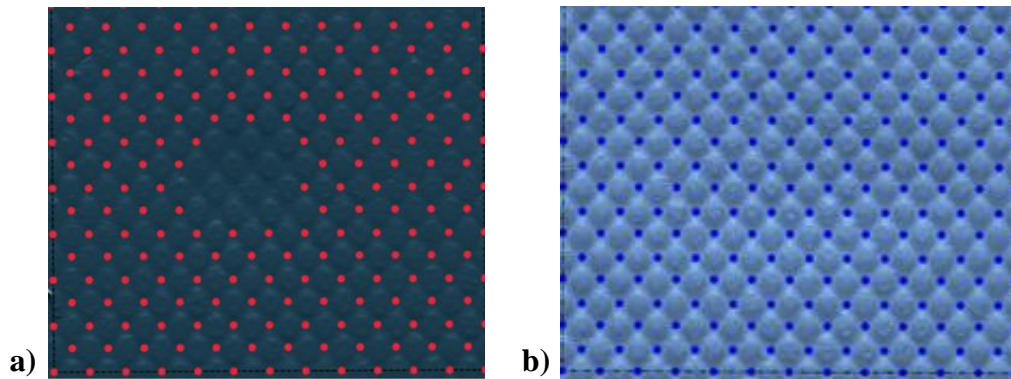


**Figure 60 a) Control regions defined for the undamaged surface fit surrounding an individual dent, b) control regions defined for the damaged surface fit surrounding an individual dent**

A deviation analysis is then performed within Geomagic Design X, where the perpendicular distance between the damaged and undamaged surface fits is extracted in order to provide the dent depth. The dent depth is shown as a contour plot in Figure 61 a), where green represents the undamaged panel, and yellow and orange represent different dent depths. The area and diameter of the dent was automatically extracted using the image processing software ImageJ by creating a black and white image, as shown in Figure 61 b).

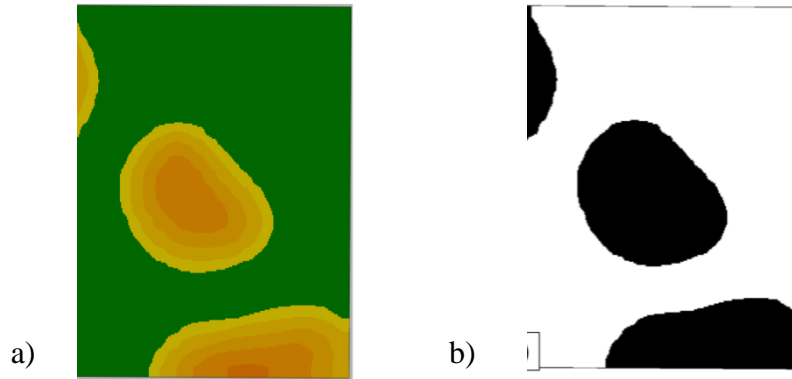


**Figure 61 a) Deviation analysis results showing the deepest part of the dent in orange, b) black and white image used for extracting the dent area and diameter**

The accuracy of the 3D laser scanning method was evaluated by comparing the dent depth and area to measurements obtained with the manual procedure currently used in the field. The difference was 0.22 mm in the dent depth and 6.3% in the dent area. Laser scanning has the potential to provide an efficient, accurate and repeatable method for determining dent depth and area in the field. Work is presently underway to automate this method.

### 8.1.1 REFERENCES

- [26] Reyno T., Marsden C., Wowk D., “Surface damage evaluation of honeycomb sandwich aircraft panels using 3D scanning technology”, *NDT&E International*, 97 (2018), pp. 11-19.

## 8.2 Numerical Modelling of Composite Material and Structural Failure Behaviours

Gang Li, NRC Aerospace

### 8.2.1 COHESIVE ZONE MODELING OF A UNIDIRECTIONAL CFRP DCB TEST ON PROGRESSIVE FAILURE [27]

A parametric study was conducted using 2D FE models combined with cohesive elements to simulate progressive failure behaviour of a composite double cantilever beam (DCB) specimen in Mode I static loading. The bilinear traction-separation law was used to govern the cohesive elements. Effects of selected key factors: increment step size, cohesive element length, cohesive strength, and stiffness, were investigated. Acceptable numerical results were successfully sorted by the peak load convergence and then a tight fracture toughness,  $G_{IC}$ , agreement degree specified between the input and the output values. The NRC method would give closer  $G_{IC}$  values than the

relevant ASTM method using the numerical results, as compared with the input value. With a small difference, say 5% in  $G_{IC}$ , almost identical load-displacement variation profiles were obtained, by the models using different mesh conditions and different cohesive parameters. Discussion was also provided regarding the minimum number of the cohesive elements within the cohesive zone length, and modelling robustness using the cohesive elements in this study [27].

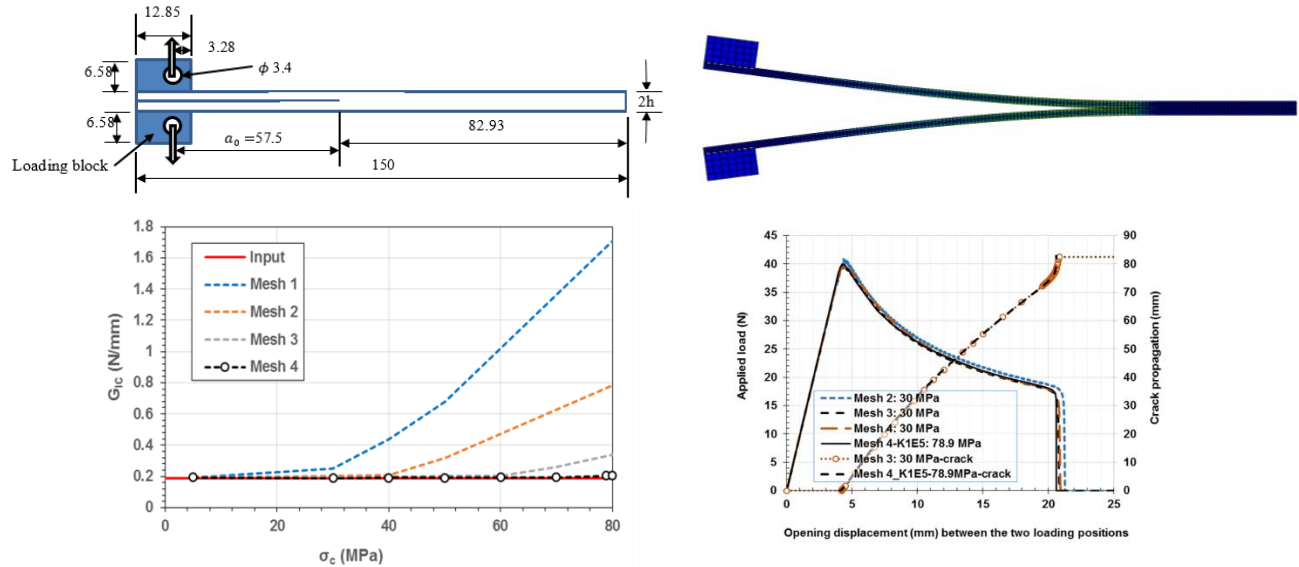


**Figure 62 A quasi-static CFRP DCB test and cohesive zone modeling of progressive failure**

### 8.2.2 PROGRESSIVE FAILURE OF A BONDED 3D COMPOSITE SECTION [28]

A 3D finite element model combined with cohesive surface behaviour was created via ABAQUS CAE code, version 6.14r2, to simulate progressive failure behaviour of a bonded composite section structure. Only the cohesive failure at the adhesive surfaces was considered in this modelling analysis. The effect of the adhesive layer was represented by the cohesive behaviour at the interfaces between the panel and the 3D stiffener. Three-dimensional continuum shell elements were used to mesh the composite parts and 3D stress elements were used to mesh the steel fixtures. The predicted peak failure load was employed to guide the experimental rig design, test coupon preparation, and to ensure that the testing was successfully conducted. Excellent agreement in the peak failure load within 3% difference was obtained between the numerical and the experimental result.

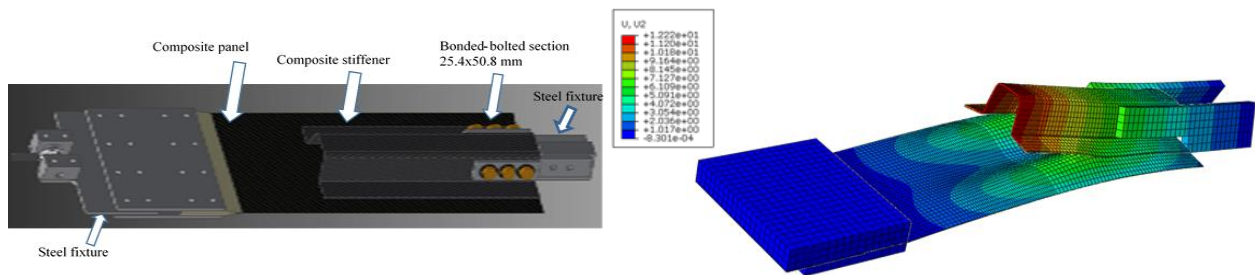


**Figure 63 Failure strength prediction of a bonded composite structure**

### 8.2.3 REFERENCES

- [27] G. Li, G. Renaud, M. Liao, “Assessment of cohesive elements on simulating progressive failure behavior of a unidirectional laminated DCB Specimen Configuration”, NRC, Laboratory Technical Report, LTR-SMM-2019-0032, 2019.
- [28] G. Li, C. Li, “Numerical assessment of the effects of dimension and layup on a bonded composite section joint design”, The CASI ASTRO 18 Conference, 15-17 May 2018, Quebec City, Canada.

## 9.0 FATIGUE AND STRUCTURAL INTEGRITY OF NEW MATERIAL AND MANUFACTURING

### 9.1 Measurement of the Resistance to Fracture of 7249-T76511 Aluminium Extrusion

Y. Bombardier, NRC Aerospace

During the course of the P-3C/CP-140 Service Life Assessment Program (SLAP), Lockheed Martin Aeronautics (LMA) and the United States Navy (USN) undertook a program to identify a newer aluminium (Al) alloy capable of reducing the susceptibility of the P-3C fleet to corrosion and stress corrosion cracking. This development program led to the selection of Al 7249-T76511 extrusion (Al 7249) as the material of choice to replace the original Al 7075-T6511 (Al 7075) for all new wings. The initial Al 7249 test results showed that the material properties of Al 7249 were equal to or superior to Al 7075 in every instance that was tested. To reduce material testing costs, it was assumed that the overall fatigue performance of Al 7249 was similar to Al 7075, enabling P-3C operators to employ the extensive data set previously generated for Al 7075. Subsequent testing has shown that this assumption was optimistic and that further material evaluation was required. The current test results indicate that the fatigue crack growth threshold of Al 7249 is significantly lower than that of Al 7075, allowing cracks to develop and grow more rapidly at very low stress intensity factor ranges. It was also found that Al 7249 does not exhibit the same level of crack growth retardation as Al 7075 for structures subjected to loading spectra with loads producing high stresses, resulting in shorter crack growth lives and reduced inspection intervals.

In an attempt to extend the current inspection intervals, the National Research Council Canada (NRC) was tasked to measure the crack growth resistance ( $K_R$ ) of Al 7249 as a function of material thickness to accurately establish the residual strength capability of the CP-140 structures instead of relying on the unsubstantiated assumption that Al 7249-T76511 has equivalent or better crack growth resistance than the original material, Al 7075-T6511.

The fracture toughness of 7249-T76511 aluminium (Al 7249) was tested according to the ASTM E561 standard method using middle-cracked tension specimens. Four specimen thicknesses were tested: 0.090, 0.110, 0.270, and 0.400 inch. For the tested thicknesses, it was observed that the fracture toughness of Al 7249 unexpectedly increased as a function of thickness. This unexpected trend can be explained by the fact that the fracture toughness can gradually decrease as thickness decreases when plane stress conditions prevail, because the volume of material available for plastic deformation energy absorption decreases. Despite this unexpected trend, where there was a reduction in fracture toughness for thinner specimens, the results show that Al 7249 has higher fracture toughness than the original alloy used for the P-3C/CP-140 wing

(7075-T6511) along the L-T direction. By comparison, the fracture toughness of Al 7249 aluminium extrusion is equal to or better than 7075-T76511 aluminium extrusion.

### 9.1.1 REFERENCES

- [29] Y. Bombardier, “Measurement of the resistance to fracture of 7249-T76511 aluminium extrusion”, NRC, Laboratory Technical Report, LTR-SMM-2017-0056, Ottawa, 2017.

## 9.2 Application of Multifunctional Mechanical Metamaterials

Ali Shanian<sup>1</sup>, Francois-Xavier Jette<sup>1</sup>, Mahtab Salehii<sup>1</sup>, Minh Quan Pham<sup>1</sup>, Megan Schaezner<sup>1</sup>, Genevieve Bourgeois<sup>1</sup>, Katia Bertoldi<sup>2</sup>, Andrew Gross<sup>2</sup>, Farhad Javid<sup>2</sup>, David Backman<sup>3</sup>, Scott Yandt<sup>3</sup>, Miklos Gerendas<sup>4</sup>, Tobias Meis<sup>5</sup>, Karsten Knobloch<sup>6</sup>, Friedrich Bake<sup>6</sup>, and Dieter Peitsch<sup>7</sup>

<sup>1</sup>Siemens Canada, <sup>2</sup>Harvard University, <sup>3</sup>NRC Aerospace, <sup>4</sup>Rolls-Royce Deutschland, <sup>5</sup>Siemens AG, <sup>6</sup>German Aerospace Center (DLR), <sup>7</sup>TU Berlin

Mechanical metamaterials have attracted great interest due their ability to attain material properties outside the bounds of those found in natural materials. Many promising mechanical metamaterials have been designed, fabricated, and tested; however, these metamaterials have not been subjected to the rigorous requirements needed to certify their use in demanding industrial applications that require multifunctional behaviour. This multidisciplinary research program details an auxetic multifunctional metamaterial that has been optimized to outperform conventional designs for cooling systems commonly used in space, transportation, energy and nuclear industries. Experimental testing performed to certify this material for use in gas turbines have shown that in comparison to conventional designs, the metamaterial increases structural life by orders of magnitude, while also providing more efficient cooling and maintaining acoustic damping characteristics (Figure 64). This auxetic multifunctional metamaterial offers an agile and economical solution for the realization of next generation components.

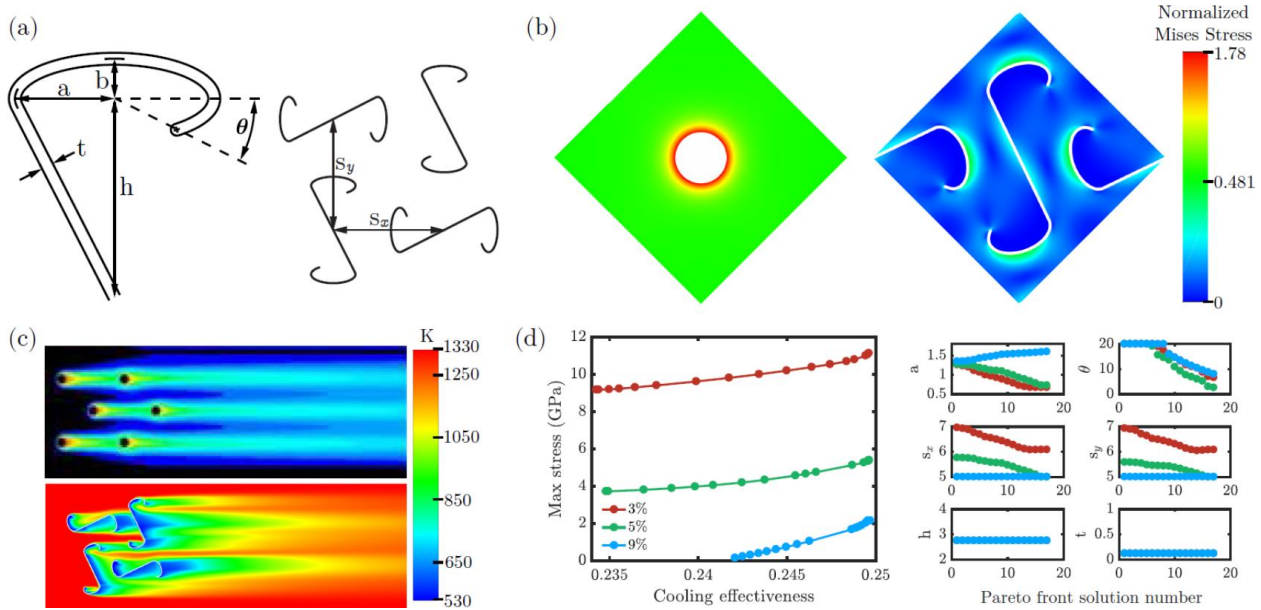


**Figure 64 (a) The six geometric parameters that define the S-slot metamaterial. During optimization, the parameter  $b$  is held constant. (b) One of the mechanical simulations from the optimization of S-slot geometry compared to the conventional design of circular holes.**

**Both are subjected to the same level of equibiaxial strain with periodic boundary conditions. Contours of von Mises stress are normalized by the value of stress present in an unperforated plate loaded in the same manner. (c) One of the fluid flow simulations from the optimization of the S-slot geometry compared to the conventional design. Contours correspond to the near wall gas temperatures. (d) Pareto fronts from the multi-objective optimization at three values of porosities, and the values of the S-slot geometric parameters for each solution on the Pareto front.**

### 9.2.1 REFERENCES

- [30] F. Javid, J. Liu, A. Rafsanjani, M. Schaezner, M.Q. Pham, D. Backman, S. Yandt, M.C. Innes, C. Booth-Morrison, A. Shanian and K. Bertoldi, "Architected porous materials with enhanced fatigue life", *Advanced Materials*, 2017-05-05.

### 9.3 Durability and Damage Tolerance of Additive Manufacturing Polymer Parts for Aerospace Application\*

H. El Fazani, J. Coil, J. Laliberté, Carleton University

\* Paper being presented at ICAF2019

Additive manufacturing (AM) technology has great advantages due to its ability to create lightweight structure with complex geometries that can suite most industries including aerospace. AM has been receiving a lot of attention from industry, research, as well as academia [31]. However, there is a current need to better understand the material behaviour of AM printed parts. The lack of research publications on fatigue analysis for AM polymer parts manufactured was discussed in [32] and [33]. For this reason, more fatigue testing must be carried out to gain a better understanding of the material behaviour. The fatigue crack propagation behaviour for AM polymers continues to be an active area of study in the aerospace industry.

The objective of this research is to study the application of damage tolerance and fatigue evaluation to polymer parts made by AM technology. Therefore, the fatigue characteristics of polymer parts made by the Stratasys BST 1200es fused deposition machine (FDM) were tested experimentally, including the influence of building orientation on the fatigue life of the AM parts. The crack growth in AM polymer specimens was also monitored, as well as the effect of stress intensity factor on the crack growth.

The material used to manufacture the AM parts was a commercial polymer acrylonitrile-butadiene-styrene (ABS) P430. The fatigue coupon design and dimensions followed the ASTM standard. The layout for flat and on-edge samples are illustrated in Figure 65. In this study, the flat specimens were manufactured at different angles of orientation ( $0^\circ$ ,  $22.5^\circ$ ,  $45^\circ$ ,  $67.5^\circ$ , and  $90^\circ$ ), and the on-edge parts were built with ( $0^\circ$ ,  $45^\circ$  and  $90^\circ$ ) orientations. The proposed test matrix and number of test coupons is presented in Table 8.

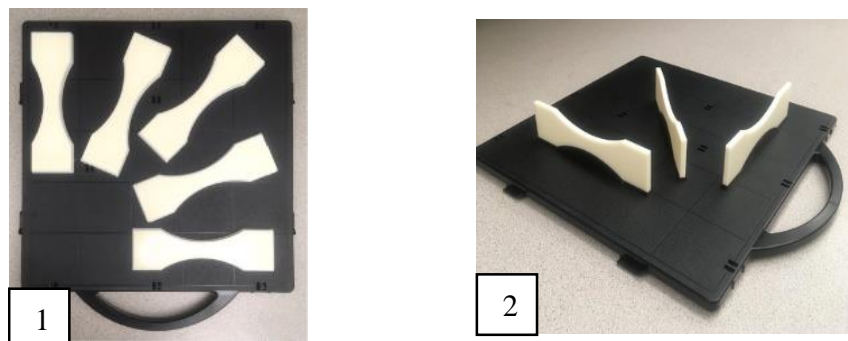
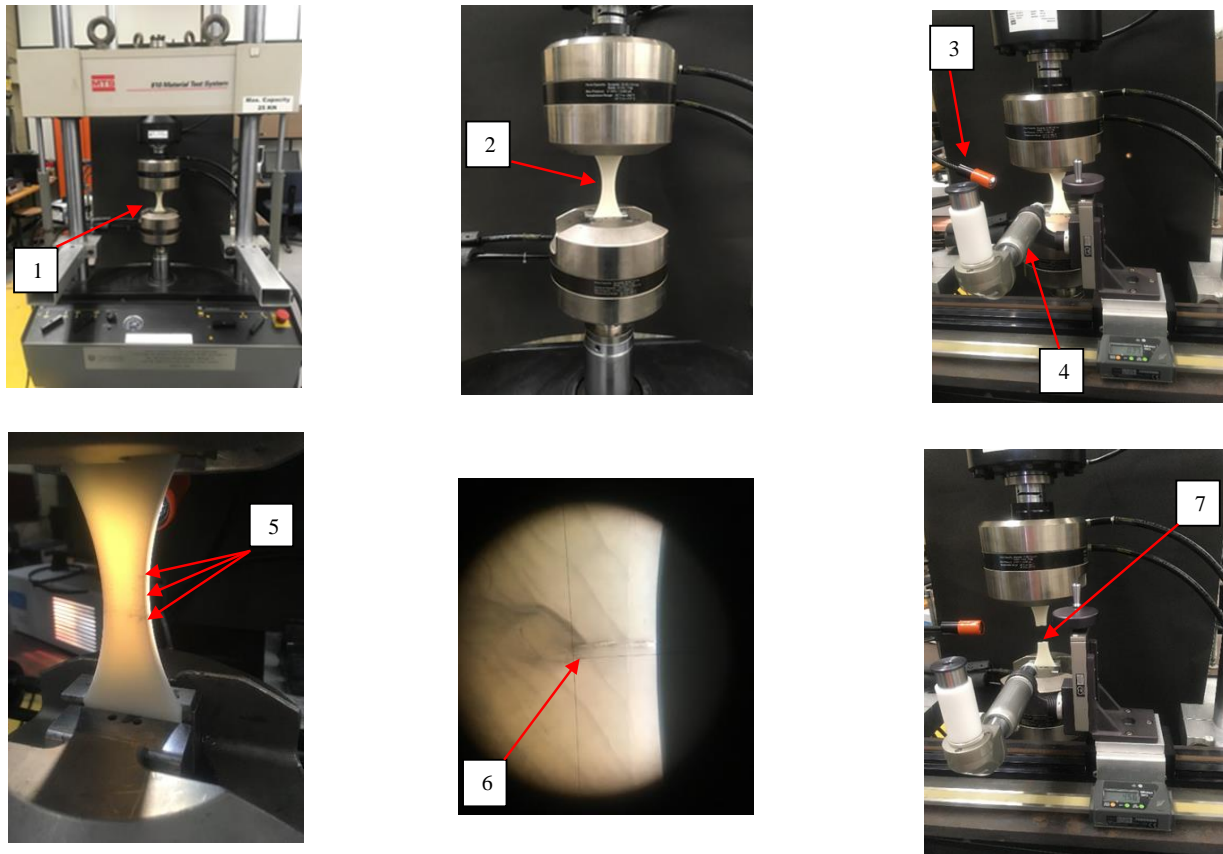


Figure 65 Fatigue coupon: 1. Flat specimen, 2. On-edge specimen

**Table 8 Material test matrix**

AM process and orientations		Minimum number of acceptable fatigue test					Total
		0°	22.5°	45°	67.5°	90°	
Stratasys BST 1200es (FDM)	Flat	4	3	4	3	7	21
	On edge	3	-	3	-	3	9
Total		7	3	7	3	10	30



**Figure 66 Fatigue Testing: 1. Specimen mounted at 25 kN MTS load frame, 2. Close-up of specimen in fatigue testing, 3. Light source 4. Travelling microscope, 5. Multiple crack sites, 6. Single crack length measurements, 7. Specimen at failure.**

Fatigue analysis was conducted and both fatigue crack formation and crack propagation were investigated. However, the focus of this study was on crack formation. The fatigue test was based on measuring the crack length of AM specimens caused by low cyclic fatigue loading. As shown in Figure 66 an optical microscope was used to track the crack formation. Also, multiple cracks were measured within the same AM specimen. The relation between crack length, for individual

crack and multiple cracks, versus the number of fatigue cycles was obtained. The variation of fatigue lives with specimen build orientations was discussed including the influence of building sides on fatigue life. This research will also help identify which fatigue test methods are suitable for polymer AM components.

### 9.3.1 REFERENCES

- [31] C. Lindemann, T. Reiher, U. Jahnke, and R. Koch, "Towards a sustainable and economic selection of part candidates for additive manufacturing," *Rapid Prototyp. J.*, vol. 21, no. January, pp. 216–227, 2015.
- [32] C. W. Ziemian, R. D. Ziemian, and K. V. Haile, "Characterization of stiffness degradation caused by fatigue damage of additive manufactured parts," *Mater. Des.*, vol. 109, pp. 209–218, 2016.
- [33] S. Ziemian, M. Okwara, and C. W. Ziemian, "Tensile and fatigue behaviour of layered acrylonitrile butadiene styrene," *Rapid Prototyp. J.*, vol. 21, no. 3, pp. 270–278, 2015.
- [34] H. Fazani, J. Laliberté, "Durability and Damage Tolerance of Additive Manufacturing Polymer Parts for Aerospace Application", *Proceedings of the International Committee on Aeronautical Fatigue and Structural Integrity (ICAF 2019)*, Krakow, Poland, Jun 2019.

## 9.4 Case Study: In-Service use of Additively Manufactured Aircraft Structural Components

R. Amos, D. Backman, F. Kirby, NRC Aerospace

The ability to additively manufacture aircraft structural components on demand is of great interest, especially to maintenance and repair organizations who struggle with repair and replacement of legacy structures. To better understand how to produce a certified part that could be used in an aircraft, a candidate aircraft structural component was selected and a building block approach to building and testing the part was employed. This case study details the implementation of many of the key steps required for eventual certification, including: extensive characterisation of the manufacturing process, non-destructive inspection of the candidate parts, and structural testing of the candidate structure to ultimate load. For the structural test, the digital image correlation method was used to determine full field strain in over a significant portion of the structure, while marker tracking was used to measure the displacement of fasteners under loading. The results of the testing showed that the candidate part was able to withstand both design limit and ultimate loads with strains remaining in the elastic range.

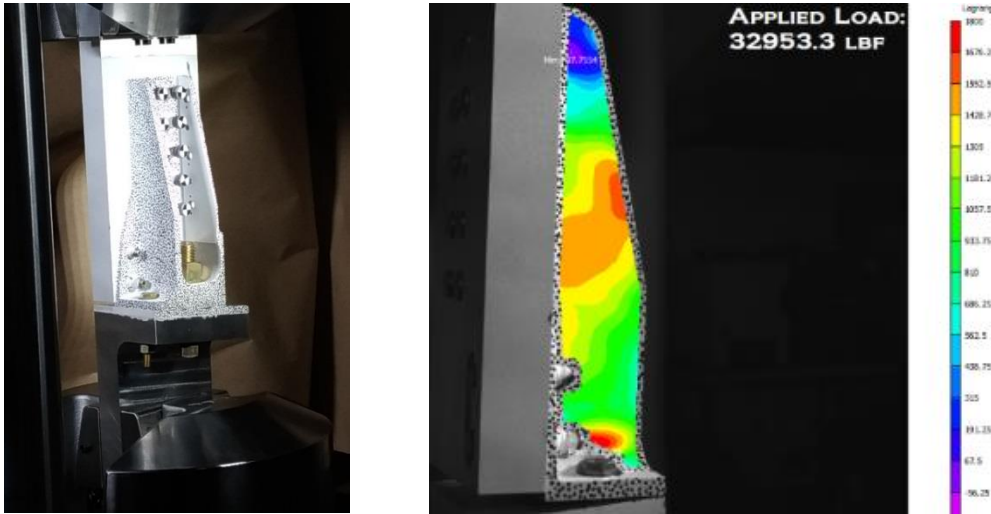


**Figure 67** Static test of an additively manufactured aircraft structural corner fitting, using digital image correlation technique

## 9.5 Deformation and Evolution of Life in Crystalline Materials – An Integrated Creep Fatigue Theory

X. Wu, NRC Aerospace

An integrated creep-fatigue theory (ICFT) was developed starting with the understanding of the physical nature of basic materials – crystalline structures and imperfections (dislocations and vacancies), and the kinetics of their movements in a microstructure strengthened by mechanisms involving the interactions of dislocations with various point defects (solute atoms), line defects (dislocations themselves), planar defects (grain boundaries and interfacial discontinuities) and volume defects (precipitates and inclusions), as described in Chapters 1-4 [35]. The ICFT deals with deformation and crack growth processes involving creep, low-cycle fatigue (LCF), high-cycle fatigue (HCF), and thermomechanical fatigue (TMF) and their life prediction for various engineering materials, described in the remaining Chapters of [35].

Regarding creep (Chapter 5), a deformation-mechanism based true-stress (DMTS) creep model is first developed with consideration of the oxidation effect. The DMTS model describes the entire creep curve behaviour including the primary, secondary and tertiary stages, and predicts the creep life with specified failure mode, i.e. transgranular or intergranular fracture. Furthermore, with consideration of oxidation, which is missing in other creep life prediction methods, it is shown that the DMTS model can truly predict long-term creep life ( $> 10^4$  hours) based on short-term creep tests ( $< 10^4$  hours), as warranted by the physical mechanisms.

Regarding LCF (Chapter 6), first, the Tanaka-Mura model is modified with the corrected dislocation dipole pileup strain formulation and thus the fatigue crack nucleation life is predicted just based on the material's Burgers vector, Poisson's ratio, elastic modulus and surface energy, without resorting to experiments, for the first time in the 150-year history of fatigue study. For high temperature LCF, the ICFT model evaluates the life evolution by considering internally distributed damage via creep and intergranular embrittlement, as well as oxidation. Thus, the ICFT model describes the many-faceted phenomena of LCF including the crossover-behaviour, the temperature, and frequency dependence of LCF life. Demonstrations are shown for ductile cast iron, austenitic cast steel, and Co/Ni base superalloys.

Regarding TMF (Chapter 7), it is shown that the TMF behaviours and life under various TMF conditions including in-phase (IP), out-of-phase (OP) and constrained TMF can be sufficiently described using the LCF-calibrated ICFT model. This further proves that complicated TMF behaviours are merely manifestation of the underlying physical deformation and damage mechanisms under the given loading profiles (or boundary conditions). This approach can save a lot of testing efforts in characterization of TMF for components.

Regarding HCF (Chapter 8), particular emphasises are given to HCF problems with imposed cold dwell and prior creep history. The cold dwell damage is related to accumulation of Zener-Stroh-Koehler (ZSK) dislocation pile-ups, and prior creep history effect is related to grain boundary voids/crack formations, even during steady-state creep. Both phenomena are governed by the same ICFT damage equation, where a linear damage accumulation rule does not work in these cases.

The microscopic crack nucleation and growth are treated as either Zener-Stroh-Koehler (ZSK) or Bilby-Cottrell-Swinden (BCS) dislocation pile-ups in anisotropic materials (Chapter 9). Hence, short crack behaviour can be described by the extended slip band (ESB), the blocked slip band (BSB) and the propagated slip band (PSB) models, composing the corresponding dislocation pile-up solutions for anisotropic materials, especially for the initial stage of crack growth.

The macroscopic or long crack growth behaviour has been well known in terms of linear elastic fracture mechanics (LEFM), for which a restricted slip reversal (RSR) model has been developed to describe transgranular fatigue crack growth rate (Chapter 10). The applicability of LEFM lies in the K-similitude with fatigue crack growth rate data generated from standard coupons containing long cracks. However, load-shedding tests could cause crack closure, which violates the K-similitude and affects the "fatigue threshold". An energy approach is developed to derive a new definition of the "effective stress intensity factor range", conforming to the Irwin-Kies approach. Furthermore, creep crack growth is considered as a grain boundary slip dominated process driven by stress-relaxation by multi-deformation mechanisms in the crack-tip zones.

Special topics on advanced gas turbine materials such as single crystal Ni-base superalloys, thermal barrier coatings and ceramic matrix composites are also discussed (Chapters 11-13).

Finally, component-level life cycle management approaches for gas turbine engine components against common component damage modes are discussed (Chapter 14). Both the safe-life and damage-tolerance approaches are reviewed, and the holistic structural integrity process (HOLSIP) approach is discussed from the ICFT point of view. A case study of nozzle guide vane using the ICFT approach is described. A new 3D weight function is introduced, which allows fracture mechanics analyses without meshing for the crack growth. Fracture analyses of gas turbine blade and spacer are then performed using this weight function method. There is still more work regarding the four stages of HOLSIP: i) crack nucleation, ii) short crack, iii) long crack, and iv) unstable fracture, which are also described in [35].

#### 9.5.1 REFERENCE

- [35] X. Wu, Deformation and Evolution of Life in Crystalline Materials: An Integrated Creep-Fatigue Theory, 1<sup>st</sup> Edition, CRC Press Published April 15, 2019; ISBN 9781138296732 - CAT# K35630.

## **10.0 ACKNOWLEDGEMENTS**

The NRC programs, Defence Technologies and Sustainment (DTS) and Aeronautical Product Development and Certification (APDC) provided support for the NRC's effort to prepare this ICAF National Review.

Special thanks to all the organizations and authors who have contributed the various inputs to the Canadian National Review for ICAF2019.

Special thanks to Marko Yanishevsky for closely reviewing this report.